haematologica
Journal of the Ferrata Storti Foundation

BCAT1 is a NOTCH1 target and sustains the oncogenic function of NOTCH1

by Valeria Tosello, Ludovica Di Martino, Adonia E. Papathanassiu, Silvia Dalla Santa, Marco Pizzi, Lara Mussolin, Jingjing Liu, Pieter Van Vlierberghe, and Erich Piovan

Received: March 29, 2024.
Accepted: August 23, 2024.

Citation: Valeria Tosello, Ludovica Di Martino, Adonia E. Papathanassiu, Silvia Dalla Santa, Marco Pizzi, Lara Mussolin, Jingjing Liu, Pieter Van Vlierberghe, and Erich Piovan. BCAT1 is a NOTCH1 target and sustains the oncogenic function of NOTCH1. Haematologica. 2024 Sept 5. doi: 10.3324/haematol.2024.285552 [Epub ahead of print]

BCAT1 is a NOTCH1 target and sustains the oncogenic function of NOTCH1

Valeria Tosello*[1], Ludovica Di Martino*[2], Adonia E. Papathanassiu[3], Silvia Dalla Santa[2], Marco Pizzi[4], Lara Mussolin[5], Jingjing Liu[6], Pieter van Vlierberghe†[7], Erich Piovan[2, 8]**

[1]Basic and Translational Oncology Unit, Veneto Institute of Oncology IOV-IRCCS, Padua, Italy, [2]Department of Surgery, Oncology and Gastroenterology, University of Padua, [3] Ergon Pharmaceuticals, LLC, Washington DC, United States of America, [4]Surgical Pathology & Cytopathology Unit, Department of Medicine - DIMED, University of Padua,[5]Unit of Onco-hematology, stem cell transplant and gene therapy, Department of Women's and Children's Health, University of Padua, [6]Department of Computational Biology, St. Jude Children's Research Hospital, Memphis, TN, USA, [7]Department of Biomolecular Medicine, Ghent University, Ghent, Belgium, [8]Immunology and Molecular Oncology Unit, Veneto Institute of Oncology IOV-IRCCS, Padua, Italy

†Deceased.

* these two authors contributed equally to the work

**Correspondence: Dr. Erich Piovan erich.piovan@unipd.it

Running title: BCAT1 sustains the oncogenic function of NOTCH1 and represents a therapeutic target

CONFLICT OF INTEREST

There are no financial conflicts of interest to declare.

ACKNOWLEDGEMENTS

We thank Sonia Minuzzo for providing T-ALL xenografts and Laura Bonaldi for help with epifluorescence microscopy. We are grateful to Ilaria Talli for technical assistance in setting up methylation specific assays. Special thanks to Jiyang, Yu and Angela Grassi for doing preliminary gene expression profiling analysis and help with bioinformatics analyses concerning the various datasets used in the present study. We are especially grateful to our co-author, Pieter van Vlierberghe, who recently passed away, for his enthusiastic contribution, warmth and friendship.

FUNDING

This work was supported by the Italian Foundation for Cancer Research (Fondazione AIRC) grants to E.P. (IG2018#22233); Ex 60% to E.P (University of Padova). There are no conflicts of interest to declare.

AUTHOR CONTRIBUTIONS

L.D.M. performed ChIP analyses, performed some in vitro experiments with inhibitors, performed qRT-PCR experiments and helped in writing the first draft of the manuscript; V.T. generated NOTCH1-dependent mouse T-ALLs, performed in vitro and in vivo therapeutic experiments and helped in writing the first draft of the manuscript; A.E.P. provided the BCAT inhibitor, helped in designing in vivo therapeutic experiments and helped in writing the manuscript; L.D.M. and S.D.S. helped in setting up the protocol for performing the immunophenotypic characterization of the leukemia in *Bcat1* WT and KO mice and performed some analyses; L.M. performed patient selection and provided clinical data; M.P. performed and helped in

interpreting IHC results; J.L. helped in bioinformatical analyses. P.V.V. helped in analyzing ChIP-seq data and provided reagents; E.P. designed and performed some experiments, directed research, analyzed data and wrote the paper. All the authors read and edited the manuscript.

DATA AVAILABILITY STATEMENT: The study utilized, in part, publicly available datasets (Gene Expression Omnibus, Chinese Leukemia Genotype-Phenotype Archive). Raw data for this study were generated at HMT (Tokyo, Japan) and Active Motif (Waterloo, Belgium). Derived data supporting the findings of this study are available from the corresponding author upon reasonable request.

Word count: Abstract: 168; Main text: 6079

ABSTRACT

High levels of branched-chain amino acid (BCAA) transaminase 1 (BCAT1) have been associated with tumor aggressiveness and drug resistance in several cancer types. Nevertheless, the mechanistic role of BCAT1 in T-cell acute lymphoblastic leukemia (T-ALL) remains uncertain. We provide evidence that Bcat1 was over-expressed following NOTCH1-induced transformation of leukemic progenitors and that NOTCH1 directly controlled BCAT1 expression by binding to a BCAT1 promoter. Further, using a NOTCH1 gain-of-function retroviral model of T-ALL, mouse cells genetically deficient for *Bcat1* showed defects in developing leukemia. In murine T-ALL cells, Bcat1 depletion or inhibition redirected leucine metabolism towards production of 3-hydroxy butyrate (3-HB), an endogenous histone deacetylase inhibitor. Consistently, BCAT1 depleted cells showed altered protein acetylation levels which correlated with a pronounced sensitivity to DNA damaging agents. In human NOTCH1-dependent leukemias, high expression levels of BCAT1 may predispose to worse prognosis. Therapeutically, BCAT1 inhibition specifically synergized with etoposide to eliminate tumors in patient-derived xenograft models suggesting that BCAT1 inhibitors may have a part to play in salvage protocols for refractory T-ALL.

INTRODUCTION

T-ALL is an aggressive hematological cancer accounting for ≈ 15% of pediatric and ≈25% of adult ALL cases, requiring intensive chemotherapy regimens[1, 2]. Notwithstanding improved cure rates, especially in pediatric cases, a significant fraction of patients (~15%) relapse. Children and adults with relapsed T-ALL face poor prognosis due to low remission rates and increased morbidity and mortality with salvage therapy. There is no doubt that more effective treatment strategies are needed, especially for refractory T-ALL. It is generally accepted that T-ALL is a heterogeneous disease, the result of a wide spectrum of genetic lesions and environmental cues that cooperate to promote leukemogenesis[3, 4] leading to the aberrant growth of immature T-cell progenitors. Gain-of function mutations in NOTCH1 are amongst the most common genetic alterations found in T-ALL[5]. NOTCH1 plays an important physiological role in promoting T-cell lineage and cell growth during thymic development. Its activation following ligand binding requires proteolytic cleavage by γ-secretase-containing protease complexes as well as translocation of the cleaved NOTCH1 intracellular domain (NICD) to the nucleus to facilitate the transcription of numerous downstream targets[6]. NOTCH1 gain-of function mutations (mutNOTCH1) in T-ALL determine the activation of NOTCH1 in the absence of a ligand and/or prevent termination of NOTCH1 signaling in the nucleus. Constitutive NOTCH1 signaling in T-ALL is linked to the transcriptional activation of numerous anabolic pathways involved in cell growth such as ribosome biosynthesis, protein translation and nucleotide and amino acid metabolism [7, 8]. In addition to its transcriptional activities, NOTCH1 is a direct, negative regulator of DNA damage response (DDR) through binding and inhibiting of the ATM (Ataxia-Telangiectasia Mutated) Ser/Thr kinase[9]. This links

NOTCH1 activation to the high number of genetic alterations found in T-ALL, which are thought to be driven by errant DNA repair.

The present study reports that, in addition to its direct effect on the HR pathway, mutNOTCH1 indirectly regulates DDR by upregulating BCAT1. Specifically, we found that BCAT1 was a transcriptional target of mutNOTCH1, which was expressed early in the process of leukemogenesis and shown to regulate not only branched chain amino acid (BCAA) levels but also ketone body synthesis (3-hydroxybutyrate, 3-HB). 3-HB accumulation in BCAT1 deficient cells modified protein acetylation levels and altered DDR resulting in accentuated DNA damage and cell death, especially when combined with a genotoxic insult. The increased chemosensitivity to double strand break (DSB)-inducing agents, observed in T-ALL models following BCAT1 inhibition, suggests that BCAT1 is a novel therapeutic target in T-ALL.

METHODS

Western blotting

Total cell lysates were prepared using RIPA lysis buffer supplemented with phosphatase inhibitor cocktail set I and II (Sigma-Aldrich, Merck, Darmstadt, Germany) and protease inhibitor cocktail tablets (Roche, Burgess Hill, UK) and normalized for protein concentration using the BCA method (Pierce, Pero, Italy). For Western blotting, protein samples were separated on 4-12% gradient Tris-Glycine or 3-8% Tris-Acetate SDS-PAGE Gels (Invitrogen) and transferred to PVDF membrane (Millipore). Antibodies against tubulin (TU-02), MYC and p53 (DO-1) were from Santa Cruz Biotechnology (Dallas, TX, USA); antibodies recognizing Cleaved NOTCH-1 (ICN1; Val 1744), β-actin, p21, BCAT2, BCAT1, Ku-80, Ku-70, Histone H3, cleaved PARP-1, cleaved caspase 3, phosphorylated H2AX (pS139), phosphorylated DNA-PKcs (pS2056), total DNA-PKcs, phosphorylated ATM (pS1981), total ATM, phosphorylated CHK2 (pT68), total CHK2, phosphorylated TP53 (pS15), acetylated p53 (K382) and GADPH were from Cell Signaling Technology (Danvers, MA, USA). Acetyl-Histone H3 Antibody Sampler Kit (#9927) was also from Cell Signaling Technology. Mouse anti-BCAT1 (BD Pharmingen, Oxford, U.K) was also used. The BioRad ChemiDoc XRS Imager was used to capture the signals from the blots.

Chromatin Immunoprecipitation (ChIP) qPCR

ChIP assays were performed using the SimpleChIP plus Enzymatic Chromatin IP kit (Cell Signaling Technology, #9005) following the manufacter's protocol. Briefly, 4 $x10^6$ cells were fixed with formaldehyde in a final concentration of 1% for 10 minutes at room temperature. The crosslinking reaction was quenched with a 5M glycine solution, and the cells were then centrifuged, washed twice with ice-cold PBS and lysed. Cell nuclei were prepared and chromatin was digested with micrococcal nuclease, then sonicated. The sheared chromatin was immunoprecipitated with human Notch-1 intracellular domain antibody (R&D Systems, Minneapolis, MN; Cat#AF3647). Normal sheep IgG (Cat#5-001-A, R&D Systems) was used as a non-specific antibody control for immunoprecipitation. Following an overnight incubation with antibodies, 30 μl of Protein G Magnetic Beads was added at 4°C for 2 h. Beads were washed, and chromatin was eluted. Crosslinks were reverted according to kit instructions. The DNA was purified using DNA Purification Buffers and Spin Columns (Cell Signaling Technology #14209) following kit instructions. The immunoprecipitated DNA was subjected to real-time PCR reaction using ChIP primer sets (listed in *Online Supplementary Table S1*), which were designed to include the promoter and negative regions for BCAT1 gene. HES1 promoter region was used as positive control. Fold enrichment was calculated as a ratio of amplification efficiency of ChIP sample over that of the IgG. More specifically, the amplification efficiency (AE) of each primer set was used to determine the amplification efficiency of the ChIP sample and the IgG

sample as follows: % ChIP = AE(Input Ct – ChIP Ct) x (dilution factor; Fd)(100); % IgG = AE(Input Ct – IgG Ct) x(Fd)(100); Fold Enrichment = % ChIP / % IgG.

Statistical Analyses

Results were expressed as mean value ± Standard Deviation (SD). Student's *t*-test and nonparametric *t*-test (Mann-Whitney) were used where appropriate. A non-parametric test (Fisher's exact test) was used to compare qualitative data. The Kaplan–Meier method was used to estimate the distributions of overall survival (OS). OS was considered as the time from diagnosis to date of death. The log-rank test was used to compare survival distributions. All statistical tests were two sided, unpaired and $P< 0.05$ was considered statistically significant ($*P< 0.05$, $**P< 0.01$, $***P< 0.001$). Analysis of drugs' interaction was performed using Combenefit software[10]. The sample size for animal xenograft experiments was determined on the basis of prior studies that yielded a two-tailed statistical test with ~80% power to detect a twofold change in tumour burden (α=0.05). All attempts at replication were consistent for all animal and cell culture experiments.

Mouse experiments

The study was approved by the Institutional Review Board (OPBA) of the University of Padova (protocol code 238591; 25 June 2019) and the Italian Ministry of Health (DGSAF 0006112; 177/2020-PR; 10/03/2020).

Information on cell lines and primary leukemia samples, mouse transplantation experiments and studies, flow cytometry and analysis of T-cell distribution, quantitative real-time PCR, total histone extraction, immunohistochemistry, immunoprecipitation of acetylated proteins, neutral comet assay, analysis of publicly available datasets, RNA-sequencing and gene-set enrichment analysis, steady state metabolite profiling, stable-isotope tracing experiments, analysis of ChIP-seq databases, cell viability assays and flow cytometry, plasmids, lentiviral constructs and viral production, luciferase reporter experiments, methylation specific PCR (MSP) methods are detailed in the *Online Supplementary Materials and methods section*.

RESULTS

NOTCH1 upregulates BCAT1 expression in *NOTCH1* mutated human T-ALL by binding to a BCAT1 promoter. To understand the role that BCAT1 plays in T-ALL development, we analyzed gene expression data from a NOTCH1-induced murine T-ALL (NIC) model. In that model, overexpression of an activated, intracellular form of Notch1 (*ICN1*) in transplanted Lin-negative murine hematopoietic cells leads to the development of an abnormal $CD4^+CD8^+$ double positive (DP) T cell subset at 2 weeks of transplantation followed by the rise of a highly tumorigenic DP leukemic population at 6-8 weeks of transplantation[11, 12]. In the gene set of Figure 1A, Bcat1 was highly upregulated in leukemic DP cells compared to normal DP cells. The increase in Bcat1 expression occurred early in T-ALL development as evident from the heat map of *Online Supplementary Figure S1A*, and was unique among other enzymes involved in BCAA metabolism (eg, Bcat2, Bckdha, and Bckdhb), whose expression did not exhibit a specific pattern (*Online Supplementary Figure S1A*). To confirm the above observations, we compared transcript and protein levels of Bcat1 and Bcat2 in thymocytes isolated from normal C57/BL6 mice and leukemic cells obtained from spleens of mice bearing T-ALL tumors. The tumors were induced through overexpression of an activated form of NOTCH1 lacking a major portion of the extracellular domain (*ΔE-NOTCH1*). As in the case of the NIC model, the development of leukemia in the *ΔE-NOTCH1* model (NOTCH1-T tumors) was associated with increased Bcat1 levels (Figure 1B). On the other hand, the gene expression of Bcat2, the mitochondrial isoform of

BCAT, was not consistently altered with the development of leukemia, although a decrease was observed in the protein levels in NOTCH1-T tumors (*Online Supplementary Figure S1B, C*). The results suggest that the expression of Bcat1 and Bcat2 in NOTCH1-T tumors may be anti-correlated. Since Bcat1 and Bcat2 are metabolic enzymes, we attempted to identify a leukemia-specific metabolic signature by extracting metabolites from NOTCH1-T tumors (N=3) and murine thymic tissue (N=3). We quantified 112 metabolites by using a highly sensitive capillary electrophoresis-time-of-flight mass spectrometry (CE-TOFMS) and capillary electrophoresis-tandem mass spectrometry (CE-MS/MS) (*Online Supplementary Figure S1D*). While thymic tissue preferentially expressed metabolites associated with lipid oxidation (e.g., carnitine and citric acid) as well as purine and pyrimidine metabolism, metabolites found elevated in NOTCH1-T tumors were linked to glycolysis (lactic acid) and TCA cycle replenishment (succinic, fumaric, and malic acids) indicating a significant metabolic shift with development of leukemia (*Online Supplementary Figure S1E*). This metabolic feature was maintained when heavily infiltrated thymuses were used as a source of leukemia (*Online Supplementary Figure S2A*). NOTCH1-T tumors were also characterized by increased concentrations of BCAAs (*Online Supplementary Figures S1F, S2B*). While BCAA biosynthesis was identified as a significantly enriched pathway in NOTCH1-T tumors by metabolite set enrichment analysis (*Online Supplementary Figure S1E*), active uptake could not be excluded as the tumors showed increased expression of the neutral amino acid transporter *slc7a5* (LAT1) compared to normal thymic tissues (*Online Supplementary Figure S1G*).

To determine if BCAT1 overexpression is also a characteristic of human T-ALL, we utilized a publicly available dataset, which profiled both normal human thymocyte populations and bone marrow samples of childhood T-ALL patients at the time of diagnosis[13]. We found that BCAT1 was highly expressed in numerous T-ALL samples (*Online Supplementary Figure S1H*). To confirm that human T-ALL is indeed linked to increased BCAT1 expression, we used a comprehensive microarray data set[14, 15] consisting of T-ALL patients (N=57) and thymocyte subsets (7 thymocyte and mature T-cell subsets derived from 3 independent donors). BCAT1 expression was again found to be significantly upregulated in a fraction of T-ALL specimens compared to thymocyte subsets (Figure 1C). T-ALL can be subclassified into three differentiation stages based on cluster of differentiation (CD) surface markers, such as early/precortical, cortical, and mature/postcortical. To identify patient groups with upregulated BCAT1 expression, we utilized a well-characterized T-ALL gene dataset (TARGET cohort), obtained from 264 pediatric T-ALL patients[16]. We found BCAT1 to be preferentially expressed in the cortical (CD1a positive) T-ALL immunophenotypical subgroup (*Online Supplementary Figure S1I*). Since *NOTCH1* activating mutations are highly prevalent in the cortical subgroup[3], we hypothesized that NOTCH1 regulates BCAT1 expression. Sub-diving the TARGET cohort of patients into *NOTCH1/FBXW7*-mutated and *NOTCH1/FBXW7* wild-type disclosed that the former had higher BCAT1 levels compared to *NOTCH1* wild-type patients (*Online Supplementary Figure S1J*). This observation was confirmed in two independent T-ALL cohorts composed of 37 diagnostic pediatric samples included in the Children's Oncology Group P9404 study[17] and 130 pediatric and adult samples from the Shanghai Institute of Hematology project with known *NOTCH1* mutational status (*Online Supplementary Figure S1K, L*)[18]. We then analyzed BCAT1 expression in a comprehensive panel of T-ALL cell lines. *Online Supplementary Figure S1M* discloses a heterogeneous pattern of BCAT1 protein expression, which was not evidently correlated with the mutational status of NOTCH1, as detected by the presence of ICN1, although BCAT1 transcript expression did correlate with HES1 expression (*Online Supplementary Figure S1N*). *HES1* gene is a well-known NOTCH1-target gene. We also evaluated the methylation status of *BCAT1* promoter in a cell line panel and determined that gene methylation status controlled BCAT1 expression in a particular cell line (*Online Supplementary Figure S1O, P*). We also analyzed the transcript and protein levels (Figure 1D) of BCAT1 in previously generated patient derived xenografts (PDX)[19, 20]. PDX samples possessing activated NOTCH1 (*NOTCH1/FBXW7* mutant/NICD1-positive cases) showed higher BCAT1 levels compared to NICD1-negative cases (Figure 1D). Finally, we evaluated BCAT1 and HES1 expression levels using immunohistochemistry in primary T-cell lymphoblastic leukemia/lymphoma (T-ALL/T-LBL; N=10), PDX samples (N=10) and normal human thymuses (N=3). We found weak expression of all three markers in normal thymus (*Online Supplementary Figure S3A*). The staining pattern for BCAT1 and HES1 was rather heterogeneous in leukemia samples (*Online Supplementary*

Figure S3B, C), however we found a statistically significant association between BCAT1 expression and HES1 staining (Fisher's exact test $P < 0.05$; *Online Supplementary Figure S3C*). We used HES1 staining as a surrogate for NOTCH1 activation status as Sanger based sequencing of *NOTCH1* and *FBXW7* genes from FFPE material failed in most patient cases. On the other hand, we found no association between BCAT2 and HES1 staining (*Online Supplementary Figure S3D*). These results further suggest that NOTCH1-activated leukemia cases express higher levels of BCAT1. Based on the above evidence, we hypothesized that NOTCH1 activation leads to BCAT1 overexpression.

To additionally evaluate whether BCAT1 represents a novel NOTCH1 downstream target gene, we treated NOTCH1-T tumor-bearing mice (5 independent tumors) with the gamma secretase inhibitor dibenzazepine (DBZ) and subjected vehicle-control (DMSO) and treated (DBZ) tumors to transcriptomic analysis. We found that Bcat1 gene expression was highly downregulated following in vivo NOTCH1 inhibition (*Online Supplementary Figure S4A*). Downregulation of Bcat1 was also observed following similar analysis of *HDΔPEST NOTCH1* (*NOTCH1* mutant allele harboring both HD and PEST domain mutations) leukemias treated ex-vivo with DBZ[21] (data not shown). Further, treatment of human *NOTCH1* mutant T-ALL cell lines (in vitro) and PDX samples (in vivo) with DBZ markedly reduced BCAT1 transcript and protein levels (Figure 1E and *Online Supplementary Figure S4B, C*). To determine whether NOTCH1 directly regulates BCAT1 expression in T-ALL, we analyzed deposited chromatin immunoprecipitation followed by next-generation sequencing (ChIP-seq) data of NOTCH1 chromatin binding sites in HPB-ALL cells, which are NOTCH1-mutant and MYC expressing T-ALL cells[22]. We found numerous NOTCH1 peaks in the BCAT1 locus; particularly prominent was a peak of $\approx$ 0.5 kb near the BCAT1 transcription start site (TSS) (Figure 1F). In the vicinity of this peak region, a RBPJ site was found upstream of the TSS. To functionally characterize the potential role of this NOTCH1 binding region in BCAT1 gene regulation, we inspected Encyclopedia of DNA Elements (ENCODE) data for epigenetic histone marks in this region in T-ALL cells. These analyses revealed bona fide promoter features associated with this region, including occupancy and high levels of DNA polymerase II (Pol II) and high levels of histone H3 Lys4 trimethylation (H3K4me3) (*Online Supplementary Figure S5*). Transposase-accessible chromatin with sequencing (ATAC-Seq) data also support an open chromatin state in this region (*Online Supplementary Figure S5*). Local ChIP experiments using specific primers centered around this region were performed in PF382 cells, which are NOTCH1 mutant and present modest levels of MYC protein expression (*Online Supplementary Figure S4C*). This analysis confirmed NOTCH1 binding in this area of the BCAT1 promoter region (Figure 1F). Based on these results, we proposed that this NOTCH1 bound region could function as an important regulatory element driving BCAT1 expression in T-ALL cells. Consistent with that hypothesis, luciferase reporter assays in ICN1 transfected HEK 293T cells showed a dose dependent activation of a reporter construct containing this ~0.5kb region of the BCAT1 promoter (including the upstream RBPJ binding site) (*Online Supplementary Figure S4D*). Reporter activity was severely reduced following mutation of the RBPJ binding site (*Online Supplementary Figure S4D*). Further, ICN1 induced reporter activity was progressively reduced using CB103, a highly selective and potent inhibitor of the CSL-NICD gene transcription complex[23] (*Online Supplementary Figure S4E*). On the other hand, knockdown of MYC or the use of JQ1[24] only modestly affected ICN1 induced reporter activity (*Online Supplementary Figure S4F, G*), strongly suggesting that MYC does not play a major role in regulating the activity of this region. Coherently, in HPB T-ALL cells (*Online Supplementary Figure S4H*), luciferase reporter assays showed strong activation of this BCAT1 promoter reporter construct. Further, in HPB T-ALL cells reporter activity could progressively be reduced using CB103 (*Online Supplementary Figure S4I*) or following inactivation (deletion or mutation) of the RBPJ binding site, suggesting a prominent role for NOTCH1 in regulating reporter activity in T-ALL cells (*Online Supplementary Figure S4J*). This notion was further strengthened by the observation that forced increased expression of ICN1 in HPB T-ALL cells augmented BCAT1 promoter reporter activity but had very modest effects on the transcriptional activity of the BCAT1 promoter construct having the RBPJ binding site mutated (*Online Supplementary Figure S4K*).

Canonical functions of BCAT1 in T-ALL. To examine the role of Bcat1 in T-ALL development, we used a NOTCH1-dependent T-ALL mouse model *(ΔE-NOTCH1*). Transduced BM progenitor cells (GFP+Lineage-cKit+Sca1+) from *Bcat1 KO* and *Bcat1 WT* were transplanted into lethally irradiated C57BL/6J hosts (*Online Supplementary Figure S6A*). Despite no evidence of engraftment defects three weeks post-transplant, mice receiving *Bcat1 KO ΔE-NOTCH1* GFP+ cells showed a significant delay in succumbing to leukemia respect to mice receiving *Bcat1 WT ΔE-NOTCH1* GFP+ cells (Figure 2A). The immunophenotype of established leukemias was similar amongst genotypes (*Online Supplementary Figure S6B*). We thus hypothesized that Bcat1 may be implicated in cell cycle progression or apoptosis of T-ALL cells. To examine this, we evaluated Edu incorporation and Annexin V staining in leukemic cells obtained from diseased animals. *Bcat1 KO* T-ALL cells showed a decrease in the proportion of cells in the S-phase of the cell cycle (Figure 2B) and a modest increase in apoptotic cells (*Online Supplementary Figure S6C*). These results suggest that Bcat1 promotes survival and proliferation of *NOTCH1*-mutant T-ALL. We thus examined the in vitro and in vivo effects of BCAT1 gene depletion by short-hairpin RNA (shRNA) in human leukemia cell lines expressing high levels of the protein. Bcat1 silencing was associated with cell cycle arrest at the G1 phase (Figure 2C and *Online Supplementary Figure S7A*), inhibition of proliferation (Figure 2D), and induction of apoptosis (*Online Supplementary Figure S7B*) in vitro and decreased tumor growth in vivo (Figure 2E, F, *Online Supplementary Figure S7C*). Different cell lines exhibited differential sensitivity to the effects of BCAT1 depletion, which was also dependent on the type of assay used. Whereas BCAT1 silenced MOLT4 cells were far more apoptotic than CCRF-CEM cells in vitro (*Online Supplementary Figure S7B*), the opposite was true for tumor growth in vivo. Indeed, BCAT1 silencing in CCRF-CEM cells strongly affected their growth in vivo (Figure 2E), whereas, in MOLT4 cells, it yielded only a modest reduction in tumor burden and a moderate increase in survival (Figure 2F, *Online Supplementary Figure S7C*). BCAT1 silenced DND41 cells also recorded a high degree of apoptosis (*Online Supplementary Figure S7B*). We speculate that loss of BCAT1 in human T-ALL is associated with cell cycle arrest, apoptosis, and delayed tumor growth in vivo.

To determine the putative mechanism behind the functional dependence of *NOTCH1*-mutant T-ALL cells on Bcat1, gene expression analysis was performed by RNA-seq on leukemic cells isolated from spleens of diseased mice at the moment of sacrifice. Comparison of gene expression profiles of *Bcat1 WT* and *Bcat1 KO ΔE-NOTCH1* tumors identified 470 differentially expressed genes (≥2 Fold change, $P<0.05$, FDR≤0.1; Figure 3A and *Online Supplementary Table S2*). The majority of these genes showed decreased expression in *Bcat1 KO ΔE-NOTCH1* tumors (data not shown). Gene set enrichment analysis (GSEA) identified four significantly different pathways: "G2M checkpoint", "mitotic spindle", "epithelial mesenchymal transition", and "E2F targets", all downregulated in *Bcat1 KO ΔE-NOTCH1* cells (*Online Supplementary Table S3*; Figure 3B). On the other hand, GSEA analysis identified 18 significantly different pathways upregulated in *Bcat1 KO ΔE-NOTCH1* cells, including "DNA repair", "apoptosis", and "p53 pathway" (*Online Supplementary Table S3*; Figure 3C). These results are consistent with our functional data and suggest that Bcat1 may be implicated in regulating the DNA damage response (DDR). To follow-up on this possibility, we evaluated the levels of γH2AX, a surrogate marker of DNA damage and double strand breaks (DSB) abundance in Bcat1 depleted cells. We found that Bcat1 KO or BCAT1 depleted cells had higher basal levels of γH2AX compared to Bcat1 expressing cells (Figure 3D).

Subsequently, we examined the metabolic impact of Bcat1 depletion on *ΔE-NOTCH1* leukemias. Briefly, we extracted metabolites from *Bcat1 WT* and *Bcat1 KO ΔE-NOTCH1* tumors, and quantified 56 metabolites by mass spectrometry to examine the metabolic impact of *Bcat1* loss on *ΔE-NOTCH1* leukemias (Figure 3E). We found N=19 differentially expressed metabolites between the pairs of compared *Bcat1 WT* and *Bcat1 KO ΔE-NOTCH1* tumors (Figure 3E). Of these, four metabolites (leucine, glutamine, 3-hydroxy-butyrate (3-HB) and lactic acid) were consistently modulated in other compared tumors (data not shown). Further, we performed $^{13}C_6$-Leu stable-isotope tracing experiments to track the metabolic fate of BCAA in *ΔE NOTCH1* leukemias. The results, which are shown in *Online Supplementary Figure S8*, indicated that $^{13}C_6$-Leu was readily taken up by *Bcat1 WT* tumors and that *Bcat1 KO* tumors had increased levels of (m+6)

Leu compared to *WT* tumors, presumably due to lack of Bcat1. Again, a relevant amount of labeled leucine was incorporated in 3-HB in both groups, with *Bcat1 KO* tumors showing increased levels of (m+2 and m+3) 3-HB compared to *WT* tumors (*Online Supplementary Figure S8*). On the other hand, major TCA metabolites (with the exception of citrate) exhibited very low isotopic labeling indicating that *ΔE-NOTCH1* leukemias probably do not utilize BCAAs for the replenishment of the TCA cycle. This result may however be influenced by our experimental approach using $^{13}C_6$-Leu bolus injection rather than constant infusion.

The BCAT1 inhibitor, ERG245, recapitulates the functional consequences of Bcat1 depletion. Given our observations that BCAT1 could be a therapeutic target in T-ALL, we evaluated the effects of a novel BCAT1-specific inhibitor, ERG245[25]. Treatment of *ΔE NOTCH1 Bcat1 WT* leukemias with ERG245 was highly apoptotic and induced a potent cell cycle arrest (Figure 4A, B and *Online Supplementary Figure S9A, B*). Interestingly, *ΔE NOTCH1 Bcat1 KO* leukemias were almost refractory to this drug, even at high concentrations (Figure 4C). On the other hand, human T-ALL cell lines and PDX samples were less sensitive to the effects of ERG245, with only high doses determining effects on viability or cell cycle (Figure 4D, E; *Online Supplementary Figures S9C, D and S10A, B*). We further performed $^{13}C_6$-Leu stable-isotope tracing experiments to examine the metabolic impact of BCAT1 inhibition on *ΔE-NOTCH1* leukemias. Briefly, NOTCH1-T-tumor bearing mice were treated in vivo with vehicle control or ERG245[25], and perfused with $^{13}C_6$- Leu just prior sacrifice. Cellular metabolites from snap-frozen spleens were then extracted and quantified. The results, which are shown in *Online Supplementary Figure S11*, indicated that $^{13}C_6$-Leu was readily uptaken by the tumors and that tumors treated with ERG245 had increased levels of (m+6) Leu compared to tumors treated with vehicle-control, presumably due to inhibition of Bcat1 (*Online Supplementary Figure S11*). Two major metabolic events were observed with BCAT1 inhibition: a) a partial break in the TCA cycle between citrate and succinate, and b) increased synthesis of 3-HB. In *Online Supplementary Figure S11*, accumulation of citrate and isocitrate are noted with a concomitant decrease in the levels of succinate and fumarate. A similar TCA cycle break was reported by Ko et al. in LPS-stimulated macrophages treated with a different but structurally related BCAT1 inhibitor[26]. Considering that accumulation of TCA components previously noted in NOTCH1-T tumors (*Online Supplementary Figure S1D*), the break in the TCA cycle with BCAT1 inhibition constitutes a significant metabolic shift. Again, with the exception of citrate, major TCA metabolites exhibited limited isotopic labeling indicating that NOTCH1-T tumors may not utilize BCAAs for the replenishment of the TCA cycle, at least under our experimental conditions of bolus injection. ERG245- driven inhibition of BCAT1 induced a modest decrease in the levels of isoleucine and valine (data not shown) in tandem with an increase in the isotopic labeling of citrate and 3-HB. Acetyl-CoA or succinyl-CoA (and propionyl-CoA) are the main end-products of BCAA metabolism, with acetyl-CoA that can be used to synthesize citrate and/or ketone bodies such as acetoacetate and 3-HB. These findings are similar to the metabolic effects obtained in *Bcat1 KO ΔE-NOTCH1* tumors (*Online Supplementary Figure S8*). We speculate that, following BCAT1 inhibition or depletion, there is a shift towards leucine and 3-HB synthesis. 3-HB is known to act as an energy source in the absence of sufficient glucose and to inhibit class I histone deacetylases (HDACs)[27], thus influencing the acetylation state of proteins and/or the epigenetic regulation of genes.

BCAT1 depletion increases chemosensitivity of T-ALL cells and is dependent on its enzymatic activity. Given that our results implicate BCAT1 in regulating DDR, we examined if the cytotoxicity of DSB-inducing agents increases in the absence of BCAT1. The data suggest that BCAT1-depletion significantly enhances the sensitivity of murine and human T-ALL cells to etoposide (Figure 5A-C and *Online Supplementary Figure S10C, D*). *ΔE- NOTCH1 Bcat1 KO* leukemias were particularly sensitive to etoposide (Figure 5A). In Figure 5B, early apoptotic CCRF-CEM cells (Annexin$^+$ Sytox Red$^-$) and late apoptotic or necrotic CCRF-CEM cells (Annexin$^+$ Sytox Red$^+$) were evident at 48h of etoposide treatment; both populations increased significantly when etoposide was combined with BCAT1 depletion (Figure 5B). Similar results were obtained with DND41 (*Online Supplementary Figure S10C*) and MOLT4 cells (*Online*

Supplementary Figure S10D). Increased chemosensitivity in BCAT1-depleted cells was also observed when cells were exposed to other drugs such as doxorubicin (*Online Supplementary Figure S10E-F*). To understand the effect of BCAT1 silencing on etoposide-induced DNA damage, we examined the presence of DNA DSBs in CCRF-CEM cells transduced with shBCAT1 after treatment with etoposide for different time periods by determining the levels of γH2AX, a surrogate marker of DSB abundance (Figure 5C and *Online Supplementary Figure S12A*). Additionally, we performed a neutral comet assay to determine the extent of DNA damage (DSB). In this assay, the % tail DNA can be used to quantitate DNA damage. We found that BCAT1-depleted cells exposed to etoposide presented considerably more tail DNA compared to control cells, especially at the 6h timepoint (Figure 5D). We also examined the phosphorylation status of key proteins that control activation of different DNA DSB repair pathways (DNA-PK for c-NHEJ pathway and ATM for HR pathway) or cell cycle arrest (CHK2 and p53). *Online Supplementary Figure S12B* indicates that both c-NHEJ and HR pathways were involved in repairing etoposide-induced DNA damage. Whereas control and BCAT1-depleted CCRF-CEM cells exhibited similar rates of ATM phosphorylation, DNA-PK was subject to an accentuated phosphorylation in BCAT1-depleted cells (*Online Supplementary Figure S12B*). Interestingly, increased DNA sensing was not associated with DNA DSB repair but with further DNA damage, as intimated by the dramatic increase in the levels of γH2AX in BCAT1-depleted cells compared to control cells (Figure 5C and *Online Supplementary Figure S12A, B*). The combination of BCAT1 silencing and etoposide treatment was also associated with increased levels of phosphorylated CHK2 and p53 (*Online Supplementary Figure S12B*). Cleaved PARP-1 was observed only at 24h of etoposide treatment suggesting that the failure of the cells with depleted BCAT1 to repair DNA DSBs leads to extensive DNA damage and eventually apoptosis (*Online Supplementary Figure S12A*).

We next determined whether the metabolic function of BCAT1 contributes in modulating the sensitivity to DNA damaging agents. To this end we constructed a BCAT1 catalytic-inactive mutant where we abolished transaminase activity through mutation of lysine 222 to alanine ($BCAT1^{K222A}$)[28]. Next, we analyzed the phenotypic impact of expressing wild-type BCAT1 ($BCAT1^{WT}$) and $BCAT1^{K222A}$ in BCAT1 depleted CCRF-CEM cells treated with etoposide. We found that overexpression of $BCAT1^{WT}$ was able to partially rescue the phenotype of BCAT1 depleted cells (*Online Supplementary Figures S13A and S12C*), while $BCAT1^{K222A}$ overexpressing cells maintain sensitivity to etoposide much like parental BCAT1 depleted cells (*Online Supplementary Figure S13A and S12C*). These data suggest that BCAT1 catalytic activity is required for maintaining resistance to DNA damaging agents such as etoposide. Since we found 3-HB (a putative HDAC inhibitor) to accumulate in *Bcat1 KO* and ERG245 treated murine T-ALL, we evaluated whether this metabolite could be implicated in modulating sensitivity to etoposide. CCRF-CEM cells treated with increasing doses of 3-HB showed sensitization to the cytotoxic effects of etoposide (*Online Supplementary Figure S13B*). Similar results were obtained in a human T-ALL PDX model (PDX#47; *Online Supplementary Figure S12D-F*). Interestingly, the well-known HDAC inhibitor, NaB, was also highly effective in sensitizing cells to the cytotoxic effects of etoposide (*Online Supplementary Figures S13B and S12D-F*), further suggesting a common mode of action between 3-HB and NaB. Following up on these observations, we initially determined whether Bcat1/BCAT1 depletion or inhibition could modulate the epigenetic state (acetylation) of histones. We found H3K27 acetylation to be consistently increased in Bcat1 KO and BCAT1 depleted cells (*Online Supplementary Figure S12G, H*), similarly to 3-HB treated cells (*Online Supplementary Figure S12I*). Interestingly, increased acetylation of proteins implicated in DDR response (p53, Ku-70, Ku-80) was also found in BCAT1 depleted cells, especially after etoposide treatment (*Online Supplementary Figure S12J*). These results suggest that altered acetylation of signaling proteins may contribute to the chemo-sensitizing effect of BCAT1 depletion/inhibition.

BCAT1 overexpression correlates with poor survival and its pharmacological inhibition synergizes with DNA-damaging chemotherapy in T-ALL cells. To investigate the putative clinical relevance of high BCAT1 expression, we used the TARGET T-ALL cohort composed of over 260 T-ALL patients[16]. Using the mean BCAT1 expression level as the cut-off for subdividing high and low BCAT1 expression, we found that BCAT1 levels had a prognostic significance (*Online Supplementary Figure S14A*).

Another disease characterized by frequent constitutive activation of the NOTCH1 signaling cascade (by mutational and non-mutational mechanisms) is chronic lymphocytic leukemia (CLL)[29, 30]. We also evaluated the prognostic significance in a profiled CLL cohort (N=107) with known clinical response (survival)[31]. Using the mean BCAT1 expression level as the cut-off for subdividing high and low BCAT1 expression, BCAT1 levels were also found to have a prognostic significance (*Online Supplementary Figure S14A*). These results suggest that BCAT1 may have a prognostic significance in these two NOTCH1-dependent leukemias and may further represent a valid therapeutic target.

Following-up on our observation that knock-down of BCAT1 increased the sensitivity of T-ALL cells to DNA damaging agents, we investigated whether pharmacological inhibition of BCAT1 using ERG245 could also improve the antitumor efficacy of DNA damaging agents. We found that ERG245 potentiated the effects of DNA damaging drugs such as etoposide (Figure 6A, B; *Online Supplementary Figures S14B, C and S15A-C*), cytarabine (*Online Supplementary Figure S15C*) and doxorubicin (*Online Supplementary Figure S15C*) in T-ALL cell lines (MOLT4, CCRF-CEM, and DND41) and PDX cells (Figure 6C, D and *Online Supplementary Figures S14D-J, S15D, E and S16A-C,*). The combinatory effect of ERG245 and a DNA-damaging agent was synergistic in most cases and most pronounced for etoposide (*Online Supplementary Figure S15C*). Levels of γH2AX increased dramatically following addition of ERG245 to T-ALL cells treated with etoposide (Figure 6B and *Online Supplementary Figures S14F, S16A*). That increase was accompanied by induction of apoptosis as indicated by the presence of cleaved PARP-1. Next, we used a xenograft-based approach to test the effects of combining BCAT1 inhibition with etoposide in in vivo models of T-ALL. We injected luciferase expressing PDX#27 (PDX#27-luc) cells into NSG mice and treated them with vehicle, ERG245 (30mk/kg, three times a week), etoposide (15mg/kg, twice a week) or the combination of the two drugs for 14 days. Tumor burden was evaluated using bioluminescence, $hCD45^+$ staining, and spleen weight as human T-ALL is characterized by elevated levels of $CD45^+$ blasts and splenomegaly. Whereas etoposide treatment decreased tumor burden by almost one-log unit of bioluminescence compared to vehicle, the combination of etoposide and ERG245 decreased it by almost two-log units (Figure 6D). The efficacy of the combination treatment was additionally reflected in the other markers used to assess tumor growth: mice treated with etoposide and ERG245 exhibited lower levels of human $CD45^+$ blasts in the peripheral blood (PB; *Online Supplementary Figure S16B*), spleen and bone marrow (not shown). Further, these mice did not show splenomegaly (*Online Supplementary Figure S16C*). Actually, our results suggest that mice in the combination group experienced almost complete elimination of tumor cells (N=5; blasts <1%) in PB, and all mice had experienced partial remission (>90% reduction of blasts compared to vehicle treated mice at day 28) in target organs (bone marrow, spleen). In contrast, mice that received etoposide monotherapy exhibited much smaller tumor burden decreases, while almost complete elimination of tumor cells (blasts <1% in any compartment) were absent in that group. Impact on overall survival was not evaluated. Similar results were obtained in another highly aggressive PDX model, PDX#19. Here, luciferase expressing PDX#19 (PDX#19-luc) cells were injected into NSG mice and treated with vehicle, ERG245 (30mk/kg, three times a week), etoposide (10mg/kg, twice a week) or the combination for 10 days before evaluating tumor burden (*Online Supplementary Figure S14G-J*). The data again highlight that BCAT1 inhibition greatly potentiates the antitumor activity of etoposide in vivo.

DISCUSSION

The present study elucidates the unique role that BCAT1 plays in T-ALL. BCAT1 is the cytosolic enzyme commonly responsible for the reversible transfer of an amino group from leucine, isoleucine, and valine to alpha-ketoglutarate (α-KG) to form glutamate and the corresponding α-ketoacid[32]. Here, we report that BCAT1 is a downstream target of mutated NOTCH1. Mutations that activate NOTCH1 signaling are found in more than 65% of all T-ALL cases and considered a hallmark of the disease. Our experiments revealed that Notch1 binds to Bcat1 promoter and increases Bcat1 gene transcription early in the process of

leukemogenesis in experimental models of T-ALL, as well as in clinical samples of patients suffering from the disease. Such an increase confers metabolic and other advantages to the leukemic cells. Compared to thymic tissues, we show that NOTCH1-T tumors exhibit elevated levels of TCA cycle metabolites. For the same tumors, we report a break in the TCA cycle with BCAT1 inhibition and impaired metabolic activity as determined by the downregulation of many essential metabolites. At the same time, BCAT1 inhibition or Bcat1 depletion appears to redirect leucine metabolism towards synthesis of leucine and 3-HB, an HDAC inhibitor, suggesting that BCAT1 may also regulate protein acetylation. Indeed, we find increased acetylation of histones (H3K27) and repair proteins (Ku70/Ku80) in Bcat1/BCAT1 depleted cells. Another interesting finding was that BCAT1 depletion or inhibition resulted in increased levels of γH2AX, a marker of increased DNA damage. Although we do not provide any direct experimental evidence, this may be linked to an anti-oxidant role for the BCAT1 CXXC motif, normally buffering intracellular reactive oxygen species (ROS)[33].

Deletion of Bcat1 seems associated with faulty DDR and induction of apoptosis, especially following exposure to DNA damaging agents. Collectively, our study indicates that NOTCH1 upregulates BCAT1 to metabolically reprogram the cells and to ensure cell survival upon DNA damage possibly through altered 3-HB synthesis and protein acetylation (see Figure 7). This is in line with numerous studies suggesting that NOTCH1 controls oncogenic pathways that promote cell proliferation and survival, metabolic reprogramming, and resistance to chemotherapy through transcriptional activation of downstream target genes. Although non-canonical functions have previously been assigned to BCAT1 and linked to its redox state[25, 28, 34], increased sensitivity to etoposide in BCAT1 depleted cells seems to be dependent on its transaminase activity. We speculate that following BCAT1 depletion/inhibition, cells adapt increasing ketone body synthesis (3-HB) which initially has growth-promoting effects (through its anti-oxidant effect at low concentrations), but as it accumulates, it paradoxically promotes cell death through its capacity to inhibit HDACs[35, 36] and promote protein acetylation. This accumulation of 3-HB seems to potentiate the cytotoxic effects of DNA damaging agents such as etoposide. We hypothesize that NOTCH1 directly[9] and indirectly (through BCAT1 upregulation) represses DDR in order to promote cell survival in the presence of a genotoxic insult. The same mechanism might be at play during leukemogenesis, which allows for the accumulation of genetic lesions, the survival of the cells, and ultimately the onset of T-ALL.

The role of BCAT1 in leukemia and other cancers is currently an active area of research. Numerous reports have indicated that BCAT1 is a risk-factor in multiple cancers: its expression is associated with tumor progression, increased chemoresistance, and poor prognosis[37, 38]. In agreement, our experiments suggest that high BCAT1 expression correlates with poor survival in NOTCH1-driven malignancies (T-ALL, B-CLL) and that inhibition of BCAT1 increases the chemosensitivity of T-ALL cells towards cytotoxic drugs, known to induce DSBs, such as the topoisomerase II inhibitor etoposide. In two aggressive PDX models, the combination of ERG245 and etoposide markedly reduced tumor burden, almost completely cleared $CD45^+$ blasts from the blood, and abolished splenomegaly in the majority of the treated animals indicating that BCAT1 could be a novel therapeutic target in T-ALL particularly in salvage protocols.

REFERENCES

1. Terwilliger T, Abdul-Hay M. Acute lymphoblastic leukemia: a comprehensive review and 2017 update. Blood Cancer J. 2017;7(6):e577.
2. Pui CH, Robison LL, Look AT. Acute lymphoblastic leukaemia. Lancet. 2008;371(9617):1030-1043.
3. Belver L, Ferrando A. The genetics and mechanisms of T cell acute lymphoblastic leukaemia. Nature reviews Cancer. 2016;16(8):494-507.
4. Bongiovanni D, Saccomani V, Piovan E. Aberrant Signaling Pathways in T-Cell Acute Lymphoblastic Leukemia. Int J Mol Sci. 2017;18(9).
5. Weng AP, Ferrando AA, Lee W, et al. Activating mutations of NOTCH1 in human T cell acute lymphoblastic leukemia. Science. 2004;306(5694):269-271.
6. Ferrando AA. The role of NOTCH1 signaling in T-ALL. Hematology Am Soc Hematol Educ Program. 2009;353-361.
7. Palomero T, Lim WK, Odom DT, et al. NOTCH1 directly regulates c-MYC and activates a feed-forward-loop transcriptional network promoting leukemic cell growth. Proc Natl Acad Sci U S A. 2006;103(48):18261-18266.
8. Weng AP, Millholland JM, Yashiro-Ohtani Y, et al. c-Myc is an important direct target of Notch1 in T-cell acute lymphoblastic leukemia/lymphoma. Genes Dev. 2006;20(15):2096-2109.
9. Vermezovic J, Adamowicz M, Santarpia L, et al. Notch is a direct negative regulator of the DNA-damage response. Nat Struct Mol Biol. 2015;22(5):417-424.
10. Di Veroli GY, Fornari C, Wang D, et al. Combenefit: an interactive platform for the analysis and visualization of drug combinations. Bioinformatics. 2016;32(18):2866-2868.
11. Li X, Gounari F, Protopopov A, Khazaie K, von Boehmer H. Oncogenesis of T-ALL and nonmalignant consequences of overexpressing intracellular NOTCH1. J Exp Med 2008;205(12):2851-2861.
12. Sanda T, Li X, Gutierrez A, et al. Interconnecting molecular pathways in the pathogenesis and drug sensitivity of T-cell acute lymphoblastic leukemia. Blood. 2010;115(9):1735-1745.
13. Ng OH, Erbilgin Y, Firtina S, et al. Deregulated WNT signaling in childhood T-cell acute lymphoblastic leukemia. Blood Cancer J. 2014;4(3):e192.
14. Van Vlierberghe P, Ambesi-Impiombato A, Perez-Garcia A, et al. ETV6 mutations in early immature human T cell leukemias. J Exp Med. 2011;208(13):2571-2579.
15. Thandapani P, Kloetgen A, Witkowski MT, et al. Valine tRNA levels and availability regulate complex I assembly in leukaemia. Nature. 2022;601(7893):428-433.
16. Liu Y, Easton J, Shao Y, et al. The genomic landscape of pediatric and young adult T-lineage acute lymphoblastic leukemia. Nat Genet. 2017;49(8):1211-1218.
17. Gutierrez A, Sanda T, Grebliunaite R, et al. High frequency of PTEN, PI3K, and AKT abnormalities in T-cell acute lymphoblastic leukemia. Blood. 2009;114(3):647-650.
18. Chen B, Jiang L, Zhong ML, et al. Identification of fusion genes and characterization of transcriptome features in T-cell acute lymphoblastic leukemia. Proc Natl Acad Sci U S A. 2018;115(2):373-378.
19. Agnusdei V, Minuzzo S, Frasson C, et al. Therapeutic antibody targeting of Notch1 in T-acute lymphoblastic leukemia xenografts. Leukemia. 2014;28(2):278-288.
20. Bordin F, Piovan E, Masiero E, et al. WT1 loss attenuates the TP53-induced DNA damage response in T-cell acute lymphoblastic leukemia. Haematologica. 2018;103(2):266-277.
21. Saccomani V, Grassi A, Piovan E, et al. miR-22-3p Negatively Affects Tumor Progression in T-Cell Acute Lymphoblastic Leukemia. Cells. 2020;9(7):1726.
22. Ngondo-Mbongo RP, Myslinski E, Aster JC, Carbon P. Modulation of gene expression via overlapping binding sites exerted by ZNF143, Notch1 and THAP11. Nucleic Acids Res. 2013;41(7):4000-4014.
23. Lehal R, Zaric J, Vigolo M, et al. Pharmacological disruption of the Notch transcription factor complex. Proc Natl Acad Sci U S A. 2020;117(28):16292-16301.
24. Winter GE, Mayer A, Buckley DL, et al. BET Bromodomain Proteins Function as Master Transcription Elongation Factors Independent of CDK9 Recruitment. Mol Cell. 2017;67(1):5-18.

25. Lodi F, Certo M, Elkafrawy H, et al. BCAT1 inhibition affects CD8+ T cell activation, exhaustion, and tumoral immunity by altering iron homeostasis. bioRxiv. 2023 Feb 26. doi: 10.1101/2023.02.25.530034 [preprint not peer-reviewed]
26. Ko JH, Olona A, Papathanassiu AE, et al. BCAT1 affects mitochondrial metabolism independently of leucine transamination in activated human macrophages. J Cell Sci. 2020;133(22):jcs247957.
27. Shimazu T, Hirschey MD, Newman J, et al. Suppression of oxidative stress by beta-hydroxybutyrate, an endogenous histone deacetylase inhibitor. Science. 2013;339(6116):211-214.
28. Francois L, Boskovic P, Knerr J, et al. BCAT1 redox function maintains mitotic fidelity. Cell Rep. 2022;41(3):111524.
29. Fabbri G, Rasi S, Rossi D, et al. Analysis of the chronic lymphocytic leukemia coding genome: role of NOTCH1 mutational activation. J Exp Med. 2011;208(7):1389-1401.
30. Fabbri G, Holmes AB, Viganotti M, et al. Common nonmutational NOTCH1 activation in chronic lymphocytic leukemia. Proc Natl Acad Sci U S A. 2017;114(14):E2911-E2919.
31. Herold T, Jurinovic V, Metzeler KH, et al. An eight-gene expression signature for the prediction of survival and time to treatment in chronic lymphocytic leukemia. Leukemia. 2011;25(10):1639-1645.
32. Ananieva EA, Powell JD, Hutson SM. Leucine Metabolism in T Cell Activation: mTOR Signaling and Beyond. Adv Nutr. 2016;7(4):798S-805S.
33. Hillier J, Allcott GJ, Guest LA, et al. The BCAT1 CXXC Motif Provides Protection against ROS in Acute Myeloid Leukaemia Cells. Antioxidants (Basel). 2022;11(4):683.
34. Harris M, El Hindy M, Usmari-Moraes M, et al. BCAT-induced autophagy regulates Abeta load through an interdependence of redox state and PKC phosphorylation-implications in Alzheimer's disease. Free Radic Biol Med. 2020;152:755-766.
35. Rodrigues LM, Uribe-Lewis S, Madhu B, Honess DJ, Stubbs M, Griffiths JR. The action of beta-hydroxybutyrate on the growth, metabolism and global histone H3 acetylation of spontaneous mouse mammary tumours: evidence of a beta-hydroxybutyrate paradox. Cancer Metab. 2017;5:4.
36. Rojas-Morales P, Pedraza-Chaverri J, Tapia E. Ketone bodies, stress response, and redox homeostasis. Redox Biol. 2020;29:101395.
37. Ananieva EA, Wilkinson AC. Branched-chain amino acid metabolism in cancer. Curr Opin Clin Nutr Metab Care. 2018;21(1):64-70.
38. Luo L, Sun W, Zhu W, et al. BCAT1 decreases the sensitivity of cancer cells to cisplatin by regulating mTOR-mediated autophagy via branched-chain amino acid metabolism. Cell Death Dis. 2021;12(2):169.
39. Chen CS, Wang YC, Yang HC, et al. Histone deacetylase inhibitors sensitize prostate cancer cells to agents that produce DNA double-strand breaks by targeting Ku70 acetylation. Cancer Res. 2007;67(11):5318-5327.
40. Hada M, Kwok RP. Regulation of ku70-bax complex in cells. J Cell Death. 2014;7:11-13.

Figure legends

Figure 1. BCAT1 is upregulated during NOTCH1-dependent transformation. (A) Heat map showing the top 50 most down-regulated and up-regulated genes between normal double positive (DP) cells and *ICN1*-induced DP leukemic cells (NIC Tumors). (B) Expression levels (qRT-PCR; left) of *Bcat1* in thymocytes obtained from 6-8 weeks old C57/Bl6 mice and leukemic cells from six *ΔE-NOTCH1* T-ALL tumors (NOTCH1-T). Significance was calculated using an unpaired two-tailed t-test. ***P*< 0.01. Western blot (right) showing protein expression levels of ICN1 and Bcat1. β-actin and tubulin are shown as loading controls. Graphical representation of Bcat1/β-actin ratios (extreme right). Bars represent mean values. ICN1: intracellular NOTCH1. (C) Box plot showing the expression of BCAT1 mRNA in T-ALL patients (N=57) and thymocyte subsets (7 thymocyte and mature T-cell subsets derived from (N=3) independent donors; quantile-normalized microarray results downloaded from GSE33469 and GSE33470. $CD3^+$ and $CD3^-$ DP cells were grouped together. $CD1^+$ and $CD1^-$ $CD34^+$ cells were grouped together. Boxes represent first and third quartiles and line represents the median. Statistical analysis between groups was performed using unpaired two-sided t-test. (D) BCAT1 transcript (top) and protein levels (bottom) in total human thymus, *NOTCH1* wild-type and *NOTCH1* activated/mutated patient derived T-ALL xenografts (PDX). Significance was calculated using a nonparametric t-test (Mann-Whitney). ***P*< 0.01. ICN1, MYC and PTEN protein levels are also shown. β-actin is shown as loading control. (E) PDX samples were treated in vivo with DBZ (10 μg/kg every 8 hours for a total of 3 injections) or vehicle (DMSO) for 24h before analysis of BCAT1 transcript levels. For statistical analysis, an unpaired t-test was used. ***P*< 0.01, ****P*< 0.001. (F) NOTCH1 ChIP-seq binding (left) in the BCAT1 locus in HPB T-ALL cells. Inset shows the location of ChIP-qPCR amplicons near NOTCH-1 peak region (P1-P2) and in a negative control region (NL). Chromatin from PF382 cells was subjected to ChIP using a NOTCH1 antibody (right). The indicated regions (P1, P2 and NL) were PCR amplified from the precipitated and input DNA. Fold enrichment was calculated as a ratio of amplification efficiency of ChIP sample over that of the IgG control. Shown are means ± SD (N ≥ 3). For statistical analysis, an unpaired t-test was used. ****P*< 0.001.

Figure 2. Functional effects of BCAT1 depletion. (A) Kaplan-Meier survival curves of overall survival in lethally irradiated C57BL/6J hosts transplanted with BM cells (WT or KO for *Bcat1*) transduced with *ΔE-NOTCH1* allele. Data from two independent transplantation experiments were pooled together. Log-rank Mantel-Cox test was performed to calculate *P* value. ****P*< 0.001. Shaded area represents 95% CI. (B) Representative plots (left) and bar graph representation (S-phase fraction; right) of ex vivo EdU incorporation in *ΔE-NOTCH1* leukemias WT and null for *Bcat1*. Data for bar graph is shown as mean ± SD. Significance was calculated using an unpaired two-tailed t-test. ****P*< 0.001. (C) Representative plots (left) and bar graph representation (S-phase fraction; right) of MOLT4 cells transduced with shCTRL, shBCAT1 #1 or shBCAT1 #2 seven days post-puromycin selection and assessed for EdU incorporation by fluorescence-activated cell sorting (FACS) analysis. Data for bar graph is shown as mean ± SD. Significance was calculated using an unpaired two-tailed t-test. ****P*< 0.001. (D) T-ALL cells were transduced with control vector (shCTRL) or vector containing shRNA sequences against BCAT1 (shBCAT1 #1, shBCAT1 #2). Expression of BCAT1 and tubulin was analyzed by immunoblotting seven days post transduction (left panels) in DND41 and MOLT4. Starting from seven days post-puromycin selection, cell proliferation was evaluated by determining cell number (DND41) or ATP levels by bioluminescence (MOLT4). Significance was calculated using an unpaired two-tailed t-test. **P*< 0.05, ***P*< 0.01. (E) Representative images of bioluminescence (top) and quantitative analysis of tumor burden (bottom) in NSG mice xenografted with CCRF-CEM cells expressing luciferase and transduced with shCTRL or shBCAT1 (#1 and #2). Analysis after 15 days post-transplant is shown. Significance was calculated using an unpaired two-tailed t-test. ***P*< 0.01. (F) Representative images of bioluminescence (top) and quantitative analysis of tumor burden (bottom) in NSG mice xenografted with MOLT4 cells expressing luciferase and transduced with shCTRL or shBCAT1 (#1 and #2). Analysis after 15 days post-transplant is shown. Significance was calculated using an unpaired two-tailed t-test. **P*< 0.05, ***P*< 0.01.

Figure 3. Canonical functions of Bcat1. (A) Heat map representation of the top down-and up-regulated genes between *ΔE-NOTCH1* tumors *WT* or *KO* for *Bcat1*. Two independent *WT* and *KO* tumors were analyzed. Bcat1 gene is highlighted in red. (B) Gene set enrichment analysis (GSEA) identified three significantly enriched gene sets involved in cell cycle regulation downregulated in *Bcat1 KO* T-ALL cells. The normalized enrichment score (NES) and the nominal *P* value are illustrated. (C) Gene set enrichment analysis (GSEA) identified three significantly enriched gene sets involved in DNA damage response upregulated in *Bcat1 KO* T-ALL cells. The normalized enrichment score (NES) and the nominal *P* value are illustrated. (D) Immunoblots of γH2AX, p21 and Bcat1 in tumors *WT* or *KO* for *Bcat1* (top). α-Tubulin is shown as loading control. T-ALL cells (CCRF-CEM, DND41, MOLT4) transduced with shCTRL/CAS9 or shBCAT1 (#1 and #2)/sgBCAT1 were analyzed by immunoblotting for γH2AX and BCAT1 (bottom). β-actin is shown as loading control. (E) Heatmap representation (left) of the top 50 differentially expressed metabolites identified by capillary electrophoresis time-of-flight mass spectrometry (CE-TOFMS) between *ΔE-NOTCH1* leukemias wild-type and KO for *Bcat1*. Metabolites that are significantly and consistently differentially expressed in multiple comparisons are highlighted in red. Volcano plot (right) showing differentially expressed metabolites (≥1.5 fold change, $P<0.05$; in red and blue) identified by capillary electrophoresis time-of-flight mass spectrometry (CE-TOFMS) between *ΔE-NOTCH1* leukemias wild-type and KO for *Bcat1*. Metabolites that are significantly and consistently differentially expressed in multiple comparisons are encircled.

Figure 4. ERG245, a BCAT1 specific inhibitor mimics the functional consequences of Bcat1 depletion. (A) Representative plots of apoptosis in *ΔE-NOTCH1* leukemia wild-type for *Bcat1* (WT#6) treated in vitro for 48h with PBS (vehicle) or increasing doses of ERG245 (200 μM- 1 mM). (B) Representative plots of *ΔE NOTCH1* leukemia wild-type for Bcat1 (WT#6) treated in vitro for 48h with PBS (vehicle) or increasing doses of ERG245 (200 μM-500 μM). Cells were then assessed for EdU incorporation by fluorescence-activated cell sorting (FACS) analysis. (C) Representative cell viability analysis in *ΔE-NOTCH1* tumors WT (WT#3) or KO (KO#3, #1) for *Bcat1*. Murine T-ALL cells were treated *in vitro* for 48h with PBS (vehicle) or increasing doses of ERG245 (100 μM- 1 mM). Data is shown as mean ± SD. (D) Representative plots of T-ALL cell lines (CCRF-CEM, DND41) treated in vitro for 72h with PBS (vehicle) or ERG245 (300 μM). Cells were then assessed for EdU incorporation by fluorescence-activated cell sorting (FACS) analysis. (E) Representative plots of PDX#27 treated in vitro for 72h with PBS (vehicle) or increasing doses of ERG245 (300 μM- 1 mM). Cells were then assessed for EdU incorporation by fluorescence-activated cell sorting (FACS) analysis.

Figure 5. BCAT1 loss induces a dysfunctional DNA damage response following etoposide treatment. (A) Representative cell viability analysis (left) in *ΔE-NOTCH1* tumors *WT* (WT#1) or *KO* (KO#6) for *Bcat1*. Murine T-ALL cells were treated *in vitro* for 48h with DMSO (vehicle) or increasing concentrations of etoposide (25-100 nM). Data is shown as mean ± SD. Significance was calculated using an unpaired two-tailed t-test. *$P< 0.05$, **$P< 0.01$. Quantification of apoptosis (right) in *ΔE-NOTCH1* tumors *WT* (WT#1) or *KO* (KO#6) for *Bcat1* treated in vitro for 48h with DMSO (vehicle) or increasing concentrations of etoposide (25-100 nM). Data is shown as mean ± SD. Significance was calculated using an unpaired two-tailed t-test. *$P< 0.05$, **$P< 0.01$. (B) Representative plots of apoptosis (top) in CCRF-CEM T-ALL cells transduced with shCTRL or shBCAT1 (#1 and #2) and treated in vitro for 48h with DMSO (vehicle) or etoposide (100 nM or 1 μM). Quantification of apoptosis (bottom) in CCRF-CEM T-ALL cells transduced with shCTRL or shBCAT1 (#1 and #2) and treated in vitro for 48h with DMSO (vehicle) or etoposide (100 nM– 2 μM). Significance was calculated using an unpaired two-tailed t-test. ** $P< 0.01$, *** $P< 0.001$. (C) Expression of cleaved PARP-1 and phosphorylated γH2AX was analyzed by immunoblotting in CCRF-CEM T-ALL cells transduced with shCTRL or shBCAT1 (#1 and #2) and treated in vitro for 48h with DMSO (vehicle) or etoposide (1 μM). β-actin and GADPH are shown as loading controls. (D) Representative neutral comet images (left) performed in CCRF-CEM cells infected with a control shRNA (shCTRL) or BCAT1-targeting

shRNAs (shBCAT1#1, shBCAT1#2) either untreated or after etoposide treatment (1µM) for 2 or 6 hours. Dot plot (right) showing individual percentages of comet tail DNA. The median value of 50-80 nuclei per experimental condition is indicated. Statistical analysis was conducted by using the Mann-Whitney test. Data are representative of 2 independent experiments.

Figure 6. BCAT1 specific inhibition increases response to DNA-damaging agents, especially etoposide, in vitro and in vivo. (A) Representative plots of apoptosis in MOLT4 T-ALL cells treated with vehicle (DMSO), BCAT1 inhibitor (ERG245), etoposide (Etop; 50-75 nM) or the combination (ERG245 + Etop) for 48h. (B) Representative plots of annexin V staining (left panels) in DND41 T-ALL cells treated with vehicle (DMSO), BCAT1 inhibitor (ERG245), etoposide (Etop) or the combination (ERG245 + Etop) for 48h. Western blot analysis (right panels) of PARP-1 (total or cleaved PARP-1), and phosphorylated γH2AX in DND41 cells treated for 48h with DMSO (vehicle), ERG245 (200 µM), etoposide (Etop; 500 nM) or ERG245 + Etop. GADPH was used as protein loading control. (C) Representative plots (left) and bar graph representation (right) of apoptosis (Annexin V positive) in ex vivo obtained PDX#39 cells treated with vehicle (DMSO), BCAT1 inhibitor (ERG245), etoposide (Etop; 50-250 nM) or the combination (ERG245 + Etop) for 48h. Significance was calculated using an unpaired two-tailed t-test. ** $P<0.01$, *** $P<0.001$. (D) Representative images of bioluminescence (left) in NSG mice xenografted with PDX#27 cells expressing luciferase (PDX#27-luc) and treated with vehicle (DMSO), BCAT1 inhibitor (ERG245; 30 mg/kg three times a week), etoposide (Etop; 15 mg/kg twice a week) or the combination (ERG245 + Etop). Analysis before (day 13 post-transplantation) and 15 days after start of treatment (day 28 post-transplantation) is shown. Quantitative analysis of tumor load (right) via in vivo bioluminescence imaging of NSG mice xenografted with PDX#27-luc after treatment (day 28 post-transplantation) with vehicle (DMSO), BCAT1 inhibitor (ERG245), etoposide (Etop) or the combination (ERG245 + Etop). Significance was calculated using an unpaired two-tailed t-test. ** $P<0.01$, *** $P<0.001$. n.s.=not significant.

Figure 7. Schematic illustration of the proposed role of BCAT1 in regulating T-ALL response to DNA damaging agents in BCAT1 high and BCAT1 silenced/functionally inhibited T-ALL cells. BCAT1 inhibition induces a partial break in the TCA cycle between citrate and succinate leading to citrate accumulation and directing leucine metabolism towards 3-HB synthesis. 3-HB is known to act as an energy source in the absence of sufficient glucose and as it builds-up it inhibits class I histone deacetylases (HDACs), leading to increased acetylation of proteins such as histones and DNA damage response proteins (including KU70 and KU80) modifying their activity[39, 40] and possibly priming cells to the deleterious effects of DNA damaging agents. Following the exposure to DNA damaging agents (etoposide) this leads to accentuated DNA damage leading to cell death.

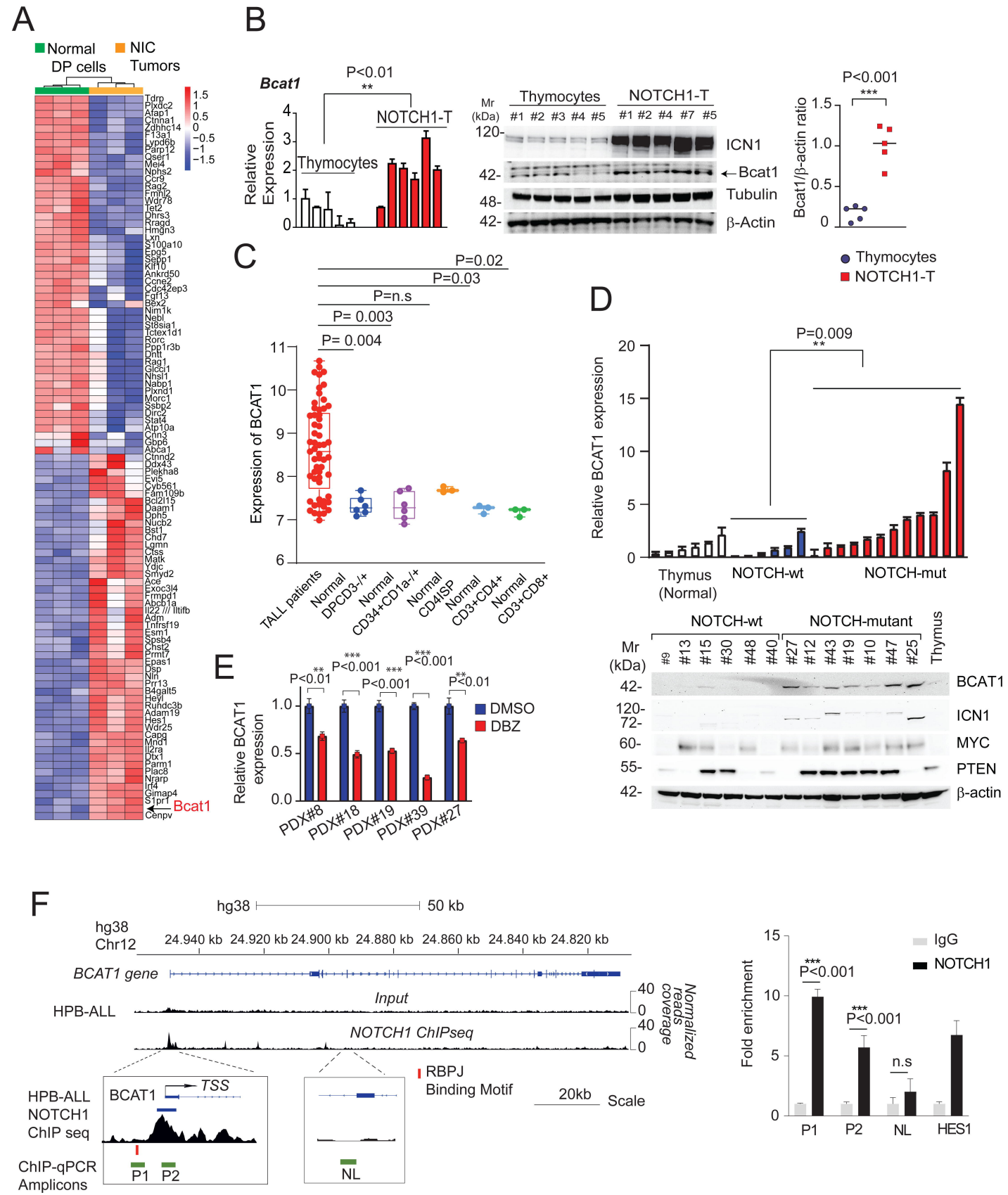
A
Normal
NIC
DP cells
Tumors
Bcat1
B
Bcat1
P<0.01
**
NOTCH1-T
Thymocytes
Relative Expression
Mr (kDa)
#1 #2 #3 #4 #5
#1 #2 #4 #7 #5
120-
42-
48-
42-
ICN1
←Bcat1
Tubulin
β-Actin
P<0.001
***
Bcat1/β-actin ratio
C
P=0.02
P=0.03
P=n.s
P= 0.003
P= 0.004
Thymocytes
NOTCH1-T
Expression of BCAT1
TALL patients
Normal
DPCD3-/+
Normal
CD34+CD1a-/+
Normal
CD4ISP
Normal
CD3+CD4+
Normal
CD3+CD8+
D
P=0.009
**
Relative BCAT1 expression
Thymus (Normal)
NOTCH-wt
NOTCH-mut
NOTCH-wt
NOTCH-mutant
Thymus
Mr (kDa)
#9 #13 #15 #30 #48 #40 #27 #12 #43 #19 #10 #47 #25
42-
120-
72-
60-
55-
42-
BCAT1
ICN1
MYC
PTEN
β-actin
E
P<0.01
**
P<0.001
***
P<0.001
***
P<0.001
***
P<0.01
**
Relative BCAT1 expression
DMSO
DBZ
PDX#8
PDX#18
PDX#19
PDX#39
PDX#27
F
hg38
50 kb
hg38
Chr12
24.940 kb 24.920 kb 24.900 kb 24.880 kb 24.860 kb 24.840 kb 24.820 kb
BCAT1 gene
HPB-ALL
Input
NOTCH1 ChIPseq
Normalized reads coverage
HPB-ALL
NOTCH1
ChIP seq
BCAT1
TSS
ChIP-qPCR
Amplicons
P1
P2
NL
RBPJ
Binding Motif
20kb
Scale
IgG
NOTCH1
Fold enrichment
***
P<0.001
***
P<0.001
n.s
P1
P2
NL
HES1

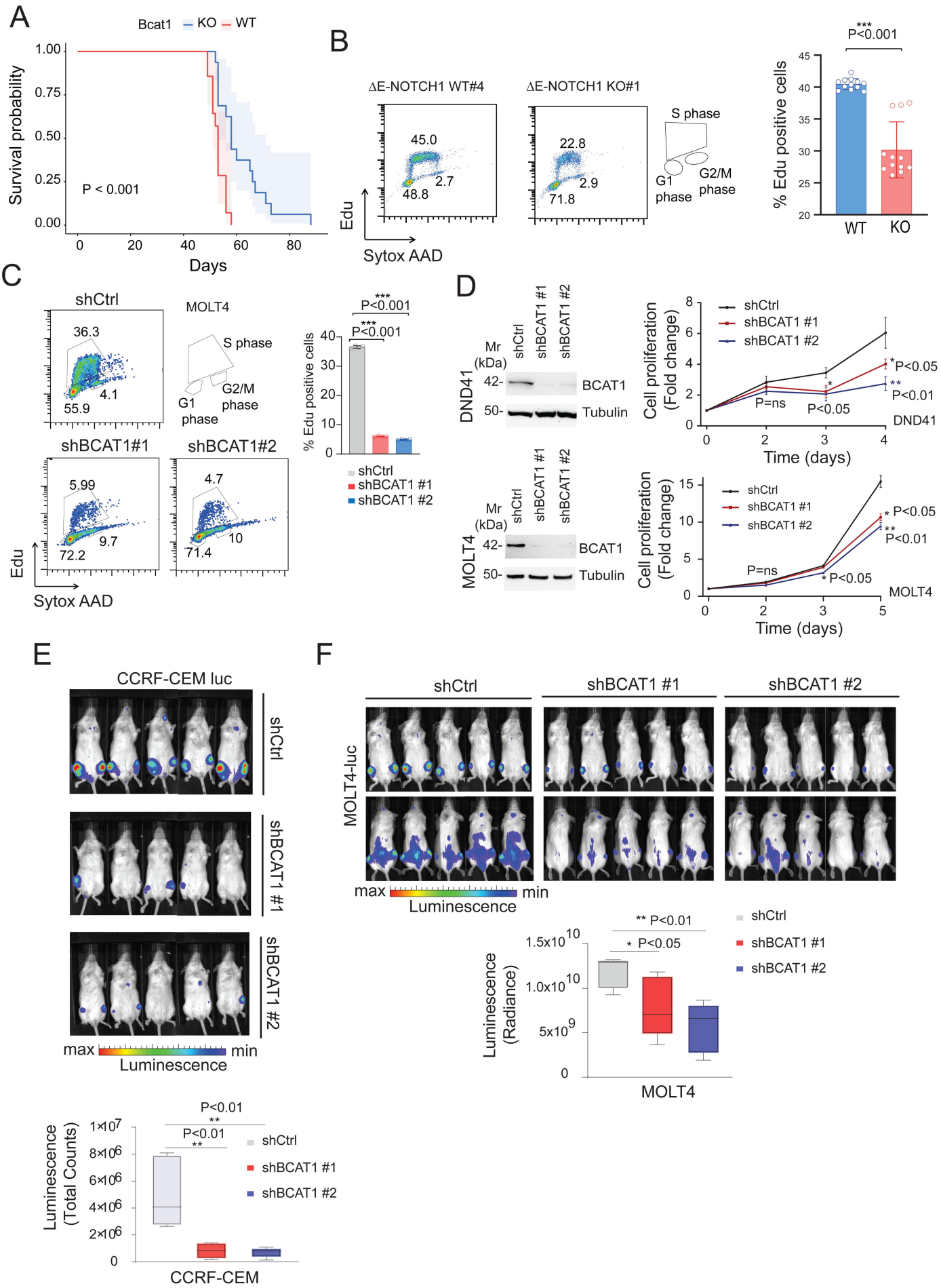
A
Bcat1 KO WT
Survival probability
1.00
0.75
0.50
0.25
0.00
P < 0.001
0
20
40
60
80
Days
B
ΔE-NOTCH1 WT#4
ΔE-NOTCH1 KO#1
45.0
2.7
48.8
22.8
2.9
71.8
Edu
Sytox AAD
S phase
G1 phase
G2/M phase
***
P<0.001
% Edu positive cells
45
40
35
30
25
20
WT
KO
C
shCtrl
MOLT4
36.3
4.1
55.9
S phase
G1 phase
G2/M phase
shBCAT1#1
shBCAT1#2
5.99
9.7
72.2
4.7
10
71.4
Edu
Sytox AAD
***
P<0.001
***
P<0.001
% Edu positive cells
40
30
20
10
0
shCtrl
shBCAT1 #1
shBCAT1 #2
D
DND41
Mr (kDa)
shCtrl
shBCAT1 #1
shBCAT1 #2
42-
BCAT1
50-
Tubulin
MOLT4
Mr (kDa)
shCtrl
shBCAT1 #1
shBCAT1 #2
42-
BCAT1
50-
Tubulin
Cell proliferation (Fold change)
shCtrl
shBCAT1 #1
shBCAT1 #2
P=ns
P<0.05
*P<0.05
**P<0.01
DND41
Time (days)
Cell proliferation (Fold change)
shCtrl
shBCAT1 #1
shBCAT1 #2
P=ns
*P<0.05
*P<0.05
**P<0.01
MOLT4
Time (days)
E
CCRF-CEM luc
shCtrl
shBCAT1 #1
shBCAT1 #2
max
min
Luminescence
P<0.01
**
P<0.01
**
Luminescence (Total Counts)
1×10^7
8×10^6
6×10^6
4×10^6
2×10^6
0
shCtrl
shBCAT1 #1
shBCAT1 #2
CCRF-CEM
F
shCtrl
shBCAT1 #1
shBCAT1 #2
MOLT4-luc
max
min
Luminescence
** P<0.01
* P<0.05
Luminescence (Radiance)
1.5x10^10
1.0x10^10
5x10^9
0
shCtrl
shBCAT1 #1
shBCAT1 #2
MOLT4

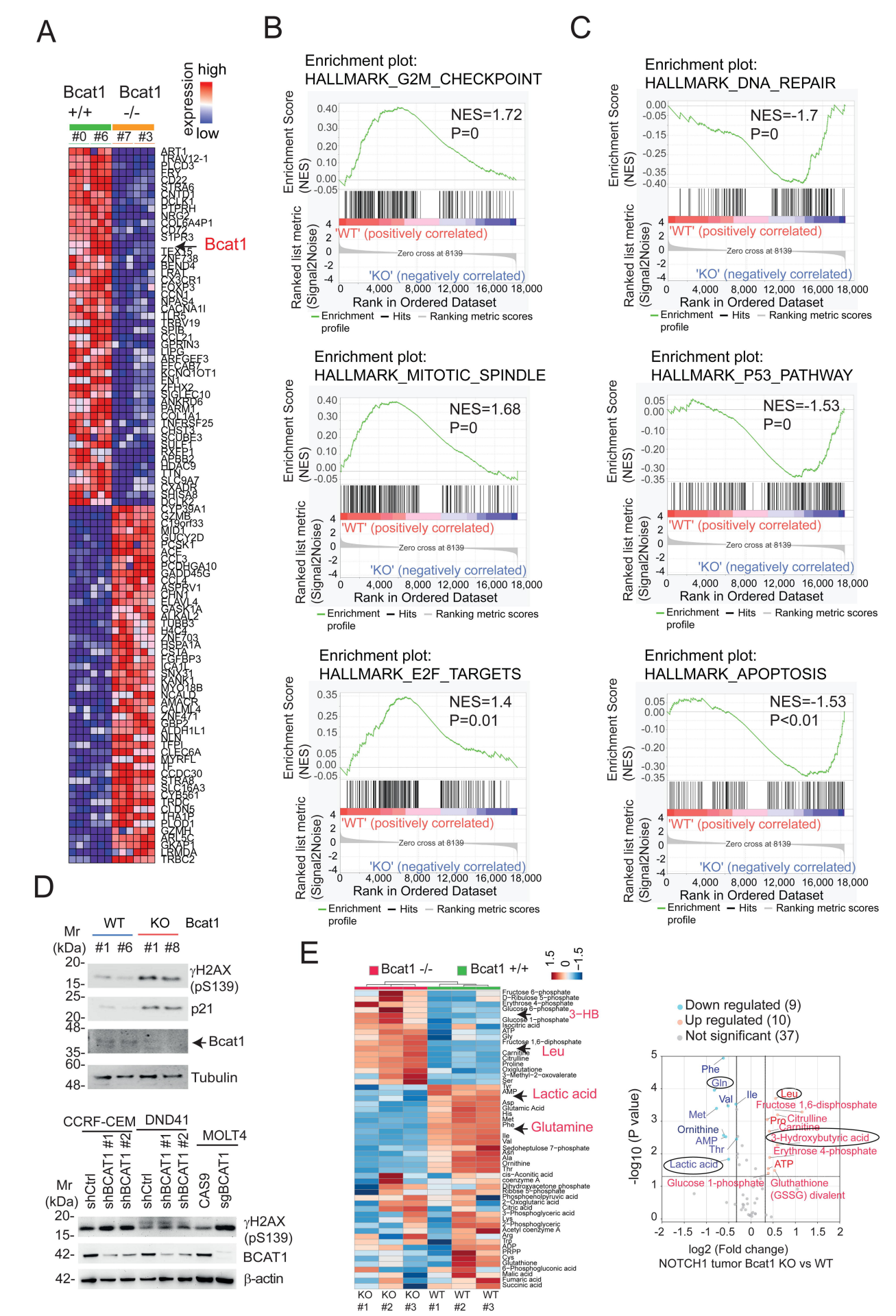
A
Bcat1 +/+
Bcat1 -/-
#0 #6 #7 #3
expression
high
low
Bcat1
B
Enrichment plot:
HALLMARK_G2M_CHECKPOINT
NES=1.72
P=0
Enrichment Score (NES)
Ranked list metric (Signal2Noise)
'WT' (positively correlated)
Zero cross at 8139
'KO' (negatively correlated)
Rank in Ordered Dataset
Enrichment profile
Hits
Ranking metric scores
Enrichment plot:
HALLMARK_MITOTIC_SPINDLE
NES=1.68
P=0
Enrichment plot:
HALLMARK_E2F_TARGETS
NES=1.4
P=0.01
C
Enrichment plot:
HALLMARK_DNA_REPAIR
NES=-1.7
P=0
Enrichment plot:
HALLMARK_P53_PATHWAY
NES=-1.53
P=0
Enrichment plot:
HALLMARK_APOPTOSIS
NES=-1.53
P<0.01
D
Mr (kDa)
WT
KO
Bcat1
#1 #6 #1 #8
γH2AX (pS139)
p21
Bcat1
Tubulin
CCRF-CEM
DND41
MOLT4
shCtrl
shBCAT1 #1
shBCAT1 #2
CAS9
sgBCAT1
γH2AX (pS139)
BCAT1
β-actin
E
Bcat1 -/-
Bcat1 +/+
3-HB
Leu
Lactic acid
Glutamine
KO #1
KO #2
KO #3
WT #1
WT #2
WT #3
Down regulated (9)
Up regulated (10)
Not significant (37)
-log10 (P value)
log2 (Fold change)
NOTCH1 tumor Bcat1 KO vs WT
Phe
Gln
Val
Ile
Leu
Met
Fructose 1,6-disphosphate
Pro
Citrulline
Carnitine
Ornithine
AMP
3-Hydroxybutyric acid
Thr
Erythrose 4-phosphate
Lactic acid
ATP
Glucose 1-phosphate
Gluthathione (GSSG) divalent

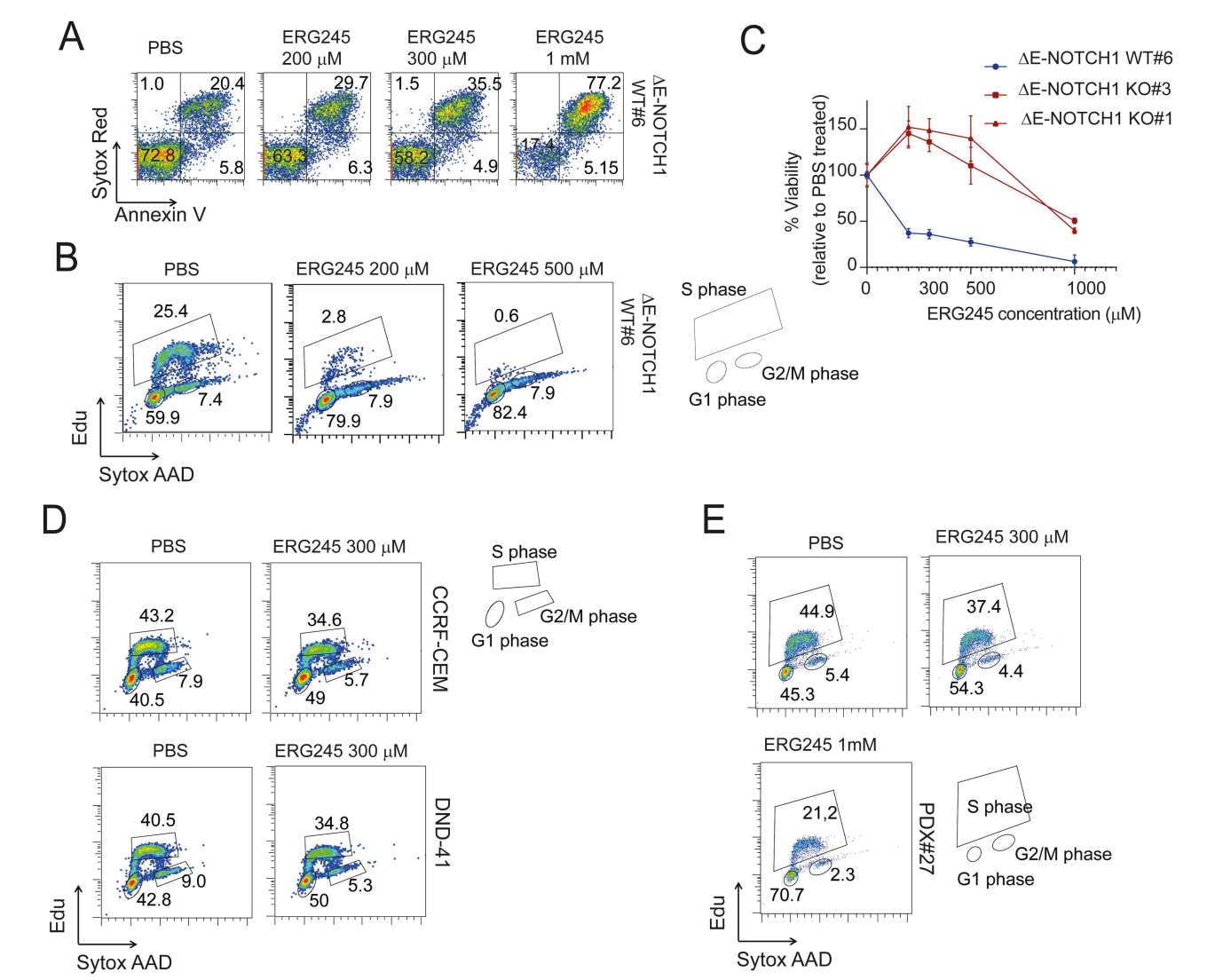
A
PBS
ERG245 200 μM
ERG245 300 μM
ERG245 1 mM
1.0
20.4
72.8
5.8
29.7
63.3
6.3
1.5
35.5
58.2
4.9
77.2
17.4
5.15
ΔE-NOTCH1 WT#6
Sytox Red
Annexin V
B
PBS
ERG245 200 μM
ERG245 500 μM
25.4
7.4
59.9
2.8
7.9
79.9
0.6
7.9
82.4
ΔE-NOTCH1 WT#6
Edu
Sytox AAD
S phase
G2/M phase
G1 phase
C
ΔE-NOTCH1 WT#6
ΔE-NOTCH1 KO#3
ΔE-NOTCH1 KO#1
% Viability (relative to PBS treated)
0
50
100
150
0
300
500
1000
ERG245 concentration (μM)
D
PBS
ERG245 300 μM
43.2
7.9
40.5
34.6
5.7
49
CCRF-CEM
S phase
G2/M phase
G1 phase
PBS
ERG245 300 μM
40.5
9.0
42.8
34.8
5.3
50
DND-41
Edu
Sytox AAD
E
PBS
ERG245 300 μM
44.9
5.4
45.3
37.4
4.4
54.3
ERG245 1mM
21,2
2.3
70.7
PDX#27
S phase
G2/M phase
G1 phase
Edu
Sytox AAD

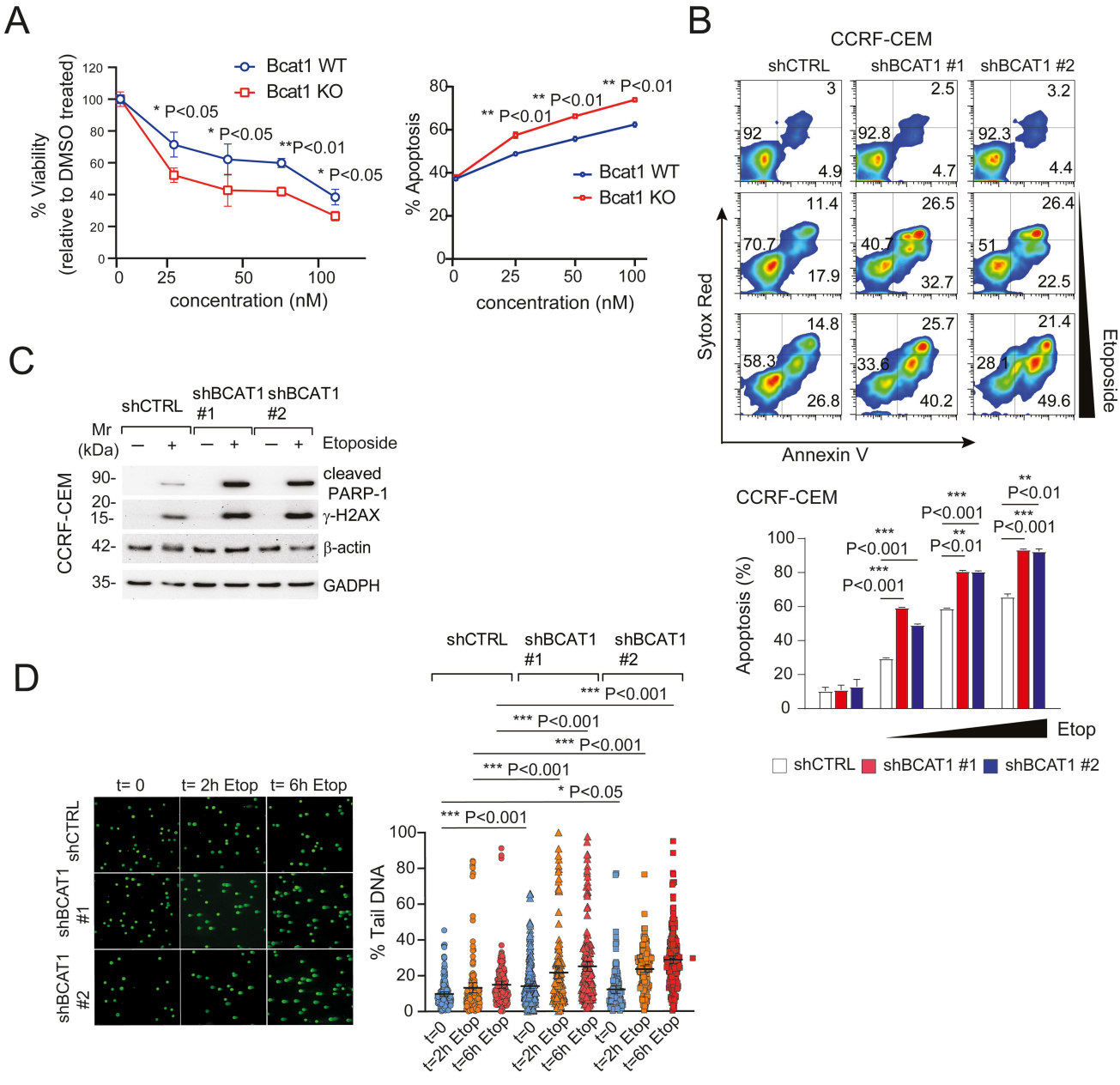
A
Bcat1 WT
Bcat1 KO
% Viability
(relative to DMSO treated)
concentration (nM)
* P<0.05
* P<0.05
**P<0.01
* P<0.05
% Apoptosis
** P<0.01
** P<0.01
** P<0.01
Bcat1 WT
Bcat1 KO
concentration (nM)
B
CCRF-CEM
shCTRL
shBCAT1 #1
shBCAT1 #2
Sytox Red
Annexin V
Etoposide
C
shCTRL
shBCAT1 #1
shBCAT1 #2
Mr (kDa)
Etoposide
CCRF-CEM
cleaved PARP-1
γ-H2AX
β-actin
GADPH
CCRF-CEM
Apoptosis (%)
*** P<0.001
** P<0.01
Etop
shCTRL
shBCAT1 #1
shBCAT1 #2
D
t= 0
t= 2h Etop
t= 6h Etop
shCTRL
shBCAT1 #1
shBCAT1 #2
% Tail DNA
*** P<0.001
*** P<0.001
*** P<0.001
*** P<0.001
* P<0.05
*** P<0.001
t=0
t=2h Etop
t=6h Etop

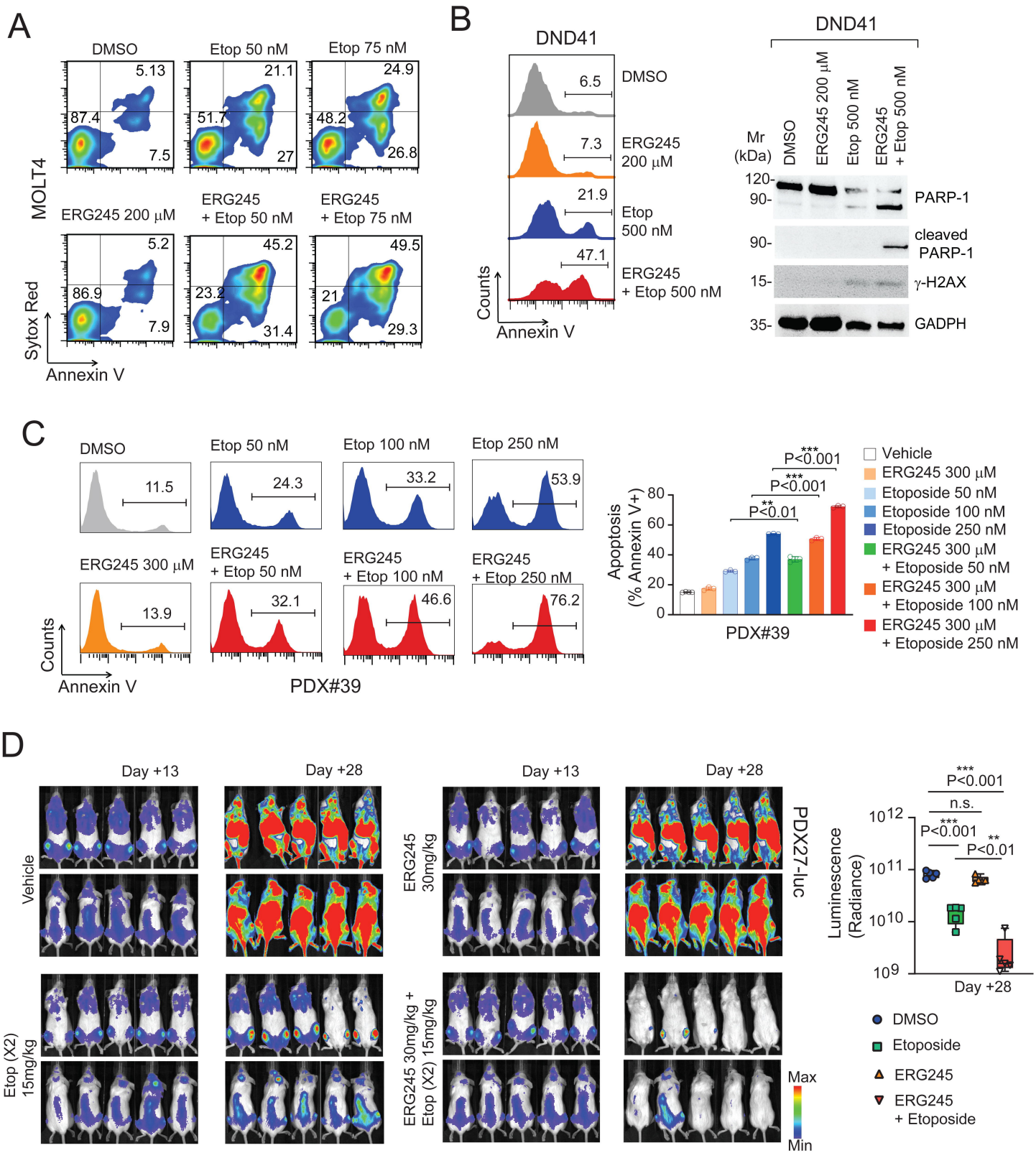
A
DMSO
Etop 50 nM
Etop 75 nM
5.13
87.4
7.5
21.1
51.7
27
24.9
48.2
26.8
MOLT4
ERG245 200 μM
ERG245 + Etop 50 nM
ERG245 + Etop 75 nM
5.2
86.9
7.9
45.2
23.2
31.4
49.5
21
29.3
Sytox Red
Annexin V
B
DND41
6.5
DMSO
7.3
ERG245 200 μM
21.9
Etop 500 nM
47.1
ERG245 + Etop 500 nM
Counts
Annexin V
DND41
Mr (kDa)
DMSO
ERG245 200 μM
Etop 500 nM
ERG245 + Etop 500 nM
120-
90-
PARP-1
90-
cleaved PARP-1
15-
γ-H2AX
35-
GADPH
C
DMSO
11.5
Etop 50 nM
24.3
Etop 100 nM
33.2
Etop 250 nM
53.9
ERG245 300 μM
13.9
ERG245 + Etop 50 nM
32.1
ERG245 + Etop 100 nM
46.6
ERG245 + Etop 250 nM
76.2
Counts
Annexin V
PDX#39
Apoptosis (% Annexin V+)
P<0.001
P<0.001
P<0.01
PDX#39
Vehicle
ERG245 300 μM
Etoposide 50 nM
Etoposide 100 nM
Etoposide 250 nM
ERG245 300 μM + Etoposide 50 nM
ERG245 300 μM + Etoposide 100 nM
ERG245 300 μM + Etoposide 250 nM
D
Day +13
Day +28
Vehicle
ERG245 30mg/kg
PDX27-luc
Etop (X2) 15mg/kg
ERG245 30mg/kg + Etop (X2) 15mg/kg
Max
Min
Luminescence (Radiance)
P<0.001
n.s.
P<0.001
P<0.01
Day +28
DMSO
Etoposide
ERG245
ERG245 + Etoposide

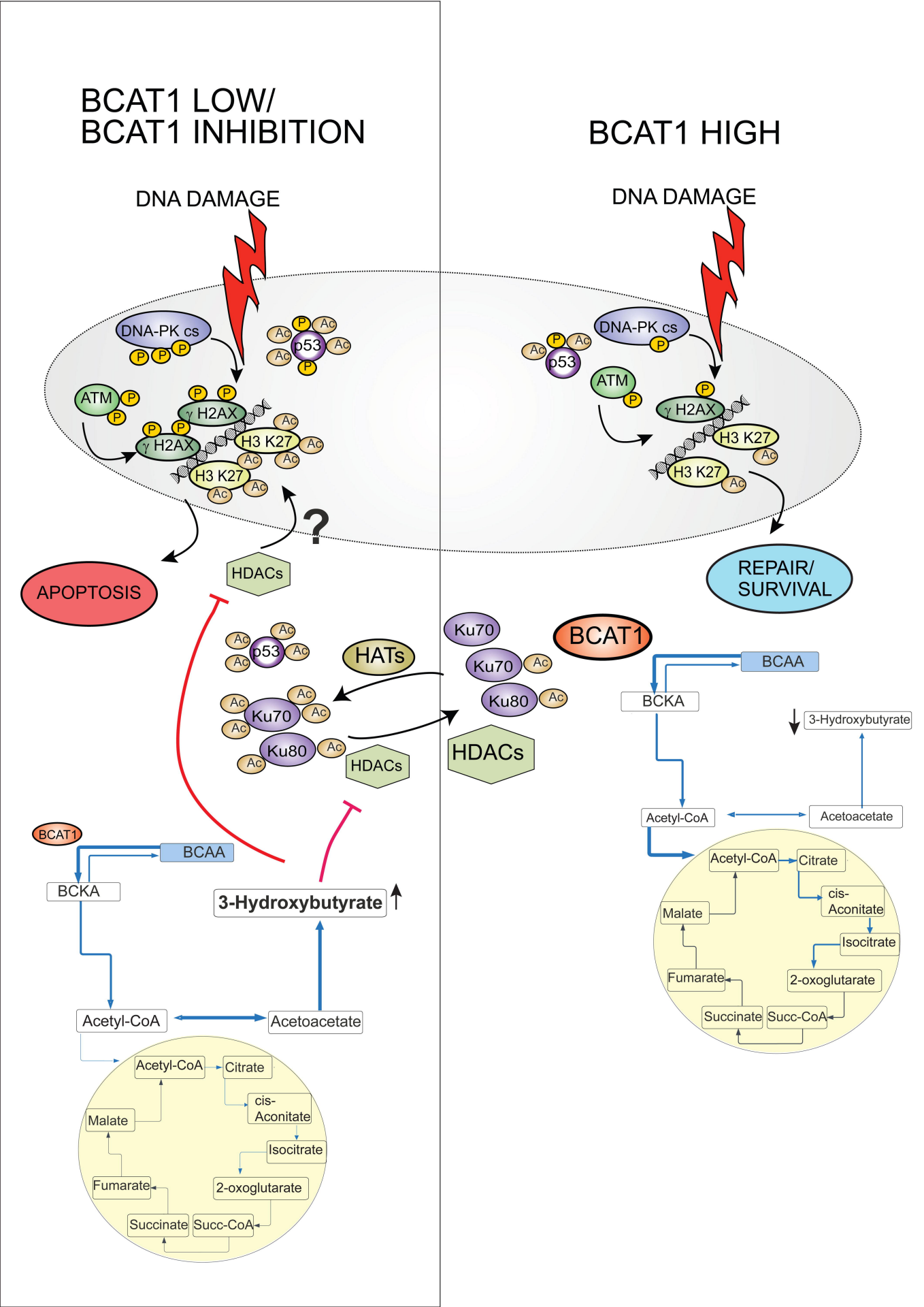
BCAT1 LOW/
BCAT1 INHIBITION
BCAT1 HIGH
DNA DAMAGE
DNA DAMAGE
DNA-PK cs
p53
ATM
γ H2AX
H3 K27
?
HDACs
APOPTOSIS
REPAIR/
SURVIVAL
HATs
Ku70
Ku80
BCAT1
BCAA
BCKA
3-Hydroxybutyrate
Acetyl-CoA
Acetoacetate
Citrate
cis-
Aconitate
Isocitrate
2-oxoglutarate
Succ-CoA
Succinate
Fumarate
Malate

BCAT1 is a NOTCH1 target and sustains the oncogenic function of NOTCH1

Valeria Tosello*, Ludovica Di Martino*, Adonia E. Papathanassiu, Silvia Dalla Santa, Marco Pizzi, Lara Mussolin, Jingjing Liu, Pieter van Vlierberghe†, Erich Piovan

†Deceased.

*these two authors contributed equally to the work

SUPPLEMENTARY DATA:

Figure S14. BCAT1 expression correlates with prognosis in NOTCH1-dependent leukemias and represents a therapeutic target in T-ALL

Figure S15. BCAT inhibition synergizes with numerous chemotherapeutic drugs to reduce cell viability

Figure S16. BCAT1 inhibition synergizes with etoposide to reduce viability

MATERIALS AND METHODS

Cell lines and primary leukemia samples. Human embryonic kidney (HEK) 293T cells were maintained in DMEM containing 10% fetal bovine serum (FBS) and 0.05 mg/ml penicillin/streptomycin. All T-ALL cell lines were maintained in RPMI-1640 media supplemented with 10% FBS and 0.05 mg/ml penicillin/streptomycin. We tested cell lines regularly for mycoplasma contamination. Primary T-ALL cells were expanded in vivo via i.v. injection in 6-8 weeks old female NOD SCID IL2Rγnull (NSG) immunodeficient mice. T-ALL cells from spleens of xenografted mice were cultured in vitro in MEM-alpha media supplemented with 10% human serum and cytokines for the duration of functional assays (48-72h). Patient derived xenograft (PDX) and cell line authentication was determined by analyzing several loci of short tandem repeats (STRs) using a commercial kit (PowerPlex 16 HS System, Madison, WI, USA). NOTCH1-induced T-ALL murine models were previously generated by transduction of bone marrow progenitors with activated forms of NOTCH1 oncogene (*NOTCH1 L1601P ΔPEST* or *ΔE-NOTCH1*)[1]. Spleens of diseased mice were used as a source of murine T-ALL cells for further studies. Thymuses from 6 weeks old normal C57/BL6 mice were obtained. Procedures involving animals and their care conformed with institutional guidelines and were authorized by local (OPBA) and national (Italian Ministry of Health) animal ethical committees.

Mouse transplantation experiments. Bcat1 knockout ($^{-/-}$; KO) mice on a C57BL/6J background were generated using the CRISPR/Cas9 technology by Cyagen, (CA, USA). NOTCH1-induced T-ALL tumors were generated in mice as previously described [2]. Briefly, bone marrow (BM) cells were collected from 6- to 12-week-old WT and *Bcat1* KO C57BL/6 mice and BM progenitors (Lin-) were purified by negative selection using magnetic sorting (Miltenyi Biotec, Bergisch Gladbach, Germany). The cells were cultured overnight in the presence of the following cytokines (all from Peprotech, London, U.K.): mIL-3 (10 ng/mL), mIL-6 (10 ng/mL), mFLT3L (50 ng/mL), mIL7 (100 ng/mL) and mSCF (50 ng/mL). The cells were then washed, resuspended in retroviral supernatant (ΔE-NOTCH1), placed in the same cytokine cocktail containing polybrene (4 μg/mL), and centrifuged at 1,290g for 90 minutes. A second round of spinoculation was performed the following day. After flow cytometric analysis of transduced progenitors, approximately 50×10^4 $Lin^-/Sca1^+/GFP^+$ cells of each genotype were injected i.v. into lethally irradiated (9 Gy) recipients (6–8-week-old C57BL/6 female mice). Mice were bled after 2–3 weeks to monitor engraftment and evaluate the presence of circulating immature T cell progenitors by flow cytometry. Tumour bearing mice were euthanized and primary tumour cells were extracted from their spleens. For in vitro studies, Δ*E-NOTCH1* tumors were cultured in RPMI-1640 supplemented with 20% FBS, mIL-7 (10 ng/mL), mIL-2 (5ng/mL) and β-mercaptoethanol. Procedures involving animals and their care conformed with institutional guidelines and were authorized by local (OPBA) and national (Italian Ministry of Health) animal ethical committees.

Flow cytometry and analysis of T-cell distribution. Peripheral Blood (PB) and spleens were harvested from WT and KO mice. Red blood cell (RBC) lysis was performed using a hypotonic solution containing ammonium chloride for all samples. Briefly, the cells were blocked for 10 minutes with CD16/CD32 (mouse BD FC Block, BD Pharmingen, Oxford, U.K.) diluted 1:100 in PBS at 4°C and subsequently stained for 30 minutes with a combination of following panel of antibodies: Cd3e-BV421/BV510 (Biolegend, London., U.K.), Cd8-BV605/PE, Cd4-FITC/APC (all from BD Pharmingen). The fixable viability stain dye (FVS780; BD) was used to analyze only viable cells. Cells were analyzed on a BD LSR II flow cytometer and acquired data was analyzed with FlowJo (Tree Star Inc., Ashland, OR).

Quantitative real-time PCR. Total RNA from human and mouse samples were extracted using Trizol reagent (Invitrogen, Thermo Fisher Scientific, Waltham, MA, USA). RNA from thymic samples were from a previous study[3]. These samples were obtained as surgical tissue discards from pediatric patients, ranging in age from 2 days to 5 years, undergoing cardiac surgery at the University Hospital of Padova, after informed consent. cDNA was generated with the Super Script First Strand Synthesis System for RT-PCR (Invitrogen) and analyzed by quantitative real-time PCR using SYBR Green PCR Master Mix (Applied Biosystems, Paisley, UK) and the HT 7900 Real-Time PCR System (Applied Biosystems). All primers were KiCqStart™ Primers from Sigma-Aldrich. Primer sequences are available upon request. Every sample was analyzed in triplicate and relative expression levels were normalized to RPL19 or β2-microglobulin expression using the ΔΔCT method.

Total histone extraction. Total histones were obtained using the EpiQuik total histone extraction kit (Epigentek, Farmingdale, NY. USA), according to the manufacturer's recommendations. Histone extracts were normalized for protein concentration using the Bradford method (Pierce).

Immunohistochemistry. All primary T-ALL (and T-cell lymphoblastic lymphoma; T-LBL) cases were retrieved from the archives of the Pathology Unit of Padua University Hospital (Padua-Italy). Patient derived xenograft (PDX) samples were previously generated[4, 5]. Immunohistochemical (IHC) analysis was performed on 4 μm-thick formalin-fixed paraffin-embedded (FFPE) tissue sections with the Bond Polymer Refine Detection kit in an automated immunostainer (BOND-MAX system; Leica Biosystems–Newcastle upon Tyne, UK), as previously described[6]. IHC analyses were run using the following primary antibodies: anti-BCAT1 (clone 51/ECA39, BD Pharmingen), anti-HES1 (clone D6P2U, Cell Signaling Technology), anti-BCAT2 (clone D8K3O, Cell Signaling Technology). Immunostains were performed on whole tissue sections. Appropriate positive and negative controls were also included. Thymic tissue (N=3) was run in parallel to assess BCAT1, BCAT2 and HES1 expression in normal T cell precursors. The following two-tiered scoring system was used to assess the expression of these markers: (i) low expressor: no staining (0) or weak positivity (+1) in <10% of tumor cells; (ii) high expressor: moderate to strong positivity (2+ to 3+) in ≥10% of tumor cells. The scoring system was based on cytoplasmic (BCAT1/BCAT2) or nuclear expression (HES1) of each marker and intensity scores were defined by comparison with positive controls (i.e. *NOTCH1* mutated PDX samples with high BCAT1 and HES1 expression documented in western blot). Specifically, strong (score 3+) positivity was attributed to cases with protein expression comparable to that of the positive controls, moderate (score 2+) positivity to cases with protein expression slightly fainter than controls, and weak (score 1+) positivity to cases with barely detectable protein expression.

Immunoprecipitation of acetylated proteins. Immunoprecipitation of acetylated proteins was performed using the Signal-seeker Acetyl-Lysine detection kit (Cytoskeleton, Inc., Denver, CO, USA) according to the manufacturer's recommendations. Briefly, cells were lysed in diluted BlastR lysis buffer containing class I and II HDAC inhibitor (Trichostatin A; TSA) and class III HDAC inhibitor (Nicotinamide). Approximately 2 mg of protein was pre-cleared with Protein G–agarose (Santa Cruz Biotechnology) at 4°C for 30 min before being incubated with Acetyl-lysine Affinity beads or Acetyl-lysine IP control beads overnight at 4°C. Beads were washed three times with BlastR-2 wash buffer and bound proteins eluted with bead elution buffer. Immune complexes were analyzed by SDS-PAGE and immunoblot.

Neutral comet assay. T-ALL cells were treated with vehicle (DMSO) or etoposide (1 μM) for 0 to 6h. The neutral comet assay was performed using the CometAssay Silver Kit (R&D Systems; #4251-050-K). Briefly, cells were

mixed with CometAssay LMAgarose (R&D Systems; 1:10[v/v]). Once the agarose had solidified, the cells were lysed with lysis solution (R&D Systems) overnight. The following day, we placed the slides briefly in neutral electrophoresis buffer (R&D Systems) before being placing them in an electrophoresis chamber containing neutral electrophoresis buffer. The slides were subjected to electrophoresis at 1V/cm for 1h at 4ºC. We washed the slides in 70% ethanol. After drying the slides at room temperature, we stained the comets with SYBR-gold (ThermoFisher Scientific, #S11494). We viewed the comets by epifluorescence microscopy. For comet analysis we used the Open Comet software[7] to quantify the percentage of DNA in the tail in at least 50 comets per condition.

Analysis of publicly available datasets. Expression data for BCAA metabolic genes in primary T-ALL patients and thymic subpopulations were obtained from GSE46170[8]. Microarray data were also obtained from GSE12948[9], GSE14959[10], E-MTAB-9279[1], CGAS00000000002[11], GSE33469[12], GSE33470[13]. RNA sequencing (RNA-seq) data of 264 pediatric T-ALL patients from St. Jude[14] was used. Gene expression data of B-cell chronic lymphocytic leukemia (B-CLL) patients analyzed with HGU133+2.0 Affymetrix GeneChip arrays (N = 107) was obtained from Gene Expression Omnibus (GSE22762)[15]. BCAT1 expression levels were extracted and used to generate Kaplan–Meier survival plots. The mean BCAT1 expression level was used as cut-off to define high and low BCAT1 expression.

RNA-sequencing and gene-set enrichment analysis. Total RNA from the spleens of ΔE-NOTCH1 leukemia-bearing WT and *Bcat1* KO C57BL/6 mice was extracted using the RNAeasy Mini Kit (Qiagen, Hilden Germany), according to the manufacturer's instructions. Library preparation and paired-end RNA sequencing using Illumina NextSeq 500, as well as downstream data analysis, were performed by Active Motif (Waterloo, Belgium). Sequenced reads were mapped to the genome using the STAR aligner with default settings and uniquely mapped reads were counted. Normalized counts per million and differential gene expression were determined with DESeq2. Hierarchical clustering of Z score and log fold-change expression values used in heatmaps was carried out using GenePattern software[16]. RNAseq data was also analyzed using iDEP[17]. Gene set enrichment analysis (GSEA) analysis was performed using gene sets from the Molecular Signature Database at the Broad Institute (https://www.gsea-msigdb.org/gsea/msigdb/index.jsp) as previously described[18] using GenePattern software. Primary data has been deposited in GEO (GSE267966) and will be released September 1 2024.

Steady state metabolite profiling. Spleens (N=3) and thymuses (N=2) from *ΔE-NOTCH1* leukemia bearing mice and thymic tissue from 6 weeks old normal C57/BL6 mice (N=3-5) were obtained. Flash-frozen tissue (spleen or thymus) was subsequently analyzed by Capillary Electrophoresis Time-of-Flight Mass Spectrometry (CE-TOFMS; Ω-scan analysis, HMT, Tokyo, Japan). For in vivo experiments, we analyzed flash-frozen tissue (spleen) from *ΔE-NOTCH1* leukemia bearing mice with WT (N=3) and *Bcat1* KO genotype (N=3) by CE-TOFMS (C-scope analysis, HMT, Tokyo, Japan). Further, *ΔE-NOTCH1* leukemia bearing mice (N=3 each) were injected intraperitoneally (i.p.) with three doses of ERG245 (30mg/kg), which is a potent BCAT1 inhibitor, at 8 h intervals or vehicle (PBS). Identification of known chemical entities was based on comparison to metabolomics library entries of purified standards and was performed by HMT. Heatmap representation of metabolites identified by CE-TOFMS in NOTCH1-induced (*ΔE-NOTCH1*) leukemia cells treated with vehicle (PBS) or ERG245, *ΔE-NOTCH1* tumors versus normal thymic tissue or *ΔE-NOTCH1* tumors WT versus KO for *Bcat1* was performed using MetaboAnalyst[19].

Stable-isotope tracing experiments. For the stable isotope-tracing experiments using primary cells, *ΔE-NOTCH1* leukemia bearing mice were injected i.p. with three doses of ERG245 (30mg/kg) at 8 h intervals or vehicle (PBS). Ten minutes before sacrifice mice were injected i.v. with $^{13}C_6$ Leu (Cambridge Isotope laboratories, Tewksbury, MA, USA) and spleens were flash-frozen. In another set of experiments, *ΔE-NOTCH1* leukemia bearing mice (WT and *Bcat1* KO) were injected i.v. with $^{13}C_6$ Leu (Cambridge Isotope laboratories) and spleens flash-frozen. Flash-frozen splenic tissue was subsequently analyzed by F-scope CE-TOFMS (HMT, Tokyo, Japan).

Analysis of ChIP-seq databases. The ChIP-seq data presented in this study were obtained from NCBI GEO under the following accession IDs: GSM959056 (HPB-ALL-NOTCH1)[20], GSM2521494 (MOLT4-PolII)[21], GSM4271227 (MOLT4-H3K4me3)[22] and GSM3693104 (ATACseq MOLT4)[23]. Fastq files from these public ChIPseq and ATACseq datasets were downloaded and mapped to human reference genome (GRCH38/hg38) using Bowtie2 (version 2.5.0)[24] with default parameters. MACS2 (version 2.2.7.1) [25] was used to call peaks. Next, Bedgraphs generated by MACS2 were converted to BigWig files with UCSC – wigtobigwig tool (version 357) and displayed using pyGenomeTracks (version 3.7) [26].

Cell viability assays and flow cytometry. We analyzed cell viability/proliferation in T-ALL cell lines via the bioluminescent method Vialight plus (Lonza, Basel, Switzerland) or by counting live cells after trypan blue staining. For assays evaluating the effects of drugs on T-ALL cell lines, viability was evaluated after 72h. In detail, human T-ALL cells (3×10^5) or mouse T-ALL cells (0.5×10^5) were seeded in 24-well flat-bottom plates and treated with increasing doses of the various compounds: Etoposide (50-500 nM), Cytarabine/Ara-C (25-100 nM), Doxorubicin hydrochloride (25-100 nM) all from Selleck (Selleck Chemicals LLC, Houston, TX), ERG245 (200-1000 μM; Ergon Pharmaceuticals, Washington DC, NW, USA). Dibenzazepine (DBZ; Syncom, Groningen, the Netherlands) was used in selected experiments. Dl-β-hydroxybutyrate (3-HB; sodium salt) and sodium butyrate (NaB) were from Sigma-Aldrich. We analyzed apoptosis after 48-72h by flow cytometry (FACS) after staining with Annexin V-FITC (Roche) or Annexin V-PE (BD Biosciences, Milan, Italy) and SYTOX Red dead cell stain (Invitrogen). Apoptosis was defined as the sum of the percentage of Annexin V^+ and Annexin V^+/ SYTOX Red^+ cells. Analysis of proliferation combined with cell cycle profile was performed using the Click-iT™ EdU Flow Cytometry Assay Kit (Life Technologies) according to the manufacturer's instructions. The samples were collected on a FACSCalibur (BD Biosciences) using Cell Quest software (BD Biosciences), and analysed with FlowJo (Tree Star Inc., Ashland, OR).

Plasmids, lentiviral constructs and viral production. For BCAT1 silencing experiments, HEK293T were transfected with pGipz non-silencing shRNA control, shBCAT1#1 (V3LH5-337223), shBCAT1#2 (V2LH5-64329) and appropriate packaging plasmids using JetPEI transfection reagent (Polyplus, Illkirch, France). Inactivation of human BCAT1 in T-ALL cells using the CRISPR-Cas9 technology was achieved using the guide sequence for BCAT1 (TATTAGGTCTTTAGCCTG; sgBCAT1)[27] which was cloned into LentiCRISPRV2 puro vector (Addgene #98290). BCAT1 over-expression was done using pLenti-BCAT1-Myc-DDK-P2A-Puro (RC219229L3; Origene, Rockville, MD, USA). Plasmids carrying the catalytic inactive mutant of BCAT1 (K222A) was synthesized and cloned in pLenti-Myc-DDK-P2A-Puro vector by Genewiz (ALENTA Life Sciences, Chelmsford, MA, USA). For viral production, viral supernatant from transfected cells was collected 48h after transfection, filtered and used to infect target cells. All infections of T-ALL cells were performed by spinoculation. After infection, T-ALL cells were selected for 3-7 days in puromycin before functional assays.

Luciferase reporter experiments. To perform reporter assays, BCAT1 promoter (-1407 to +195 relative to the TSS) was cloned into the pGL4.23[luc2/minP] vector (E841A, Promega, Madison, WI, USA) using Bgl II and Hind III restriction sites by Genewiz (ALENTA Life Sciences, Chelmsford, MA, USA). Constructs having the RBP-J binding site (TGGGAA) mutated or deleted were also generated. To measure the capacity of ICN1 transcription factor to induce BCAT1 expression, HEK293T cells were co-transfected with pGL4.23[luc2/minP] vector containing the above mentioned BCAT1 promoter (pGL4-BCAT1 promoter) and increasing amounts of pcDNA3-ICN1 (kind gift of A. Weng; Terry Fox Laboratory, BC Cancer Agency, Vancouver, Canada) and Renilla luciferase vector (Promega). In some experiments using HEK293T cells, pGL4-BCAT1 promoter construct with the RBP-J binding site (TGGGAA) mutated was used. To determine the effects of NOTCH1-inhibition on reporter activity, pcDNA3-ICN1 transfected cells were treated for 48h with increasing amounts of CB103 (Selleck). To evaluate the contribution of MYC to reporter activity, pcDNA3-ICN1 transfected cells were either transfected with MYC targeting hairpins (pLKO-shMYC#1 (TRCN0000039640), pLKO-shMYC#2 (TRCN0000174055)) or increasing amounts of the BRD4 inhibitor, JQ1 (Selleck). Experiments were repeated at least twice and performed at least in quadruplicate. Luciferase activity was measured 72h post-transfection by Dual-Glo Luciferase Reporter assay kit (Promega) according to the manufacturer's guidelines. For reporter assays in T-ALL cells, we resuspended 1.5 x 10^6 HPB-ALL cells in 20 µL of SF Nucleofector Solution (Lonza) with the addition of 700 ng of pGL4.23 vectors (BCAT1 promoter or control constructs) and 300 ng of pGL4.74 [hRluc/TK] Renilla luciferase reporter plasmid (Promega). Cells were electroporated (Amaxa Nucleofector; Lonza) using program CM130 and resuspended in 1 ml of RPMI / 20%FCS and incubated at 37°C/ 5% CO_2 for 48 hrs. In some experiments HPB-ALL cells were co-transfected with pcDNA3-ICN1 or treated with CB103. Experiments were repeated three times and performed at least in quadruplicate. Luciferase activity was measured 48-72h post-transfection by Dual-Luciferase Reporter assay kit (Promega). Relative luciferase activity was calculated as Firefly luciferase activity normalized against Renilla luciferase activity.

Mouse studies. NOTCH1-induced T-ALL tumors (generated using both *HD-ΔPEST* and *ΔE* alleles[1]) were secondarily transplanted intravenous (i.v.) into sub-lethally irradiated recipients (C57BL/6 females of 6-8 weeks). Tumor bearing mice were euthanized and primary tumor cells extracted from the spleens of leukemic mice. T-ALL PDX samples[4] were expanded in vivo via i.v. injection into female 6-8 weeks old NOD Rag1null IL2Rγ null immunodeficient mice (NSG mice; Charles River, Wilmington, MA, USA). Tumor bearing mice were euthanized and tumor cells extracted from the spleens of leukemic mice and used in functional assays. For the evaluation of BCAT1 function in vivo, we infected MOLT4 or CCRF-CEM control (shCTRL) or BCAT1 deficient (shBCAT1#1/ shBCAT1#2) leukemic cells with lentiviral particles expressing luciferase (FUW-Cherry-LUC) and injected them i.v. into NSG mice (5x10^6 cells/mouse; N=5 per experimental group). We evaluated disease progression by in vivo bioimaging with the In Vivo Imaging System (IVIS, Xenogen, Grantham, UK). In therapy related experiments, PDX leukemic cells (T-ALL#19 or T-ALL#27) were infected with lentiviral particles expressing luciferase (FUW-Cherry-LUC) and injected i.v. into 6–8-week-old female NSG mice. After tumor engraftment (human CD45+ blasts ≥1% in peripheral blood), we treated homogeneous groups of animals (N=5) with vehicle (DMSO/PBS), Etoposide (10 mg/kg or 15 mg/kg twice a week; intraperitoneal), ERG245 (30 mg/kg three times a week; intraperitoneal) or the combination Etoposide (10 mg/kg or 15 mg/kg twice a week; intraperitoneal) + ERG245 (30 mg/kg three times a week; intraperitoneal) for 10-15 days. We evaluated disease progression and therapy response by in vivo bioimaging with the In Vivo Imaging System IVIS Spectrum (Xenogen), spleen weight and human CD45 analysis by flow cytometry. Xenografted mice were age- and sex-matched and randomly assigned to groups. No blinding methods were used. Procedures involving animals and their care conformed with institutional guidelines and were authorized by local (OPBA) and national animal ethical committees (Italian Ministry of Health; DGSAF 0006112; 177/2020-PR).

BCAT1 promoter methylation testing by Methylation specific PCR (MSP). Genomic DNA was extracted from T-ALL cell lines (DNeasy kit, Qiagen) according to the manufacturer's instructions. A total of 500 ng of genomic DNA was bisulfite modified using EZ DNA Methylation™ Kit (Zymo Research, Irvine, CA, USA). Bisulfite modified DNA (20ng) was amplified with BCAT1 promoter specific primers (listed in *Online Supplementary Table S4*). A bisulphite-conversion specific actin beta (ACTB) PCR was performed (primers listed in *Online Supplementary Table S4*) to determine total amount of analyzed DNA. PCR conditions used are available upon request. PCR products were loaded on 2% agarose, stained with SYBR safe DNA gel stain (Thermo Fisher Scientific), and visualized under UV illumination.

Table S1: Primer sequences for amplification of BCAT1 promoter following ChIP

TARGET LOCI	DIRECTION	SEQUENCE (5' to 3')
BCAT1 ***P1***	FORWARD	CTCTGGGAAAGAGATCGGCA
BCAT1 ***P1***	REVERSE	CTGCATGCTGAGAGGACCAC
BCAT1 ***P2***	FORWARD	AATCTTCGGGCTGGGAGAGA
BCAT1 ***P2***	REVERSE	GCAGATCCCAAGGGTCGTAG
HES1 ***P1***	FORWARD	AAGTTTCACACGAGCCGTTC
HES1 ***P1***	REVERSE	GCTGTTATCAGCACCAGCTC
BCAT1 ***NL***	FORWARD	GTATCGCTCTGCTGTGAGGG
BCAT1 ***NL***	REVERSE	GTCAACACCGTGACCCGTTA

Table S2_Differentially expressed genes between Bcat1KO and Bcat1WT NOTCH1-dependent leukemias

Ensemble ID	Symbol	DETUMOR KO-DETUMOR_WT_log2FoldChange	DETUMOR KO-DETUMOR_WT_padj	DETUMOR_WT#0_1	DETUMOR_WT#0_2	DETUMOR_WT#0_3	DETUMOR_WT#6_1	DETUMOR_WT#6_2	DETUMOR_WT#6_3	DETUMOR_KO#7_1	DETUMOR_KO#7_2	DETUMOR_KO#7_3	DETUMOR_KO#3_1	DETUMOR_KO#3_2	DETUMOR_KO#3_3
ENSMUSG00000045010	Gm4779	10.64676018	6.46E-21	2.80947046	2.32265191	2.32279427	2	2.320152159	2	7.84426137	7.8406322	7.9512576	11.542683	11.497332	11.58069
ENSMUSG00000090015	Gm15446	7.217665549	1.55E-14	2	2.58616865	2	2	2	2	5.45829491	5.8780348	5.9514022	5.5837553	5.829622	6.207633
ENSMUSG00000046774	8030474K03Rik	6.937006211	1.12E-10	4.17376203	4.25078255	4.39582017	2.3198067	2.320152159	2.32024072	7.17869317	7.2143575	7.496925	10.834736	10.905635	10.83097
ENSMUSG00000031125	3830403N18Rik	6.836535449	1.38E-08	2.58660819	2	2	4.51477944	4.314811199	3.80131951	7.41663134	7.6533656	7.3008695	10.645245	10.687365	10.629257
ENSMUSG00000095574	Trbv12-1	6.774001762	1.21E-15	3.32488899	3.32409844	2.58640584	2.3198067	2.320152159	2.32024072	5.99882775	6.0397503	5.9279464	9.1124347	9.0759958	9.231708
ENSMUSG00000076465	Trbv5	6.574131389	6.64E-08	6.46413927	6.57331899	6.73208315	4.23953538	4.452152566	4.45251622	13.2868952	13.400864	13.28948	7.2655037	7.3974477	7.4738522
ENSMUSG00000076873	Trdv5	6.308259504	6.57E-17	3.70385559	3.70294367	3.46218583	3.31555453	3.900368117	3.57933023	6.6992374	6.6817489	6.2639549	10.216645	10.338571	10.242446
ENSMUSG00000086391	1700042O10Rik	6.12351583	5.55E-13	2.80947046	2	2.58640584	2.3198067	2.582001393	2	5.12817554	5.2050447	5.1266377	7.4249784	7.3003549	7.1780377
ENSMUSG00000018849	Wwc1	6.038304381	0.014249	2.58660819	2	2.32279427	2.3198067	2.320152159	2	6.7669798	6.7896504	6.9159751	2	2	2
ENSMUSG00000059256	Gzmd	5.92430055	2.22E-05	2	2	2	2	2	2	3.99906228	2.3209407	2.9985073	4.3912513	3.6980072	
ENSMUSG00000076472	Trbv15	5.073432964	1.20E-13	8.53235509	8.3655153	8.60790762	8.75764398	8.879916979	8.7925193	10.9874367	10.968046	11.026306	14.622336	14.622023	14.594324
ENSMUSG00000093954	Gm16867	4.994891262	1.78E-11	3.32488899	3.00180885	3.17232976	2.3198067	2.582001393	2.32024072	7.56863151	7.2713083	7.4889326	5.2842203	4.9969249	5.1275786
ENSMUSG00000102364	Ighv8-5	4.679381387	0.000424	2.32291573	2.32265191	2.32279427	5.41661938	5.60653695	5.34992256	6.35636259	6.3876093	6.5517291	10.012709	9.9287142	9.8372877
ENSMUSG00000069306	H4c17	4.567884131	0.0001886	2	2	2	2	2	2.58214912	3.32117796	4.2440258	3.805222	2.8067906	3.3198201	3.9054796
ENSMUSG00000039058	Ak5	4.565594415	0.0118454	2	2	2.58640584	2.3198067	2	2.8037367	5.55344488	5.6958767	5.7251591	2.3216648	2	2.3215434
ENSMUSG00000084997	Gm15471	4.065396929	5.95E-05	2.58660819	2.8089055	2.58640584	3.31555453	3.45377331	3.16523297	7.10731028	7.0826646	7.0845638	3.1691935	3.5826201	3.4582072
ENSMUSG00000022156	Gzme	4.029909245	0.0002217	2	2.32265191	2.58640584	2	2.320152159	2.58214912	2.80681915	3.1671805	3.5829719	5.2842203	4.4565564	5.042703
ENSMUSG00000036242	Armh4	3.932010222	0.0087328	3.00246783	2.32265191	2.32279427	2.80280525	2	2.58214912	6.0432195	5.8533786	5.6976827	2.3216648	2	2.8065305
ENSMUSG00000078161	Erich3	3.786469008	0.0037746	2	2.32265191	2.58640584	2.3198067	2.320152159	2	3.16923045	2.3209407	2.5839675	4.9057492	4.5206589	4.3203887
ENSMUSG00000034057	Myrfl	3.757288127	9.04E-06	3.32488899	2.8089055	2.32279427	2.3198067	2	2	4.16895254	4.0836837	3.805222	5.3563635	5.2822481	5.4576822
ENSMUSG00000031137	Fgf13	3.681374957	7.68E-05	2.80947046	2.58616865	2.58640584	2.58142511	2.582001393	2.32024072	3.45863601	3.9962936	2.5839675	5.7801385	5.4230771	5.5528283
ENSMUSG00000001672	Marveld3	3.650379111	0.0385308	2	2	2	2.3198067	2.320152159	2	2.99937492	3.4562874	3.9977603	2.8067906	2	2.3215434
ENSMUSG00000070732	Rbm44	3.519759705	2.29E-05	2	3.17193469	3.46218583	2.80280525	3.694282913	3.31686005	6.30259365	6.7231634	6.9159751	3.9059249	4.5820339	4.5219723
ENSMUSG00000015437	Gzmb	3.391219953	5.42E-35	3.32488899	4.0902284	3.91006404	4.79824119	4.577548304	4.38547538	7.75366023	7.2046433	7.5284591	7.1686446	6.939114	7.3379731
ENSMUSG00000020182	Ddc	3.373616911	1.67E-05	3.32488899	3.32409844	3.46218583	2.80280525	3.45377331	3.31686005	6.98747365	6.8025878	6.5970492	3.9059249	4.1671919	4.1684284
ENSMUSG00000040170	Fmo2	3.228087338	0.0058496	3.32488899	3.4617334	3.58784774	2.99469065	3.316593717	3.31686005	7.03221076	6.7765959	6.7520113	3.4585936	2.5837918	2.3215434
ENSMUSG00000023963	Cyp39a1	3.107736897	2.19E-50	5.00431594	4.70349952	4.70410076	4.5761027	4.452152566	4.24125532	7.63539933	7.7298587	7.8108474	7.2371226	7.3274893	7.2555137
ENSMUSG00000035686	Thrsp	3.094750268	0.0021854	3.32488899	3.00180885	2.32279427	2.99469065	3.316593717	2.32024072	5.99882775	5.8533786	5.9514022	2.9993416	3.4571958	3.1688562
ENSMUSG00000006014	Prg4	3.05306881	0.0042104	3.91050864	3.17193469	3.32452507	2.3198067	2.582001393	2.8037367	6.14856716	6.0828102	6.488999	3.1691935	3.4571958	2.9990381
ENSMUSG00000076492	Trbj2-1	3.045468074	0.0057546	8.02722352	8.09631967	8.05954318	5.44976368	5.576804784	4.69328731	7.72669362	7.7162491	7.8735809	11.192211	11.130276	11.084879
ENSMUSG00000019124	Scrn1	3.020547911	0.001713	3.91050864	2.58616865	3.58784774	2.80280525	2.803546666	2.99577786	6.52236591	6.4215511	5.9971999	3.321138	3.8048451	3.3207737
ENSMUSG00000063458	Lrmda	2.932944581	1.53E-06	3.8108791	3.17193469	3.00216447	2.80280525	3.16498644	3.69459039	4.39130525	5.124905	4.2455699	6.3910631	6.2254914	6.0205618
ENSMUSG00000038233	Gask1a	2.874848371	1.46E-07	2.80947046	2.58616865	3.00216447	2.80280525	3.45377331	2.58214912	4.32092783	4.5194791	4.2455699	5.6135004	4.9511354	5.1682145
ENSMUSG00000030587	2200002D01Rik	2.771071831	2.04E-30	4.09123546	4.17273779	4.00324548	3.79976415	3.579034195	3.45405584	6.26560109	6.1450822	6.488999	6.0431569	6.3542087	6.2269969
ENSMUSG00000020890	Gucy2e	2.763132983	6.70E-19	3.588252	3.5873738	5.0912803	3.99202864	3.801002232	3.69459039	6.68529867	6.5498556	6.4565805	6.5065355	6.371694	6.4575947
ENSMUSG00000045790	Ccdc149	2.754692054	0.0003357	4.00370016	3.4617334	4.00324548	3.16402452	3.45377331	3.31686005	4.08650672	3.9962936	4.2455699	6.7800906	6.4060416	6.7530343
ENSMUSG00000021747	Cfap20dc	2.700104024	0.0228972	4.39631085	4.3952449	5.133115	2.58142511	2.582001393	2.58214912	3.45863601	3.8038253	4.4569882	7.1983912	7.0626793	7.3110069
ENSMUSG00000058740	Kcnt1	2.697415794	0.0430233	3.32488899	2.32265191	3.17232976	2.3198067	2.803546666	2	5.49071386	5.2050447	4.7523434	2.9993416	2.3212258	2.5843213
ENSMUSG00000061451	Tmem151a	2.666964075	0.0199102	3.32488899	2.58616865	2.32279427	2.3198067	2.320152159	2	4.69938173	4.4553878	4.5824738	2.5845236	2.9982436	2.9990381
ENSMUSG00000095130	Ighv1-39	2.652023111	0.0385283	5.00431594	4.52654927	5.133115	8.4652151	8.409055326	8.47545387	11.0967839	11.028489	11.061088	7.7198071	7.6404116	7.7123577
ENSMUSG00000021587	Pcsk1	2.632350056	0.0001208	2.32291573	2.58616865	2.32279427	2.80280525	2.582001393	2.32024072	3.99906228	3.9032667	4.0851792	3.321138	3.8048451	3.8059806
ENSMUSG00000018727	Cpsf4l	2.525442675	4.38E-05	5.28982865	5.61803048	5.98133135	4.51477944	4.080660667	4.51657958	6.16874406	6.2620998	6.1870014	8.2081541	8.0839996	8.3644211
ENSMUSG00000102222	Pcdhga10	2.459578891	9.12E-07	2.58660819	3.4617334	2.58640584	2.58142511	3.316593717	3.16523297	4.45840862	4.3883165	4.0851792	4.9988477	4.9038448	5.0857649
ENSMUSG00000115970	8430426J06Rik	2.446152126	0.0038826	2	2.32265191	2	2.80280525	2.320152159	2.99577786	3.80646187	3.5816684	2.9985073	3.6995281	3.4571958	3.9054796
ENSMUSG00000076494	Trbj2-3	2.439532288	0.0346512	6.7729351	7.00350259	6.89899826	3.45267087	2.320152159	2.8037367	7.49063046	7.5187257	7.4317104	8.7833298	8.7480617	9.0987519
ENSMUSG00000047501	Cldn4	2.439420158	6.61E-08	7.86282756	7.83010029	7.86223222	5.89696396	5.968945122	5.79950395	9.56290567	9.5284125	9.5725679	9.6280462	9.5491729	9.6810795
ENSMUSG00000073535	Gm5532	2.430863336	5.35E-13	5.7324803	5.52686336	5.5585469	5.07808018	5.277416118	5.41859685	7.14853192	7.0175762	6.8919313	8.2513657	8.3184571	8.1879265
ENSMUSG00000041789	2700046A07Rik	2.397176181	6.67E-05	3.32488899	3.17193469	3.17232976	2.80280525	2.582001393	2.32024072	3.45863601	4.5808437	4.1676023	5.0863008	4.4565564	4.9525203
ENSMUSG00000066677	Ifi208	2.346690953	2.05E-30	6.55931079	6.19324212	6.15382946	5.57521373	5.418193514	5.74705896	8.42082892	8.4171786	8.3807531	8.133128	8.2397055	7.9523029
ENSMUSG00000022206	Npr3	2.325839848	0.0031753	3.91050864	4.00271242	4.09077189	3.45267087	3.900368117	3.99366215	3.69957415	4.2440258	4.0851792	6.6425919	6.6113385	6.7530343
ENSMUSG00000076525	Igkv1-99	2.306716522	0.0085073	4.86223324	4.86109829	4.32538969	6.32973889	6.785835982	6.79920113	6.10734654	6.2620998	6.0415883	9.120226	8.993692	8.9924441
ENSMUSG00000110998	I730028E13Rik	2.221283903	0.0127299	3.17266678	2.58616865	2.58640584	2.58142511	2.582001393	2.58214912	4.52252907	4.4553878	4.4613475	2.8067906	3.1679733	2.9990381
ENSMUSG00000035299	Mid1	2.212534186	1.04E-34	5.46391545	6.06948903	6.04845802	5.7974791	5.968945122	5.82502842	7.89963731	7.8899571	7.52064	8.1019899	8.3496749	8.1579738
ENSMUSG00000043773	1700048O20Rik	2.191387831	3.01E-08	6.46413927	5.91026528	6.17401072	6.84771084	6.677945629	6.957599	7.71987247	7.877783	7.7718547	9.1909848	9.3430204	9.1928455
ENSMUSG00000063600	Egfem1	2.180291399	0.0108327	2.58660819	2.8089055	2	2.3198067	2.582001393	3.69459039	4.45840862	4.4553878	4.4569882	3.1691935	3.5826201	3.8059806
ENSMUSG00000044206	Vsig4	2.178973525	0.0480083	3.46257176	3.70294367	3.91006404	3.45267087	2.803546666	3.31686005	5.92956893	6.3876093	5.6411084	3.4585936	2.5837918	2.8065305
ENSMUSG00000040181	Fmo1	2.153740582	0.0448616	2.80947046	3.17193469	2.32279427	2.80280525	2.995556056	2.99577786	4.75382239	4.9498913	5.1266377	2.5845236	2.9982436	2.5843213
ENSMUSG00000087556	Gm15764	2.153387043	6.63E-18	4.86223324	5.0475718	4.58856814	4.79824119	5.277416118	4.74768681	6.40819937	6.9259558	6.440094	6.8316192	7.2539649	7.2927453
ENSMUSG00000042385	Gzmk	2.09948026	4.86E-05	3.32488899	3.17193469	3.00216447	3.99202864	3.45377331	3.99366215	4.95310728	5.5500663	6.0415883	4.2468879	4.9038448	4.8057055
ENSMUSG00000073551	Spink13	2.08725879	0.0384967	2.80947046	2.32265191	2.58640584	2.3198067	2.582001393	2.8037367	4.58392055	3.5816684	4.0851792	2.5845236	3.3198201	2.5843213
ENSMUSG00000052430	Bmpr1b	2.085421857	0.0361004	3.32488899	4.0902284	3.46218583	3.45267087	3.316593717	3.80131951	3.16923045	3.9962936	2.5839675	5.7801385	6.2634544	6.1067116
ENSMUSG00000059089	Fcgr4	2.054893663	1.77E-06	8.77967355	8.88316802	8.70472388	9.31135653	9.185916183	9.31126854	11.7245433	11.746606	11.710833	9.99021	9.9851836	9.8807267
ENSMUSG00000006642	Tcf23	2.043836649	0.0181576	3.32488899	3.17193469	3.32452507	2.80280525	2.582001393	2.32024072	4.52252907	4.9026068	5.2067896	3.4585936	3.1679733	3.1688562
ENSMUSG00000041608	Entpd3	2.042986086	0.032195	3.46257176	2.58616865	2.32279427	2.3198067	2.320152159	2.99577786	4.39130525	3.9962936	4.6413475	2.5845236	3.5826201	3.3207737
ENSMUSG00000020481	Ankrd36	2.01792237	0.0058397	6.21411868	6.1326921	6.37915695	5.63407184	5.664223877	5.12179534	8.70612067	8.6061315	8.6835426	5.6712117	5.9036102	6.0642797
ENSMUSG00000038305	Spats2l	2.017381088	0.0297183	4.75908943	4.17273779	4.17329055	5.63407184	5.77310734	5.63607788	7.95877159	7.9199501	7.8797067	4.6993254	4.5820339	4.9052229
ENSMUSG00000020681	Ace	1.982492872	1.47E-12	10.0231126	9.91648979	9.89609121	8.77736088	8.705428935	8.83396759	11.5851219	11.547732	11.554959	11.389929	11.257998	11.346807
ENSMUSG00000008845	Cd163	1.978349202	0.0006192	8.04377556	7.93429357	7.63359505	8.35143528	8.470978687	8.43458431	10.7825692	10.896688	10.959192	8.6097212	8.4311539	8.5294778
ENSMUSG00000076490	Trbc1	1.911096199	0.0251135	11.7140094	11.7543182	11.7995488	12.6162182	12.58286024	12.5861067	11.5050589	11.479382	11.468692	15.022784	15.032487	15.026716
ENSMUSG00000045551	Fpr1	1.890132585	0.0039771	5.93534593	5.61803048	5.83691257	5.84807889	6.014015574	5.69263533	8.35191169	8.4708451	8.4233125	5.806132	5.7781007	6.0205618
ENSMUSG00000047592	Nxpe5	1.872796349	1.99E-08	5.7324803	5.75823544	5.86200878	6.09850501	5.945870649	6.40133334	8.26555235	8.219124	8.3144631	7.043117	7.0626793	7.117072
ENSMUSG00000030474	Siglece	1.84370694	0.0015283	7.98213323	8.2275688	8.107550667	7.57454663	7.442513572	7.42636765	10.3419391	10.44525	10.369887	8.1072265	7.99654	8.1829773
ENSMUSG00000021187	Tc2n	1.843530107	0.0230554	3.17266678	3.17193469	3.17232976	3.31555453	3.45377331	3.31686005	5.24680876	5.0400503	5.4235559	2.9993416	2.9982436	3.9985569
ENSMUSG00000028444	Cntfr	1.825073705	0.028657	5.13365172	5.32518239	4.52713629	4.38371152	4.992214091	4.51657958	7.4825933	7.4381134	7.0739172	4.3208746	4.3894726	4.7532483
ENSMUSG00000004885	Crabp2	1.821040293	0.0312778	2.32291573	2.58616865	3.00216447	2.58142511	2.582001393	2.99577786	2.58454581	3.5816684	2.9985073	4.0864558	4.0847757	4.0859914
ENSMUSG00000101389	Ms4a4a	1.789361019	0.0005933	5.55910126	5.32518239	5.36145625	6.52897969	6.515048508	6.77321143	8.57240989	8.4748918	8.2402265	6.8316192	7.1962531	6.6275099
ENSMUSG00000051439	Cd14	1.759368146	0.0054447	6.21411868	6.36099128	6.43038954	6.6045073	6.898286583	6.94601321	9.0782436	9.1397493	8.9942159	6.5378985	6.7647985	6.6275099
ENSMUSG00000015224	Cyp2j9	1.75825452	0.0317202	3.00246783	3.00180885	3.58784774	2.99469065	2.803546666	2.8037367	3.99906228	2.9975301	2.9985073	4.2468879	4.5206589	5.2462057
ENSMUSG00000005131	4930550C14Rik	1.75709698	0.0009812	6.00462373	5.95757876	6.11259974	5.69062254	5.692224792	5.51584262	8.14342549	8.1849485	8.2778222	6.2466798	6.2445977	6.1681075
ENSMUSG00000028546	Elavl4	1.756052708	1.54E-05	4.00370016	4.00271242	3.58784774	2.99469065	3.579034195	3.31686005	5.55344488	5.2050447	4.9515951	4.8568457	4.7518938	4.4578572
ENSMUSG00000055170	Ifng	1.746855991	0.0295625	2.58660819	3.17193469	2.32279427	2.3198067	2.582001393	2.8037367	3.45863601	3.8038253	2.9985073	4.0864558	2.9982436	3.6991077
ENSMUSG00000001864	Aif1l	1.743265365	0.0491135	6.21411868	6.61817789	6.17401072	5.69062254	5.635668724	5.74705896	5.32080275	5.0831014	5.4235559	8.5378559	8.6830197	8.5792962
ENSMUSG00000028957	Per3	1.731367816	5.95E-05	6.41409069	6.41283643	6.11259974	6.0774525	5.968945122	5.99207333	6.61351047	7.0612931	6.8172978	8.4865377	8.4803401	8.3379493
ENSMUSG00000039956	Mrap	1.701963363	0.0012114	6.0707267	5.73126334	5.67641223	6.43279603	6.561329904	6.66430124	8.55335173	8.5147463	8.536204	6.7800906	6.7515029	6.5217212
ENSMUSG00000051359	Ncald	1.692570501	4.24E-08	5.46391545	5.17313917	5.3962317	5.27585864	5.201516736	5.34992256	6.35636259	6.2241389	6.3009452	7.3385655	7.186406	7.4493306
ENSMUSG00000068606	Gm4841	1.683355491	0.0002166	3.00246783	3.32409844	3.32452507	2.80280525	3.579034195	3.31686005	3.80646187	4.5808437	4.6413475	4.7537657	4.4565564	4.1684284
ENSMUSG00000050439	Enthd1	1.677045481	0.0166117	4.46346769	4.3952449	3.46218583	3.45267087	3.900368117	3.80131951	4.16895254	4.3883165	3.9047007	6.2082076	5.9274531	5.8808491
ENSMUSG00000000982	Ccl3	1.633805855	1.05E-09	4.00370016	4.58797599	4.17329055	4.07933474	4.692911159	4.31516673	5.78020026	5.4549378	5.3192401	5.9987653	5.9036102	5.9523961
ENSMUSG00000020811	Wscd1	1.630098733	0.0008134	6.29008118	6.00338973	6.49598681	6.0344028	5.922421116	5.85010914	6.61351047	6.5030684	6.520705	8.4825135	8.2011039	8.2601955
ENSMUSG00000079597	Cstdc4	1.624287397	0.0058219	2.80947046	2.32265191	2.32279427	3.45267087	3.45377331	3.31686005	4.39130525	4.2440258	3.9977603	4.0864558	3.9043138	3.6991077
ENSMUSG00000048899	Rimkla	1.61221484	0.0369047	3.17266678	2.8089055	3.00216447	2.58142511	4.240904489	3.57933023	4.08650672	3.5816684	3.5829719	4.7537657	4.9511354	5.2462057
ENSMUSG00000111354	Gm33914	1.607062325	0.0244665	2.80947046	3.17193469	3.17232976	3.31555453	2.320152159	2.32024072	4.32092783	3.5816684	4.3898999	3.4585936	3.8048451	3.3207737
ENSMUSG00000044927	H1f10	1.601457821	0.0315886	4.86223324	5.0906534	4.91064028	4.79824119	4.240904489	4.45251622	4.52252907	4.6397044	4.4569882	6.9760047	6.8420975	7.042528
ENSMUSG00000020090	Npffr1	1.585630454	0.0297166	4.64799974	5.36081511	5.04819618	2.99469065	3.45377331	3.31686005	5.04329531	5.2809661	5.0848276	6.1485043	6.3004439	6.3380206
ENSMUSG00000025934	Gsta3	1.552956359	0.0395583	4.81158291	4.70349952	4.86171081	4.89767527	5.48374496	5.45174579	7.22760162	7.0612931	7.4808956	4.64275	4.9038448	4.8057055
ENSMUSG00000005237	Dnah2	1.547511161	0.0261657	5.13365172	5.2511628	5.3258218	5.82300082	6.181412124	5.85010914	7.812553	7.8899571	7.8674288	5.4906532	5.6691864	5.3201962
ENSMUSG00000048215	A630023P12Rik	1.543025338	0.0421628	5.2138525	5.2511628	4.81106345	4.79824119	5.079611326	4.57791872	4.39130525	5.0831014	4.4569882	7.1072456	7.1361362	7.2172957
ENSMUSG00000047678	Gpr82	1.516011032	0.0255605	3.32488899	3.17193469	3.91006404	3.57787902	3.694282913	2.99577786	5.24680876	4.7506771	5.3896152	3.6995281	3.5826201	3.9054796
ENSMUSG00000035448	Ccr3	1.513961505	0.0018557	8.08700782	8.14311557	8.07035042	8.70027006	8.71910307	8.68162345	10.5408175	10.572498	10.608968	8.7668794	8.7811518	8.719193
ENSMUSG00000095788	Sirpb1a	1.509829569	0.0001637	5.7324803	5.55789694	5.86200878	5.27585864	5.746647149	5.48415014	7.64263078	7.5029595	7.5969875	6.1485043	6.1464304	6.3380206
ENSMUSG00000079076	Gm3086	1.503018624	0.014786	3.32488899	3.70294367	3.32452507	4.23953538	4.452152566	4.38547538	5.92956893	5.8780348	5.3192401	4.2468879	4.8043426	4.1684284
ENSMUSG00000079507	H2-Q1	1.497217623	2.38E-07	7.91173999	7.79145263	7.71848894	6.64799599	6.772782753	6.73332735	9.01556751	9.1010005	8.8888219	8.6604741	8.5814842	8.7123394
ENSMUSG00000030711	Sult1a1	1.493655249	0.0221983	7.06006581	6.89831182	6.63350779	7.18932456	7.002602482	7.32267092	9.28646995	9.2781762	9.1942501	6.7800906	7.0078214	6.6563633
ENSMUSG00000034220	Gpc1	1.488692394	0.0005159	6.95896894	7.22268701	6.87454274	7.8904072	7.712366832	7.75988327	8.1125098	8.0931604	7.8735809	9.4601699	9.3973853	9.5584186
ENSMUSG00000025885	Myo5b	1.487409412	0.0174422	5.17430934	5.13248572	5.28928485	4.38371152	3.99332894	3.69459039	5.04329531	5.3530911	4.9515951	6.7536193	6.7647985	6.3904846
ENSMUSG00000120321	Gm51802	1.48033752	2.37E-07	5.09181499	5.003164	4.09077189	4.99069578	5.079611326	4.99260313	6.50659919	6.4871292	6.6695556	5.7801385	5.9739884	5.9289391
ENSMUSG00000026712	Mrc1	1.477744609	7.03E-05	10.4153683	10.2727304	10.3890965	10.9097366	10.90101003	10.87344	12.6214886	12.694415	12.671869	11.253123	11.308806	11.23887
ENSMUSG00000033508	Asprv1	1.441381434	7.01E-05	3.17266678	3.4617334	3.32452507	4.16165755	3.801002232	4.16335188	5.04329531	4.7506771	4.6413475	5.1281166	4.8043426	4.8057055
ENSMUSG00000022181	C6	1.441208548	0.000603	8.87525409	8.81736453	8.85603734	9.07424874	9.107506694	9.06842175	11.001567	10.996474	11.017304	9.3273661	9.4803205	9.2625306
ENSMUSG00000004709	Cd244a	1.438883559	6.67E-05	6.5438785	6.17333981	6.23291401	6.21874975	5.824614865	5.96936166	8.05946424	8.0612192	8.0469067	6.9175898	6.7245383	6.8054992
ENSMUSG00000020682	Mmp28	1.434731634	0.0261657	4.46346769	4.00271242	4.58856814	3.89909685	3.694282913	4.24125532	6.12810407	6.1450822	5.7251591	4.64275	4.1671919	4.0859914
ENSMUSG00000091971	Hspa1a	1.408500479	0.0004426	3.8108791	3.00180885	3.91006404	3.89909685	3.694282913	3.80131951	5.04329531	5.1655312	5.1266377	4.64275	4.3191168	4.3907597
ENSMUSG00000042961	Egflam	1.395983545	0.0299155	5.75945423	5.13248572	5.75889322	5.19996894	4.992214091	5.27781519	7.27490625	7.3874914	7.4889326	5.1281166	5.4886509	5.2836752
ENSMUSG00000018930	Ccl4	1.393347675	1.37E-05	4.09123546	3.4617334	4.17329055	3.6930831	4.516212395	4.08100044	5.12817554	5.0831014	5.3896152	5.3563635	4.7518938	5.3905763
ENSMUSG00000059657	Stfa2l1	1.383826498	0.049347	3.00246783	2.8089055	2	3.6930831	3.694282913	3.57933023	4.39130525	4.2440258	4.5210949	3.4585936	4.4565564	3.8059806

ENSMUSG00000015854	Cd5l	1.372277129	0.0112117	11.0547707	11.0690248	11.0575647	10.2771082	10.28689573	10.2987709	12.7625851	12.749111	12.771802	10.834736	10.819064	10.810257
ENSMUSG00000054072	Iigp1	1.356089732	9.06E-30	8.04925097	8.3478669	8.4921176	8.19407762	8.120508951	8.01957931	9.73515736	9.6586386	9.6957321	9.2933121	9.4311336	9.4819021
ENSMUSG00000078190	Dnm3os	1.351121881	0.031713	4.25182216	4.0902284	3.81044603	4.94493511	4.850310455	4.74768681	6.20827055	6.5498556	6.0846517	4.4583541	4.9038448	4.5833589
ENSMUSG00000062380	Tubb3	1.347486732	4.97E-08	6.83764871	6.91038566	6.7456312	7.18932456	7.598611844	7.36678712	8.75364865	8.8989793	8.6336677	8.0967343	7.9390567	8.1928587
ENSMUSG00000025355	Mmp19	1.346021271	0.000798	5.75945423	6.1326921	5.86200878	6.61914967	6.450935812	6.515474	8.12288881	7.9551375	8.1107984	6.806085	6.6831222	6.8310331
ENSMUSG00000035042	Ccl5	1.319536213	0.0004292	5.17430934	5.36081511	5.91092831	6.23785108	6.483348273	6.38426458	7.72669362	7.6245127	7.6117839	6.7536193	6.8545874	6.6275099
ENSMUSG00000015947	Fcgr1	1.313112517	0.0007776	6.61944034	6.64732718	6.67658164	6.95548763	7.024794002	7.16170391	8.68175632	8.591297	8.7519282	7.2178869	7.4228316	7.2460537
ENSMUSG00000030087	Klf15	1.308463239	0.0238154	5.32636716	5.55789694	4.70410076	5.16047261	5.349521258	5.03696515	7.22760162	6.9838967	6.962893	5.3563635	5.2822481	5.1275786
ENSMUSG00000102748	Pcdhgb2	1.298948604	0.0313441	3.70385559	2.8089055	2.58640584	3.31555453	4.080660667	2.99577786	4.39130525	3.9962936	4.0851792	3.9990123	4.8043426	4.0859914
ENSMUSG00000063415	Cyp26b1	1.279844905	0.0041252	5.7324803	5.46271875	5.86200878	6.0774525	5.968945122	6.079505	7.76695684	7.6317802	7.5669316	6.0648508	6.1464304	6.3200999
ENSMUSG00000027954	Efna1	1.267903381	0.0437339	5.75945423	5.83625203	5.73192013	5.07808018	4.946446378	3.99366215	5.55344488	5.7233502	5.2827219	7.1983912	7.0409858	7.117072
ENSMUSG00000071716	Apol7e	1.265367583	4.31E-07	6.95896894	6.73139962	6.60406041	5.71808778	5.968945122	6.2208143	7.91165967	7.8716573	7.4808956	7.3824188	7.5664147	7.6491655
ENSMUSG00000095028	Sirpb1b	1.25418795	0.023827	4.25182216	4.58797599	4.52713629	4.69144319	4.992214091	5.24036336	6.24674292	6.6246128	6.3894728	5.3207428	4.5206589	4.9525203
ENSMUSG00000078922	Tgtp1	1.247814368	0.0002397	7.03820412	7.13279528	7.08101331	6.75793781	6.785835982	6.78626481	7.46638339	7.4463804	7.3721245	8.6097212	8.6149063	8.6985338
ENSMUSG00000079018	Ly6c1	1.246490667	3.57E-05	7.94148901	7.8364421	7.86223222	7.59691102	7.506993378	7.44294829	9.40176898	9.4108268	9.3257065	8.3296162	8.1863578	8.3947032
ENSMUSG00000045502	Hcar2	1.233419489	0.0009736	6.86274267	7.10154208	7.26160061	6.84771084	6.719355744	6.99180835	8.76363266	8.6208151	8.7009453	7.3824188	7.3003549	7.4410633
ENSMUSG00000005413	Hmox1	1.226379242	0.0079159	11.6839656	11.7148479	11.7060601	11.7074791	11.75887927	11.7745512	13.5835951	13.57814	13.57279	11.808854	11.796175	11.831363
ENSMUSG00000078780	Gm5150	1.223223821	0.003342	5.9114938	5.75823544	5.95824332	5.87272847	5.692224792	5.72010376	7.5986882	7.378879	7.5745045	6.0431569	6.0627843	6.2649621
ENSMUSG00000069792	Wfdc17	1.206534765	7.84E-05	7.81219846	7.8364421	7.79866373	8.8032378	8.66361126	8.68511223	9.84581235	9.791118	9.9248033	9.1124347	9.1411681	9.1013773
ENSMUSG00000062661	Ncs1	1.205531226	0.0303741	4.52763697	4.81045442	4.32538969	4.94493511	4.577548304	4.24125532	4.45840862	4.85372	4.804795	6.0862233	6.0841549	6.4575947
ENSMUSG00000117485	Gm19696	1.199230674	7.82E-05	3.91050864	4.25078255	4.17329055	3.57787902	4.314811199	4.38547538	5.35642361	4.85372	5.1266377	4.9057492	5.0843618	5.3558154
ENSMUSG00000106438	Gm32051	1.19244001	0.0313241	7.49667514	7.6473994	7.51993112	6.97838265	7.181167553	6.96909248	9.16868325	9.1849145	9.1133785	7.2081719	7.3094565	7.2075809
ENSMUSG00000028967	Errfi1	1.188126433	0.0002816	6.7596366	6.3957609	6.47986499	7.05576959	7.09988163	6.89871662	8.48660354	8.4171786	8.2778222	7.2933373	7.4641701	7.2742496
ENSMUSG00000030088	Aldh1l1	1.177837161	0.0001262	5.58948364	5.64718272	5.4633646	6.55966682	6.746316554	6.45136042	7.12806832	7.1347479	7.0951324	7.498558	7.263363	7.6054453
ENSMUSG00000073555	Gm4951	1.174891247	1.54E-05	6.02699627	5.93411597	6.66236611	6.48168928	6.450935812	6.65009068	7.88751393	7.9435035	7.7181689	6.8567094	7.1764912	7.2835271
ENSMUSG00000004359	Spic	1.170911007	0.0113104	9.46842793	9.63477427	9.50414772	9.64941038	9.557199537	9.62458126	11.3974951	11.357555	11.325132	9.5986026	9.7090288	9.5924101
ENSMUSG00000027488	Snta1	1.162500152	0.0065175	5.7324803	5.93411597	5.73192013	6.23785108	6.100140376	5.92283673	7.64982615	7.6245127	7.5284591	6.1686812	6.2820677	6.1479311
ENSMUSG00000021453	Gadd45g	1.160929726	1.82E-30	8.53235509	8.61090871	8.70125159	8.33378902	8.417466959	8.10540797	9.57618494	9.5668347	9.5573617	9.6189095	9.6812507	9.6828335
ENSMUSG00000047798	Cd300lf	1.156608499	0.0014401	7.52052367	7.70398571	7.3261458	7.84752678	7.824145038	7.61376735	9.26554423	9.301149	9.3212122	7.9412189	8.0733527	8.00373
ENSMUSG00000057378	Ryr3	1.154887553	0.0229388	4.95849239	4.32482117	4.86171081	4.7458302	4.577548304	4.63675592	6.10734654	5.8780348	6.6118449	5.0863008	4.5206589	5.1275786
ENSMUSG00000056486	Chn1	1.15453982	0.0008282	3.588252	3.5873738	3.81044603	4.23953538	3.900368117	3.80131951	4.80628319	4.7506771	5.0848276	4.5838651	4.5820339	4.6422398
ENSMUSG00000023913	Pla2g7	1.154129381	0.0207044	8.90273562	8.88316802	8.88998554	9.69504523	9.605853781	9.4591968	11.0835603	10.953619	11.087793	9.3385411	9.3995178	9.3109706
ENSMUSG00000066363	Serpina3f	1.151086701	0.0001003	7.16466507	6.88613607	6.96997176	7.98388262	7.957025524	8.28627212	8.75364865	8.9463808	8.8643174	8.7232093	8.7514051	8.6201469
ENSMUSG00000022257	Laptm4b	1.144331724	0.0026227	7.51261788	7.51923634	7.47996206	6.89660817	6.649663449	6.89871662	7.53015807	7.6533656	7.6765515	8.7865975	8.8699591	8.7260141
ENSMUSG00000024529	Lox	1.140649138	0.0056506	5.95881011	6.2128736	6.17401072	6.46557494	6.759610343	6.4676579	7.83797521	8.0878858	8.0026841	6.5837004	6.7108646	6.6705764
ENSMUSG00000072720	Myo18b	1.136985479	0.0001606	4.3258746	5.21267838	5.1737707	4.79824119	4.314811199	4.80010939	6.10734654	5.8533786	6.1469286	5.8567548	5.4562365	5.4245194
ENSMUSG00000052957	Gas1	1.134132543	0.0391585	4.00370016	4.70349952	4.86171081	4.89767527	4.850310455	5.03696515	5.95302658	6.3876093	6.5517291	4.7537657	4.9969249	4.9052229
ENSMUSG00000035873	Pawr	1.133034895	0.0131976	3.91050864	4.32482117	5.04819618	4.84881472	5.036574414	5.66463374	5.64270583	5.6393084	5.1672702	6.1686812	6.2820677	6.3557215
ENSMUSG00000087384	Gm15558	1.118865945	7.46E-08	6.49656573	6.51125134	6.88682232	6.97838265	7.17125377	6.89871662	8.21793488	8.2094419	8.1619616	7.6207615	7.5815208	7.6491655
ENSMUSG00000050493	Fam167b	1.118621793	0.0155165	5.46391545	6.41283643	5.95824332	5.66262426	5.451341511	5.45174579	7.54567078	7.378879	7.0845638	5.9987653	6.1259691	6.0205618
ENSMUSG00000081219	Bambi-ps1	1.115384027	0.0003126	9.35141493	9.35674017	9.43892895	8.44069483	8.49899114	8.63187329	9.68700594	9.7195933	9.6282052	10.480486	10.419611	10.501907
ENSMUSG00000030148	Clec4a2	1.113191806	0.0243288	7.24320577	7.22268701	7.16407621	8.31592423	8.166147644	8.22527572	9.49860236	9.3916902	9.4747881	8.0210711	8.0463867	8.026011
ENSMUSG00000032942	Ucp3	1.110666621	0.0103659	5.52806525	5.13248572	5.00378569	5.38269568	5.12140151	5.08000365	6.84428313	6.8154103	6.5517291	5.2842203	5.6114821	5.5218049
ENSMUSG00000032246	Calml4	1.10835106	0.0027511	4.25182216	3.8099383	4.46297179	3.79976415	3.801002232	3.45405584	5.12817554	4.9498913	5.0417695	4.8568457	4.6974661	4.3907597
ENSMUSG00000114369	Gm41077	1.10047964	0.0166682	5.86257288	5.88601365	6.25202586	6.44927858	6.220393213	5.99207333	7.73348268	7.7960448	7.6835716	6.0862233	6.4229134	6.2649621
ENSMUSG00000055150	Zfp78	1.09595329	0.0050803	3.588252	3.70294367	4.17329055	3.57787902	3.900368117	3.57933023	4.32092783	4.2440258	4.5210949	4.9057492	4.9511354	4.6422398
ENSMUSG00000052270	Fpr2	1.094051639	0.0301596	5.04872871	5.0475718	5.52751202	4.7458302	5.546446959	5.48415014	6.6992374	7.0504874	6.6695556	5.2467492	5.520353	5.4245194
ENSMUSG00000016529	Il10	1.09271069	0.0150737	5.67697062	5.70377736	5.5585469	6.71768502	6.499285457	6.38426458	7.61348494	7.7699336	7.6835716	6.5223022	6.5044343	6.4411076
ENSMUSG00000075410	Prcd	1.091847333	0.0398543	3.70385559	3.32409844	3.00216447	3.16402452	3.579034195	3.31686005	3.80646187	3.4562874	3.9977603	4.3912513	4.4565564	4.3907597
ENSMUSG00000085795	Zfp703	1.074170266	1.38E-07	8.93858183	8.79148531	8.71853007	8.33822086	8.409055326	8.38396172	9.99875445	9.8898946	9.9857095	9.2631341	9.3737167	9.3731265
ENSMUSG00000026018	Ica1l	1.073411635	5.39E-06	5.7324803	5.73126334	5.81137207	4.94493511	5.036574414	5.03696515	6.49065826	6.6246128	6.4565805	6.1686812	6.4229134	6.3904846
ENSMUSG00000021710	Nln	1.068732402	5.48E-08	9.50674147	9.42985919	9.44931575	9.71221977	9.633194774	9.75811119	10.9161242	10.970914	11.004046	10.178597	10.325171	10.251929
ENSMUSG00000026011	Ctla4	1.066366487	0.0007163	6.29008118	6.55805062	6.66236611	6.79709791	6.886216252	6.6212426	7.12806832	7.0612931	7.0305273	8.0539852	8.1258183	8.1529207
ENSMUSG00000058818	Pirb	1.065180033	0.0186079	9.08171058	9.05887072	8.89303249	8.95234329	9.03008527	9.00841711	10.6417069	10.655064	10.696593	8.9557956	9.0188799	9.0802388
ENSMUSG00000031298	Adgrg2	1.063693991	0.0452246	5.64839374	5.64718272	5.58892821	5.1198645	5.12140151	5.03696515	6.9760692	6.9609988	6.9159751	5.3207428	5.6114821	5.2462057
ENSMUSG00000027962	Vcam1	1.063222666	0.0092361	12.6237726	12.6127919	12.6749793	13.0407456	13.06624736	13.0813287	14.4697263	14.47079	14.499286	13.01375	13.039343	13.021311
ENSMUSG00000021567	Nkd2	1.060530853	0.009618	5.70499242	5.67575754	5.52751202	5.41661938	5.384265947	5.48415014	5.88147742	5.5804312	5.8552002	7.1280036	7.1155274	6.8054992
ENSMUSG00000038702	Dsel	1.057716783	0.0107457	5.04872871	5.42954425	5.36145625	5.99002889	6.239495772	5.82502842	6.16874406	5.7767759	6.3721965	7.0099511	7.3094565	7.0093625
ENSMUSG00000050105	Grrp1	1.056746936	0.0029387	4.86223324	5.003164	4.52713629	5.07808018	5.664223877	5.48415014	6.0432195	6.40468	6.6695556	5.699224	5.520353	6.0856516
ENSMUSG00000016458	Wt1	1.055317726	0.03369	5.49634687	5.75823544	5.75889322	5.19996894	5.384265947	5.41859685	7.10731028	7.0504874	7.0523854	5.6712117	5.3891376	5.6129426
ENSMUSG00000070369	Itgad	1.05107292	0.0429154	10.6577642	10.5427645	10.6051567	10.2561829	10.25674244	10.2595279	12.1315717	12.165924	12.111409	10.256075	10.311646	10.285794
ENSMUSG00000038007	Acer2	1.049573575	0.0053738	6.66294795	6.61817789	6.8496655	7.07713855	7.220155162	7.22058818	8.52624013	8.506863	8.385066	7.2178869	7.3003549	7.2269456
ENSMUSG00000032554	Trf	1.048039018	2.03E-06	10.9349194	10.86547	10.8739103	11.3638739	11.3370717	11.3811873	12.5070404	12.512237	12.495864	11.830388	11.776208	11.767502
ENSMUSG00000074677	Sirpb1c	1.046595026	0.0204598	4.3258746	4.64689376	4.58856814	4.7458302	4.850310455	5.24036336	6.32074021	6.1450822	5.9514022	5.0432368	5.166801	4.8563221
ENSMUSG00000059498	Fcgr3	1.045287348	0.0116492	9.31778344	9.22033702	9.29201043	10.5031185	10.36833577	10.4993613	11.4276349	11.423423	11.412759	10.482502	10.499327	10.472801
ENSMUSG00000050503	Fbxl22	1.040489959	0.0002225	6.66294795	6.61817789	6.39643742	6.9322234	6.691881486	6.86219799	8.1586384	8.0449794	8.089814	7.0321462	7.1764912	7.3556745
ENSMUSG00000037161	Mgarp	1.027190649	0.0263374	3.70385559	3.5873738	3.32452507	3.6930831	4.163006272	3.45405584	4.69938173	4.5194791	4.8554064	3.9059249	3.9973646	4.5219723
ENSMUSG00000075010	AW112010	1.026573344	0.0018557	9.29261232	9.36553726	9.32397078	10.2289956	10.19325252	10.2571859	11.2063762	11.24477	11.222225	10.458118	10.354048	10.378542
ENSMUSG00000037095	Lrg1	1.025607307	0.0157834	8.91478359	8.98658046	8.86226945	8.61152191	8.541940407	8.51911228	10.319554	10.372281	10.291643	8.9499783	8.6969586	8.886835
ENSMUSG00000046727	Cystm1	1.02496406	0.0231213	5.09181499	5.13248572	5.00378569	5.19996894	5.384265947	5.57721245	6.78015477	6.6817489	6.6118449	5.6712117	5.2063188	5.3201962
ENSMUSG00000008540	Mgst1	1.019282618	0.0121948	7.52052367	7.27030818	7.37054319	8.40311487	8.502948884	8.49148293	9.44996783	9.4338765	9.4064215	8.3780772	8.4436086	8.6310901
ENSMUSG00000020325	Fstl3	1.017436059	0.0391495	7.71219636	7.55043265	7.61894739	7.33835186	7.467032452	7.60642626	9.21792648	9.1725098	9.1133785	7.3562671	7.4803794	7.5603587
ENSMUSG00000001240	Ramp2	1.010163658	0.0367043	7.17471969	7.36107936	7.17413071	6.78416229	6.515048508	6.59180588	8.50655795	8.591297	8.4564786	7.1686446	7.0300155	6.8310331
ENSMUSG00000032549	Rab6b	1.009936775	0.0083023	7.08160117	7.06959683	7.18411563	6.0344028	6.057720555	5.38466829	7.53793528	7.5725886	7.5516655	7.5761394	7.7514377	7.5830781
ENSMUSG00000034271	Jdp2	1.006194766	0.0056562	6.4804436	6.55805062	6.75905321	7.7174836	7.642327755	7.60642626	8.5495097	8.5875644	8.4316758	7.7535949	7.848295	7.8246579
ENSMUSG00000014782	Plekhg4	-1.002047603	0.0354224	6.30846291	6.37848083	6.44707059	5.74503992	5.162015167	5.54685383	4.39130525	4.7506771	4.4569882	5.2082788	5.8547087	5.3201962
ENSMUSG00000036466	Megf11	-1.006170142	0.0029387	4.52763697	5.2511628	4.91064028	5.41661938	5.515436574	5.60694538	4.39130525	4.4553878	4.1676023	4.1689007	4.4565564	4.6422398
ENSMUSG00000079177	Fam228a	-1.009192353	0.0155034	4.81158291	5.49514752	5.25179848	4.4507334	5.277416118	4.51657958	4.58392055	3.8038253	4.2455699	4.3912513	3.6980072	4.1684284
ENSMUSG00000073538	E330020D12Rik	-1.009735519	0.0317202	4.91116549	4.32482117	4.17329055	5.16047261	4.850310455	4.89956435	2.99937492	3.9032667	4.0851792	3.6995281	4.3894726	4.2464084
ENSMUSG00000036698	Ago 2	-1.010235082	0.0024135	12.3807817	12.2288199	12.3208867	11.0378687	11.11264793	11.0710438	10.805302	10.807244	10.779199	10.777584	10.871474	10.834919
ENSMUSG00000050600	Zfp831	-1.017519654	0.0117188	5.81193468	5.83625203	6.13336188	7.16956531	7.07882382	7.12106866	5.92956893	5.6393084	5.2827219	5.6135004	5.6114821	5.9523961
ENSMUSG00000021680	Crhbp	-1.024015514	0.0041341	6.89958372	6.77166724	6.7985859	7.50529491	7.475113678	7.46746735	5.67127302	5.5804312	5.5822247	6.7129787	6.5044343	6.6563633
ENSMUSG00000020427	Igfbp3	-1.024875406	0.0429154	7.49667514	7.64016747	7.6115674	9.30684125	9.34870483	9.36445956	7.74023993	7.6245127	7.8858067	7.8252547	7.5279426	7.5830781
ENSMUSG00000076757	Trgc4	-1.028128608	1.89E-05	10.0533997	10.1457097	10.005717	10.8285888	10.83110894	10.8133361	9.2106463	9.2781762	9.1288913	9.700862	9.7909167	9.5868002
ENSMUSG00000070498	Tmem132b	-1.033112273	0.0033765	9.04655323	9.06967768	8.85915676	10.218216	10.23430183	10.1838651	8.8284833	8.8899154	8.9512334	8.4581296	8.4763047	8.5216584
ENSMUSG00000045410	Akr1e1	-1.046014034	0.0003015	7.24320577	7.4129214	7.28033863	8.00633488	7.830458128	8.06313181	6.8567737	6.9377316	7.0951324	6.4581745	5.9274531	6.3904846
ENSMUSG00000058881	Zfp516	-1.046216297	0.0009318	7.45603003	7.59599763	7.48804495	8.56312098	8.68118283	8.54238058	7.20823674	6.9494121	6.9513058	7.117662	7.1258686	7.3818259
ENSMUSG00000098799	Trgj4	-1.046454164	0.0090191	5.67697062	5.81071241	6.04845802	7.11894976	7.06817852	6.84981676	5.32080275	5.2050447	5.5518563	5.699224	5.829622	5.6986634
ENSMUSG00000076433	Cep295nl	-1.047520521	0.0201876	4.46346769	4.58797599	4.91064028	4.79824119	4.850310455	3.90069389	3.45863601	3.5816684	3.3201366	4.0864558	4.3191168	3.8059806
ENSMUSG00000096255	Dynlt1b	-1.060851286	1.16E-76	9.70187525	9.71268199	9.66786249	9.80158651	9.681139592	9.77621664	8.70266514	8.5838221	8.6190952	8.6569075	8.7974165	8.6563061
ENSMUSG00000077797	Snord19	-1.061848137	0.0341019	5.13365172	5.49514752	5.133115	4.38371152	4.314811199	3.99366215	3.99906228	3.8038253	3.9977603	3.5840846	4.3191168	4.0859914
ENSMUSG00000047880	Cxcr5	-1.064520704	0.0204923	6.34453832	6.41283643	6.63350779	6.78416229	6.677945629	7.02522529	4.95310728	5.0400503	4.4569882	6.3206769	5.8040913	6.3557215
ENSMUSG00000041779	Tram2	-1.072895597	0.0078559	5.88724069	5.86134738	5.83691257	6.75793781	6.957168369	7.01417209	4.80628319	5.3530911	5.520835	5.5837553	6.0190694	5.3201962
ENSMUSG00000072941	Sod3	-1.078507638	0.0043155	8.2384857	8.28897136	8.11800549	9.53245077	9.620500096	9.58030203	7.83166153	7.8899571	8.0026841	7.9412189	8.099824	8.127386
ENSMUSG00000028392	Bspry	-1.090888793	0.0025105	4.95849239	5.46271875	4.86171081	6.01238644	5.898584129	5.72010376	4.75382239	4.6397044	4.2455699	4.9057492	4.5820339	4.3203887
ENSMUSG00000025026	Add3	-1.098223881	0.0006749	8.49271663	8.57722471	8.5892432	9.73087858	9.675890398	9.73304995	8.37380407	8.2988995	8.2258716	8.0485514	7.9390567	8.020473
ENSMUSG00000030849	Fgfr2	-1.101099672	0.0397708	3.91050864	3.32409844	4.39582017	4.23953538	4.452152566	4.63675592	3.45863601	3.3189638	3.805222	3.4585936	2.9982436	3.4582072
ENSMUSG00000116895	Gm3435	-1.104863387	0.0001102	5.81193468	5.81071241	5.75889322	5.63407184	5.635668724	4.94683362	4.16895254	4.85372	4.8554064	4.3208746	4.7518938	4.8057055
ENSMUSG00000025558	Dock9	-1.1054027	0.026321	9.43744485	9.44860956	9.59301789	8.22790785	7.939610206	8.12094751	7.14853192	7.1850163	7.3807889	8.3474273	8.2957377	8.2648871
ENSMUSG00000040183	Ankrd6	-1.106314699	5.44E-07	7.9935386	7.81090587	7.88076912	8.52475219	8.587380424	8.64267941	6.89360938	6.9609988	7.1869195	7.3910318	7.4559966	7.2075809
ENSMUSG00000054999	Naaladl1	-1.108587165	0.0404492	7.27159011	7.35225497	7.2330292	5.7974791	5.77310734	5.45174579	6.06491344	5.9022768	5.752122	5.2467492	5.166801	5.5528283
ENSMUSG00000025461	Scart1	-1.108745535	0.0003814	10.2972374	10.1647347	10.1515154	10.4219345	10.3930709	10.5374958	8.60978716	8.4586366	8.5477917	9.7094957	9.6385543	9.7378651
ENSMUSG00000067586	S1pr3	-1.113544677	1.15E-09	6.02699627	6.09086585	6.17401072	6.52897969	6.366568068	6.27738043	5.20833817	5.4217814	5.1266377	5.1687544	5.2447829	5.1682145
ENSMUSG00000036863	Syde2	-1.118046865	0.028335	6.27146222	6.88613607	6.75905321	5.44976368	5.719692575	5.31431933	4.95310728	5.2050447	3.9977603	5.3911259	5.4230771	5.5528283
ENSMUSG00000023267	Gabrr2	-1.126869128	0.0347622	3.8108791	3.5873738	4.09077189	4.89767527	4.577548304	4.38547538	3.45863601	3.3189638	3.1682663	3.4585936	3.5826201	3.8059806
ENSMUSG00000041193	Pla2g5	-1.137787203	0.0283189	5.64839374	5.42954425	4.81106345	6.52897969	6.663873842	6.73332735	5.55344488	5.3530911	5.2827219	4.8062261	4.8043426	4.4578572
ENSMUSG00000032207	Lipc	-1.149288633	0.0102117	4.70461358	4.3952449	4.32538969	4.16165755	3.801002232	4.74768681	3.45863601	3.1671805	3.805222	3.6995281	3.4571958	3.5836798
ENSMUSG00000025207	Sema4g	-1.162333469	0.0085103	6.69124078	6.81084139	6.88682232	7.82243903	8.046515082	7.9224197	5.61356153	5.6958767	6.0415883	6.6134466	6.9154646	6.7123944
ENSMUSG00000115762	Gm34907	-1.164551125	0.0041252	5.17430934	4.32482117	4.46297179	4.5761027	4.452152566	4.38547538	3.45863601	3.8038253	3.805222	3.321138	3.8048451	3.9054796
ENSMUSG00000025780	Itih5	-1.169037412	0.0103638	9.17482226	9.16598155	9.10232625	8.06098283	8.166147644	7.87433013	6.61351047	6.9609988	6.9159751	8.0539852	7.9680847	8.0315279
ENSMUSG00000112963	Gm6093	-1.17462309	1.39E-06	5.88724069	6.25135289	6.46356097	5.60494292	5.799090957	6.03645139	4.8569031	4.7506771	5.2067896	5.1281166	4.9511354	4.8563221
ENSMUSG00000076606	Igkj3	-1.178496227	0.0333932	4.46346769	4.70349952	4.09077189	5.69062254	5.799090957	5.51584262	3.69957415	3.9032667	4.0851792	4.0864558	4.3894726	4.7532483
ENSMUSG00000070469	Adamtsl3	-1.180814461	0.0036128	4.3258746	4.81045442	4.52713629	5.23841273	4.992214091	5.12179534	3.45863601	3.4562874	3.9047007	4.4583541	3.9043138	4.0859914
ENSMUSG00000041538	H2-Ob	-1.182047064	0.0014073	8.00485452	7.89837251	7.89299604	8.15943499	8.335504181	8.19133107	5.95302658	6.3351506	6.1057108	7.3995936	7.4144198	7.5138174
ENSMUSG00000052912	Smarca5-ps	-1.187443277	0.0464673	4.00370016	3.9095428	4.39582017	3.79976415	3.579034195	3.57933023	2.32167809	3.4562874	3.3201366	3.321138	2.9982436	3.1688562
ENSMUSG00000105703	Gm43305	-1.194371428	0.0420977	10.2634814	10.2360244	10.2827612	10.2863119	10.24969357	10.2976318	7.55336503	7.5343214	7.7586194	9.7931048	9.7312112	9.8498329
ENSMUSG00000030660	Pik3c2a	-1.198278445	7.82E-05	8.60850717	8.49943045	8.65891885	9.76254971	9.727542183	9.62276317	8.27953643	8.0175001	8.1819295	8.037622	7.9738208	7.8746252
ENSMUSG00000003379	Cd79a	-1.199569947	0.0020327	8.00485452	8.24197234	8.14381578	8.98379888	9.049157112	9.01119943	6.71304274	7.0175762	6.6836297	7.7996065	8.0299617	7.8746252
ENSMUSG00000020363	Gfpt2	-1.200350147	0.023477	5.9114938	6.06948903	6.15382946	5.16047261	5.036574414	5.20191333	4.16895254	3.9032667	3.9047007	5.553384	4.4565564	4.8563221
ENSMUSG00000024793	Tnfrsf25	-1.214167915	0.0403755	4.00370016	3.8099383	3.32452507	3.99202864	3.900368117	3.45405584	2.80681915	3.3189638	2.9985073	2.9993416	2.8058495	3.1688562
ENSMUSG00000026866	Kynu	-1.218912651	0.0302815	5.13365172	5.36081511	5.36145625	6.96698055	6.910256766	6.92255873	4.80628319	4.9498913	4.7523434	5.6712117	5.4230771	5.3905763
ENSMUSG00000074607	Tox2	-1.227760288	2.38E-05	8.10289166	8.16847203	8.12320462	8.96958585	8.945366698	8.86198054	6.98747365	7.0175762	6.86748	7.7469003	7.5815208	7.7596622

ENSMUSG00000051379	Flrt3	-1.232971136	0.048264	3.70385559	4.00271242	4.58856814	5.07808018	5.036574414	4.57791872	2.99937492	3.3189638	3.805222	2.9993416	4.3894726	3.8059806
ENSMUSG00000024617	Camk2a	-1.247272209	0.0144383	8.51663015	8.4298382	8.41790296	6.92044908	6.836898977	6.957599	6.61351047	5.9022768	5.9971999	7.0099511	6.996595	7.0315573
ENSMUSG00000060275	Nrg2	-1.247618156	1.70E-16	7.09224949	7.14306434	7.12314247	7.50529491	7.258116828	7.59904762	6.32074021	6.0397503	6.0632807	6.0648508	6.1052135	5.9981959
ENSMUSG00000045441	Gprin3	-1.256048284	0.0004124	5.25234065	4.64689376	4.81106345	5.38269568	5.079611326	4.85069372	4.58392055	3.9032667	3.9977603	3.9059249	3.9043138	3.4582072
ENSMUSG00000054672	Scart2	-1.272668525	0.0227143	5.61923936	5.88601365	5.88667588	7.57454663	7.779162544	7.68519417	5.85681683	6.0828102	5.8798588	5.699224	5.6114821	5.7261413
ENSMUSG00000027718	Il21	-1.275021283	0.0223871	4.46346769	4.0902284	5.00378569	5.1198645	5.515436574	5.45174579	3.32117796	3.9962936	3.1682663	3.8064143	4.4565564	4.5833589
ENSMUSG00000057777	Mab21l2	-1.27816786	0.0037991	4.81158291	4.95734574	5.04819618	4.23953538	4.38511559	4.16335188	2.99937492	3.5816684	3.5829719	3.8064143	3.6980072	4.0859914
ENSMUSG00000028051	Hcn3	-1.28126743	0.0083073	6.58968881	6.30721334	6.44707059	5.41661938	5.48374496	5.24036336	4.32092783	3.9032667	4.5824738	5.2467492	5.166801	5.3558154
ENSMUSG00000027408	Cpxm1	-1.283883948	0.0041451	8.78952164	8.60720465	8.71853007	10.3633465	10.31192685	10.3903122	8.47449705	8.1499437	8.2544399	8.6816904	8.4883772	8.7429273
ENSMUSG00000020310	Madcam1	-1.292966516	0.0003175	5.39677993	5.91026528	5.3962317	6.36491562	6.383840938	6.23991717	4.45840862	5.1655312	5.2067896	5.0863008	4.1671919	4.6422398
ENSMUSG00000118012	Gm46620	-1.298518976	1.75E-34	9.22406693	9.17851613	9.15658017	8.90233964	8.948272285	8.80219052	7.80612683	7.5725886	7.8108474	7.7198071	7.7380178	7.8989746
ENSMUSG00000078866	Zfp970	-1.309978376	0.0007998	7.26219058	7.59599763	7.45543808	9.01181164	8.642238916	8.71272291	6.64265579	6.7896504	6.9396248	7.1585912	7.0189611	7.301905
ENSMUSG00000069516	Lyz2	-1.313206334	0.0285637	11.5479567	11.5310875	11.6259142	12.9519016	13.14370405	13.1057775	10.1395838	10.077223	10.176932	11.807246	11.867624	11.720031
ENSMUSG00000041670	Rims1	-1.313804088	0.0064784	7.14434313	7.38723323	7.45543808	6.29368298	6.120891544	6.05813879	5.04329531	5.124905	4.7523434	5.9760466	5.9274531	6.2649621
ENSMUSG00000089774	Slc5a3	-1.314438799	0.0052008	7.20446983	7.2129712	7.50407612	8.86903562	9.03008527	8.84648499	6.61351047	6.5951731	6.9513058	7.2275368	7.3974477	7.2555137
ENSMUSG00000073008	Gpr174	-1.316685634	0.030136	5.43073817	4.86109829	4.32538969	6.17977121	5.968945122	5.96936166	3.80646187	3.5816684	3.9977603	4.5224741	4.7518938	5.2836752
ENSMUSG00000031024	Denn2b	-1.320914846	0.022538	10.0561218	10.1199464	10.0930981	7.98388262	8.15612975	8.18148407	8.50258909	8.4087421	8.4646524	7.3995936	7.7176509	7.7794702
ENSMUSG00000053846	Lipg	-1.322042432	1.99E-05	7.83139318	7.69703261	7.8180301	7.05576959	7.161271392	7.23017273	5.69928551	5.7767759	5.6119669	6.7266531	6.6970601	6.3904846
ENSMUSG00000028064	Sema4a	-1.324243544	0.0009344	7.19462112	7.2129712	7.14375451	8.67596589	8.602214522	8.64267941	6.78015477	6.8407184	6.8172978	6.7800906	6.5202	6.9981357
ENSMUSG00000078653	Cntd1	-1.325042391	4.70E-08	5.64839374	5.49514752	5.75889322	5.44976368	5.313919113	5.60694538	4.39130525	3.9032667	4.4569882	4.64275	4.5206589	4.3907597
ENSMUSG00000018554	Ybx2	-1.326498048	0.0087525	8.02722352	8.16343627	8.23308679	6.6045073	6.450935812	6.74674493	5.99882775	5.7503104	5.6411084	6.7800906	6.7380836	6.4075571
ENSMUSG00000060924	Csmd1	-1.32672121	0.0056076	4.46346769	4.00271242	4.17329055	4.7458302	4.850310455	5.12179534	3.80646187	3.8038253	4.0851792	3.321138	3.1679733	3.1688562
ENSMUSG00000028459	Cd72	-1.333080415	1.10E-08	7.00477759	7.02587214	6.98146849	7.29341274	7.09988163	7.29553879	6.14856716	5.9022768	6.2825686	5.5837553	4.9038448	5.9050945
ENSMUSG00000037341	Slc9a7	-1.338289669	0.0001139	6.8874076	6.96928416	6.94669973	7.3646584	7.712366832	7.49952437	5.45829491	5.1655312	5.4567164	6.5685941	6.4723766	6.1681075
ENSMUSG00000028979	Masp2	-1.339868048	0.0102041	4.00370016	4.46239037	4.75857317	3.57787902	3.99332894	4.08100044	3.16923045	3.1671805	2.9985073	3.5840846	3.4571958	3.1688562
ENSMUSG00000002007	Srpk3	-1.342083403	0.0046419	5.46391545	5.28864725	4.75857317	4.5761027	4.314811199	4.74768681	3.45863601	4.3883165	3.1682663	3.4585936	3.9973646	4.1684284
ENSMUSG00000022865	Cxadr	-1.342835717	0.0017599	7.35353879	7.44647592	7.05947822	7.27503768	7.576246893	7.35807114	5.04329531	5.1655312	5.1266377	6.7401992	6.6548359	6.4900142
ENSMUSG00000041649	Klf8	-1.35750279	0.0016501	5.36200308	5.83625203	5.6478363	7.05576959	6.772782753	6.79920113	4.8569031	5.3174793	4.8554064	5.0432368	5.6114821	4.9525203
ENSMUSG00000030724	Cd19	-1.360341068	0.0236231	8.58230872	8.41296389	8.43890399	8.48932556	8.598520272	8.67110618	5.5224203	5.4217814	6.1870014	7.8628917	7.9034343	7.9523029
ENSMUSG00000024347	Psd2	-1.364066944	0.0099983	5.39677993	5.64718272	5.04819618	4.51477944	5.036574414	4.51657958	3.32117796	3.3189638	3.3201366	4.5224741	4.5820339	4.0859914
ENSMUSG00000085876	Gm12409	-1.374251358	0.0126768	4.75908943	4.32482117	5.133115	5.34795505	4.747308112	4.74768681	2.80681915	3.3189638	2.9985073	4.3208746	4.2451532	4.2464084
ENSMUSG00000056602	Fry	-1.385397548	5.13E-22	8.48060956	8.32999992	8.07035042	8.38180623	8.31763913	8.29543144	6.80614917	6.750127	6.5517291	7.0648115	7.1962531	7.2649121
ENSMUSG00000031362	Xlr4c	-1.390301011	4.79E-07	5.88724069	5.70377736	5.3962317	5.89696396	5.77310734	5.54685383	4.75382239	3.4562874	4.4569882	4.64275	4.7518938	4.5219723
ENSMUSG00000024402	Lta	-1.39237647	0.0276214	4.25182216	4.25078255	3.91006404	5.34795505	4.899179037	5.38466829	4.32092783	3.4562874	2.5839675	3.6995281	3.9973646	3.5836798
ENSMUSG00000024910	Ctsw	-1.397046538	0.0287701	5.7324803	5.2511628	5.3962317	7.60428944	7.491141583	7.67820854	5.45829491	5.3878451	5.2067896	5.4582344	5.9036102	5.8808491
ENSMUSG00000033590	Myo5c	-1.397770734	0.0242525	3.70385559	4.0902284	4.00324548	5.27585864	4.899179037	5.34992256	3.99906228	2.9975301	3.805222	3.6995281	3.8048451	3.1688562
ENSMUSG00000008193	Spib	-1.407857816	0.0002512	7.78620165	7.69703261	7.76579731	7.82243903	7.677772279	7.69906478	5.24680876	5.6958767	5.520835	6.9645094	7.0189611	6.7663305
ENSMUSG00000016918	Sulf1	-1.416982019	1.85E-05	5.58948364	5.73126334	6.23291401	6.52897969	6.663873842	6.66430124	4.80628319	5.4549378	5.2067896	5.0863008	4.8043426	4.3907597
ENSMUSG00000033805	Ephx4	-1.421924487	0.0053192	5.04872871	5.0475718	5.1737707	6.73122779	6.620815729	6.63573874	4.69938173	5.0400503	4.7523434	4.5838651	4.5206589	5.0857649
ENSMUSG00000088088	Rmrp	-1.422219324	0.0186829	5.32636716	5.98066607	5.5585469	4.79824119	4.946446378	3.69459039	3.69957415	3.4562874	3.4575315	4.3912513	4.6409042	4.0859914
ENSMUSG00000115420	Rmrp	-1.422219324	0.0186829	5.32636716	5.98066607	5.5585469	4.79824119	4.946446378	3.69459039	3.69957415	3.4562874	3.4575315	4.3912513	4.6409042	4.0859914
ENSMUSG00000021047	Nova1	-1.427812318	0.0250481	3.46257176	3.5873738	4.00324548	4.4507334	3.900368117	4.16335188	3.32117796	2.3209407	2.9985073	3.1691935	3.5826201	2.5843213
ENSMUSG00000071984	Fndc1	-1.443217626	0.0283793	4.25182216	3.9095428	3.17232976	3.99202864	3.900368117	4.16335188	3.32117796	2.3209407	2.3213312	3.1691935	3.4571958	3.1688562
ENSMUSG00000046634	Pkd1l1	-1.446006125	0.020162	6.34453832	6.2128736	6.21354557	5.31235716	4.946446378	4.51657958	4.80628319	5.3174793	4.3898999	3.4585936	4.3894726	3.6991077
ENSMUSG00000021803	Cdhr1	-1.457045945	0.0393785	3.91050864	4.32482117	3.58784774	4.89767527	5.036574414	5.12179534	3.32117796	2.5833164	2.9985073	3.1691935	4.1671919	4.0859914
ENSMUSG00000019852	Arfgef3	-1.462056759	0.0019183	6.30846291	6.11193055	5.52751202	5.87272847	6.201034321	6.31389544	3.80646187	3.4562874	4.5210949	4.9530493	5.4562365	5.3201962
ENSMUSG00000054679	Srsf12	-1.462581494	0.0350073	4.00370016	3.8099383	3.32452507	3.99202864	4.240904489	4.85069372	2.99937492	2.3209407	3.805222	3.321138	3.1679733	2.8065305
ENSMUSG00000096780	Tmem181b-ps	-1.468695733	7.19E-103	10.3712387	10.3176208	10.4305779	10.4498479	10.3994544	10.3502204	9.07557443	8.9950948	9.0468841	8.7767721	8.7876797	8.8435823
ENSMUSG00000057337	Chst3	-1.481816547	0.0051232	7.37985225	7.09097207	7.24261601	6.6045073	6.957168369	6.77321143	4.45840862	4.1660812	4.8554064	6.265538	5.9739884	6.4575947
ENSMUSG00000076608	Igkj5	-1.481857805	0.0101061	4.91116549	4.81045442	5.0912803	6.58971479	6.635311692	6.81202249	4.24694042	4.3883165	4.804795	4.8568457	4.7518938	5.1275786
ENSMUSG00000029370	Rassf6	-1.497243503	0.0033329	5.13365172	4.81045442	4.58856814	6.05608822	5.77310734	5.45174579	3.45863601	3.3189638	4.1676023	4.7537657	4.5206589	3.9985569
ENSMUSG00000094094	Igkv5-45	-1.503224865	0.0003327	6.94728585	6.78484383	7.24261601	8.20382462	8.348759273	8.20111131	6.06491344	5.6101701	5.8045815	6.8567094	6.4560766	6.6275099
ENSMUSG00000074024	4632427E13Rik	-1.506004073	0.0183732	3.91050864	5.2511628	4.52713629	3.57787902	4.240904489	4.45251622	3.32117796	3.1671805	2.3213312	3.5840846	3.6980072	3.5836798
ENSMUSG00000042474	Fcmr	-1.510012	0.0297783	5.64839374	6.1326921	5.83691257	4.38371152	4.577548304	4.16335188	3.45863601	3.1671805	3.805222	4.9530493	3.9973646	4.2464084
ENSMUSG00000034981	Parm1	-1.516062967	2.43E-06	7.71908319	7.52709889	7.82442821	8.57443542	8.462874201	8.51911228	6.35636259	6.1450822	6.0415883	7.2178869	7.0409858	6.892958
ENSMUSG00000064158	Izumo1	-1.523137007	0.0361956	3.00246783	3.5873738	3.46218583	3.57787902	3.694282913	3.80131951	2.80681915	2.9975301	3.1682663	2.5845236	2.3212258	2.3215434
ENSMUSG00000026193	Fn1	-1.527794932	5.47E-08	10.3200656	10.1735279	10.1854631	11.1574255	11.17970253	11.2028376	8.94127424	8.8279895	8.9743167	9.5183264	9.5278855	9.5641397
ENSMUSG00000027797	Dclk1	-1.529314777	5.82E-10	6.09210467	6.1326921	6.23291401	5.96731941	6.120891544	5.79950395	3.69957415	4.6397044	4.5824738	4.8568457	5.0843618	4.9052229
ENSMUSG00000042812	Foxf1	-1.533342238	0.0130082	3.588252	3.9095428	4.09077189	4.51477944	4.38511559	4.31516673	3.69957415	3.3189638	3.5829719	2.3216648	2.8058495	2.5843213
ENSMUSG00000064080	Fbln2	-1.539246571	0.0313241	8.54791047	8.50342142	8.5278407	11.103774	10.98192901	11.0968125	9.26554423	9.2069778	9.1769427	8.0647918	8.078686	8.127386
ENSMUSG00000031292	Cdkl5	-1.545843638	0.0457337	5.58948364	5.49514752	5.73192013	3.57787902	3.45377331	4.38547538	3.584129	3.1671805	3.3201366	4.3912513	3.5826201	4.0859914
ENSMUSG00000076569	Igkv5-39	-1.565061512	0.010356	8.68436352	8.73829115	8.67316823	11.1359492	11.11781883	11.0836553	8.85984723	8.5458557	8.7249617	8.9235063	8.8102975	8.9258693
ENSMUSG00000079173	Zan	-1.56993609	0.0459818	5.93534593	5.58827699	6.13336188	4.89767527	4.850310455	5.12179534	2.32167809	3.5816684	2.9985073	4.8568457	4.6974661	4.8057055
ENSMUSG00000022123	Scel	-1.57409529	0.0017336	4.52763697	4.75796789	4.09077189	5.03504949	5.239965497	5.12179534	3.16923045	3.5816684	2.5839675	3.6995281	4.1671919	3.9985569
ENSMUSG00000030468	Siglecg	-1.576620035	1.87E-05	7.4226688	7.48735052	7.69772918	6.74464461	6.898286583	6.6783732	5.42513069	5.124905	4.7523434	6.3562992	6.1052135	5.8561893
ENSMUSG00000009628	Tex15	-1.580594204	1.66E-08	6.83764871	6.99218639	7.28033863	7.77091554	7.732732257	7.67820854	5.45829491	5.3174793	5.752122	6.3206769	6.1464304	6.1880056
ENSMUSG00000029095	Ablim2	-1.589055844	0.0056401	7.27159011	6.74494743	7.24261601	5.27585864	5.546446959	4.89956435	5.08635957	5.0400503	5.3548567	4.64275	4.9511354	4.8057055
ENSMUSG00000056529	Ptafr	-1.597460561	0.0015283	5.81193468	5.55789694	5.04819618	7.23757017	7.120636493	7.14152935	5.12817554	4.9026068	4.9515951	5.0432368	5.2447829	5.2077371
ENSMUSG00000020937	Plcd3	-1.60036753	1.33E-13	6.36224328	6.51125134	6.21354557	6.89660817	6.705684016	6.56175601	5.45829491	5.2809661	4.9043022	5.0863008	4.5820339	4.9983162
ENSMUSG00000030577	Cd22	-1.604452806	6.74E-13	9.09765252	9.03976153	8.97870593	9.34697881	9.315334646	9.27004742	7.17869317	7.1244806	6.9971065	7.9987036	8.0244449	7.8684732
ENSMUSG00000094117	Igkv3-12	-1.607569239	0.037529	8.14441297	8.19339053	8.07572383	11.002705	10.60675078	10.9971844	7.8253201	7.7162491	7.6624078	8.9673603	8.9737929	8.9839326
ENSMUSG00000097352	C920009B18Rik	-1.612446157	0.0014582	5.13365172	5.67575754	5.133115	7.03407934	6.933903235	6.89871662	4.8569031	4.5194791	4.8554064	4.9530493	5.2063188	4.8563221
ENSMUSG00000029811	Aoc1	-1.614272543	0.0149563	3.46257176	4.0902284	3.91006404	4.38371152	4.747308112	4.80010939	2.58454581	3.3189638	2.9985073	2.5845236	3.9973646	3.1688562
ENSMUSG00000040899	Ccr6	-1.61646799	0.0185146	6.02699627	5.61803048	6.04845802	5.03504949	5.576804784	5.66463374	3.45863601	2.3209407	3.805222	4.9057492	5.2447829	4.3203887
ENSMUSG00000106734	Gm20559	-1.616720988	0.0006346	8.20943584	8.24674175	8.10229472	9.99643047	10.01903859	10.0167155	7.86913567	7.9140012	8.1366068	7.5836729	7.4722975	7.5294986
ENSMUSG00000039521	Foxp3	-1.619415414	0.0004575	4.58907321	4.58797599	4.58856814	4.79824119	4.850310455	4.38547538	3.16923045	2.5833164	3.1682663	3.6995281	3.1679733	4.2464084
ENSMUSG00000000903	Vpreb3	-1.628298865	0.0320876	4.64799974	4.52654927	4.81106345	5.544859	5.874346668	6.01443299	2.80681915	2.5833164	3.4575315	4.5224741	4.6974661	4.5219723
ENSMUSG00000076755	Trgv1	-1.633286157	2.74E-20	8.17478807	8.0369833	8.11278755	8.44069483	8.487052342	8.42626961	6.32074021	6.5802249	6.3894728	7.0755376	7.0626793	6.5527463
ENSMUSG00000017167	Cntnap1	-1.638540103	0.0045214	5.95881011	5.83625203	5.73192013	7.8904072	7.642327755	7.83718088	5.32080275	5.2809661	4.9515951	5.6712117	5.9036102	6.0205618
ENSMUSG00000069305	H4c18	-1.650618054	0.0124387	4.95849239	4.70349952	5.04819618	4.31342374	4.452152566	2.99577786	3.584129	3.5816684	3.4575315	2.5845236	2.8058495	3.6991077
ENSMUSG00000032327	Stra6	-1.65982315	2.15E-06	5.04872871	5.13248572	4.46297179	5.23841273	5.201516736	5.16241042	3.45863601	3.1671805	3.9047007	4.0864558	4.0847757	3.4582072
ENSMUSG00000032572	Col6a4	-1.667604134	3.14E-06	5.52806525	5.17313917	5.1737707	4.99069578	5.664223877	5.27781519	2.99937492	3.5816684	3.9977603	3.8064143	4.5206589	4.2464084
ENSMUSG00000090558	Gm17202	-1.677950473	0.0053738	5.2138525	5.0475718	5.1737707	6.66220571	6.620815729	6.70611192	3.45863601	4.1660812	4.1676023	4.7537657	5.3891376	4.8563221
ENSMUSG00000076499	Trbv31	-1.68565388	0.0360205	4.17376203	3.5873738	3.46218583	3.31555453	2.995556056	3.31686005	2.99937492	2	2.5839675	2.8067906	2.5837918	2.8065305
ENSMUSG00000104452	Ighv8-8	-1.69099715	0.0473001	7.27159011	7.22268701	7.4960828	10.6484921	10.64843895	10.708383	7.68527438	7.7500353	7.5820378	8.4622223	8.4641303	8.4939519
ENSMUSG00000092060	Bend4	-1.695638104	0.0001197	5.13365172	4.46239037	4.86171081	4.38371152	4.240904489	4.38547538	3.32117796	3.1671805	3.9047007	3.1691935	2.9982436	3.4582072
ENSMUSG00000039323	Igfbp2	-1.696835028	0.0155545	4.39631085	4.52654927	4.32538969	6.29368298	6.014015574	6.4676579	4.52252907	4.6397044	4.2455699	2.9993416	3.9973646	4.0859914
ENSMUSG00000052613	Pcdh15	-1.70526148	0.0200929	3.70385559	3.9095428	3.17232976	3.57787902	4.163006272	4.24125532	3.32117796	2	2.5839675	2.8067906	2.5837918	3.3207737
ENSMUSG00000087289	4933424M12Rik	-1.708254864	0.0246957	5.00431594	5.2511628	5.28928485	7.54417771	7.467032452	7.33160274	4.52252907	4.3883165	4.0851792	5.4250703	5.7781007	5.6986634
ENSMUSG00000027983	Cyp2u1	-1.715962379	0.0335129	3.32488899	3.70294367	3.32452507	3.79976415	3.316593717	3.69459039	2.99937492	2.5833164	2	2.3216648	3.3198201	2.3215434
ENSMUSG00000038677	Scube3	-1.716221324	0.0047091	3.17266678	4.25078255	4.17329055	3.79976415	3.99332894	4.08100044	2.80681915	2.5833164	3.4575315	2.8067906	2.5837918	2.9990381
ENSMUSG00000040627	Aicda	-1.729654183	0.0426866	5.95881011	6.00338973	5.3258218	7.04496523	7.181167553	7.34930219	3.16923045	3.1671805	3.9977603	5.5837553	5.8547087	5.9050945
ENSMUSG00000045903	Npas4	-1.736633447	0.0001111	4.86223324	4.17273779	5.0912803	5.19996894	4.577548304	4.99260313	3.32117796	2.9975301	3.1682663	3.9990123	4.0847757	3.1688562
ENSMUSG00000024459	H2-M5	-1.777632598	0.0231094	4.25182216	4.0902284	4.32538969	5.544859	5.635668724	5.89899925	2.32167809	3.4562874	2.9985073	4.0864558	3.9043138	4.5219723
ENSMUSG00000022375	Lrrc6	-1.787705838	0.0366908	3.00246783	3.17193469	3.32452507	3.45267087	3.801002232	3.31686005	2.32167809	2.3209407	2	2.9993416	2.5837918	2.8065305
ENSMUSG00000033498	Strc	-1.792551912	0.023295	3.70385559	4.58797599	4.39582017	6.34743447	6.258348698	6.40133334	3.584129	3.5816684	3.3201366	4.4583541	4.1671919	4.9052229
ENSMUSG00000062991	Nrg1	-1.792764353	0.0170643	4.25182216	3.5873738	4.17329055	4.79824119	5.036574414	4.99260313	2.80681915	2	3.1682663	4.1689007	3.1679733	3.4582072
ENSMUSG00000118541	Nrg1	-1.792764353	0.0170643	4.25182216	3.5873738	4.17329055	4.79824119	5.036574414	4.99260313	2.80681915	2	3.1682663	4.1689007	3.1679733	3.4582072
ENSMUSG00000014030	Pax5	-1.793764085	0.0008075	7.5517206	7.85530195	7.64086349	6.84771084	6.606172633	6.82473091	4.39130525	4.5808437	4.4569882	6.2275719	6.2061286	6.207633
ENSMUSG00000009545	Kcnq1	-1.805537792	0.0021064	5.13365172	5.28864725	5.67641223	3.57787902	4.314811199	4.57791872	3.32117796	3.3189638	3.805222	2.9993416	3.4571958	3.9985569
ENSMUSG00000095642	Ighv14-3	-1.812535998	0.000603	6.74621438	7.17344013	7.08101331	9.04743355	9.013534878	9.03052682	6.33866134	6.2241389	6.5970492	6.7800906	6.4395903	6.9639214
ENSMUSG00000020866	Cacna1g	-1.814934396	0.0423451	8.48060956	8.53885188	8.32168415	5.19996894	5.036574414	5.74705896	6.32074021	6.0828102	6.6118449	4.8568457	5.2063188	5.2836752
ENSMUSG00000104554	Gm4610	-1.82313928	0.0389135	3.32488899	3.70294367	3.46218583	3.31555453	4.163006272	2.99577786	2	2.9975301	2.5839675	2.8067906	2	2.9990381
ENSMUSG00000112160	BC024063	-1.827104442	0.0131606	3.17266678	4.58797599	3.32452507	5.27585864	5.239965497	4.99260313	2.99937492	3.1671805	3.805222	2.8067906	3.3198201	3.5836798
ENSMUSG00000053541	Gvin-ps6	-1.828783184	0.0037353	4.58907321	4.32482117	4.75857317	5.41661938	5.799090957	5.27781519	2.80681915	3.1671805	2.5839675	4.1689007	4.1671919	4.1684284
ENSMUSG00000096326	Ighv1-78	-1.838954393	0.0105755	5.36200308	5.39558892	5.5585469	7.92617395	7.798612743	7.94004791	4.95310728	4.85372	4.6413475	5.8814153	5.6406227	5.8808491
ENSMUSG00000098132	Rassf10	-1.840538762	0.0270067	6.63408914	6.58842747	6.32603781	4.23953538	3.900368117	4.45251622	3.32117796	3.9032667	3.3201366	4.7537657	4.5206589	4.6422398
ENSMUSG00000096410	Ighv1-19	-1.849337737	0.0243267	6.61944034	6.19324212	6.7985859	9.82229854	9.932182321	9.91639074	6.95298623	7.2431139	7.2259114	7.1686446	7.1564548	7.4493306
ENSMUSG00000094797	Igkv6-15	-1.859862179	0.031072	7.61216077	7.42979621	7.50407612	11.1244486	11.01971225	11.2052694	8.09152504	8.219124	8.2591468	8.5339726	8.6075458	8.5255734
ENSMUSG00000071178	Serpina1b	-1.861758839	0.0041252	3.46257176	3.5873738	3.91006404	4.5761027	4.850310455	4.57791872	2.80681915	2.3209407	2.9985073	3.321138	3.4571958	2.9990381
ENSMUSG00000042515	Pwwp3b	-1.870665402	0.0146837	5.58948364	5.28864725	5.25179848	8.09804089	7.824145038	7.82458214	4.75382239	4.6397044	4.5824738	5.7536681	5.9509084	5.8808491
ENSMUSG00000093894	Ighv1-53	-1.874494637	0.040826	6.0707267	6.2128736	6.09153444	9.8442762	9.923349689	10.0359696	7.23718744	7.1347479	7.2638772	7.2081719	7.0626793	7.2269456
ENSMUSG00000061947	Serpina10	-1.877594268	0.0459748	3.46257176	2.8089055	2.58640584	4.69144319	4.577548304	4.31516673	2.58454581	2.3209407	3.1682663	2.9993416	2.9982436	2.8065305
ENSMUSG00000052336	Cx3cr1	-1.901181134	1.73E-07	6.3797336	6.30721334	6.46356097	7.2184651	7.248719646	7.34047961	4.99890593	4.1660812	4.6413475	5.4250703	5.2822481	5.6986634
ENSMUSG00000051747	Ttn	-1.91998891	2.96E-06	4.91116549	5.42954425	5.88667588	6.34743447	6.649663449	6.45136042	4.16895254	3.9962936	3.9977603	4.64275	4.4565564	4.7532483
ENSMUSG00000074934	Grem1	-1.950079698	0.0126625	3.70385559	3.17193469	3.81044603	4.5761027	4.747308112	4.69328731	2.58454581	3.8038253	2.3213312	3.1691935	2.5837918	2.8065305
ENSMUSG00000021702	Thbs4	-1.960337509	0.0034411	4.81158291	4.81045442	4.81106345	5.92079904	5.692224792	5.82502842	2.99937492	2	3.9977603	4.3208746	4.1671919	4.0859914
ENSMUSG00000061603	Akap6	-1.965947253	0.016662	4.64799974	4.91002449	3.91006404	7.33835186	7.120636493	7.17168638	4.45840862	3.9962936	3.9977603	4.8568457	5.2063188	4.9052229
ENSMUSG00000044522	A730020M07Rik	-1.966367703	0.0038385	4.00370016	4.46239037	3.46218583	5.84807889	5.898584129	5.60694538	3.584129	3.1671805	3.9047007	3.6995281	3.3198201	3.8059806
ENSMUSG00000041216	Clvs1	-1.994398357	0.0313241	5.00431594	4.75796789	4.52713629	7.75774193	7.583740466	7.44294829	4.08650672	3.9962936	3.805222	5.7267029	4.8043426	5.8311007
ENSMUSG00000028003	Lrat	-1.999187979	0.0015526	3.17266678	4.00271242	3.81044603	4.07933474	4.080660667	4.24125532	2.80681915	2.5833164	2.3213312	2.5845236	2.8058495	3.3207737
ENSMUSG00000036928	Stag3	-2.01141966	0.0241236	6.23348755	5.78471251	6.54329872	3.57787902	3.579034195	3.80131951	4.39130525	4.1660812	3.5829719	3.321138	3.3198201	3.5836798

ENSMUSG00000073821	8030451A03Rik EN	-2.034526497	0.0015178	4.17376203	4.32482117	4.00324548	5.77149776	5.664223877	5.82502842	2.80681915	3.5816684	3.3201366	4.1689007	3.6980072	3.4582072
ENSMUSG00000031289	Il13ra2	-2.058257339	0.0065722	5.64839374	5.39558892	5.00378569	7.75774193	7.568714194	7.58417614	4.69938173	4.2440258	3.4575315	5.4906532	5.2822481	5.6986634
ENSMUSG00000025905	Oprk1	-2.074340283	0.036233	5.09181499	4.81045442	4.70410076	8.52863532	8.502948884	8.52301648	6.20827055	6.40468	5.6119669	4.8568457	5.3891376	4.4578572
ENSMUSG00000094689	Ighv1-81	-2.078084829	0.0143003	6.8874076	6.49530804	7.11272495	10.3934704	10.34757759	10.3380831	6.84428313	7.0826646	7.0951324	7.7866094	7.7312607	7.7395785
ENSMUSG00000034731	Dgkh	-2.078894396	0.0020105	6.82493613	6.77166724	6.77235151	9.55166062	9.576107386	9.44280291	6.47453922	6.3703341	6.4065447	6.67116	6.9154646	7.1376815
ENSMUSG00000048001	Hes5	-2.088807711	0.0428446	4.91116549	4.95734574	5.04819618	9.20860188	9.306304012	9.32475128	6.71304274	6.3703341	6.5970492	6.2082076	5.9509084	5.8808491
ENSMUSG00000039691	Tspan10	-2.100528015	0.0003964	5.09181499	5.13248572	4.91064028	6.31182357	6.276958431	6.40133334	2.99937492	3.3189638	3.3201366	4.6993254	4.5206589	4.3907597
ENSMUSG00000087670	9530036M11Rik	-2.114066048	0.0201062	3.32488899	2.58616865	3.17232976	3.79976415	3.579034195	3.57933023	2.58454581	2.3209407	2	2.8067906	2.3212258	2.5843213
ENSMUSG00000076680	Ighv6-6	-2.114257759	0.0200546	5.46391545	5.67575754	5.86200878	9.3795943	9.355287233	9.42830383	6.10734654	5.9022768	5.9279464	6.8690927	6.7108646	6.7396145
ENSMUSG00000067242	Lgi1	-2.200640717	0.0064262	4.52763697	4.3952449	4.325389669	7.14953168	7.295105165	7.20122591	5.08635957	4.5194791	4.6413475	3.9990123	3.9973646	3.9985569
ENSMUSG00000114203	Gm35279	-2.217445901	1.85E-05	4.00370016	4.52654927	4.39582017	4.89767527	4.577548304	4.08100044	3.45863601	3.3189638	3.2213312	2.8067906	2.5837918	2.9990381
ENSMUSG00000048905	Bnip5	-2.229472198	0.0404492	7.95321895	8.05340948	7.89907086	9.44493511	4.899179037	4.69328731	3.45863601	3.4562874	3.1682663	5.8814153	5.7781007	5.7261413
ENSMUSG00000040536	Necab1	-2.231610422	0.0404492	7.36236337	7.23233783	7.37926104	11.6241862	11.6426097	11.5374844	8.18859126	8.3349672	8.1468022	8.6533321	8.7176176	8.5905525
ENSMUSG00000058246	Gm10037	-2.270456851	0.0003526	4.52763697	4.0902284	3.81044603	4.23953538	3.694282913	4.31516673	2.80681915	2.5833164	3.4575315	2.3216648	2.9982436	2
ENSMUSG00000091679	Vmn2r96	-2.275034215	0.000118	4.39631085	4.32482117	3.46218583	4.38371152	4.314811199	4.51657958	2.99937492	2	3.4575315	2.8067906	2.5837918	2.8065305
ENSMUSG00000015599	Ttbk1	-2.282827469	0.0480931	3.17266678	3.00180885	2.32279427	3.31555453	3.99332894	3.90069389	2.80681915	2.3209407	2.3213312	2.8067906	2	2
ENSMUSG00000096638	Ighv2-9	-2.313943793	0.0120474	4.46346769	3.8099383	4.395820117	7.49739099	7.642327755	7.58417614	3.80646187	3.9962936	4.5824738	4.9988477	5.0413056	4.7532483
ENSMUSG00000103749	Pcdhgb5	-2.32085305	0.0062016	3.32488899	3.17193469	4.00324548	4.07933474	3.99332894	3.99366215	2.32167809	2.3209407	3.4575315	2.5845236	2	2.3215434
ENSMUSG00000034634	Ly6d	-2.323074219	0.0074472	10.1910288	10.1016343	10.0930981	13.29557	13.24981526	13.4378543	10.810127	10.892912	10.810801	8.9175571	8.6295157	8.9406057
ENSMUSG00000108187	4930511E03Rik	-2.326454041	0.0294049	4.64799974	5.64718272	4.81106345	3.31555453	2.320152159	3.45405584	2.58454581	2.3209407	2.5839675	2.8067906	3.4571958	3.3207737
ENSMUSG00000086638	4930405A21Rik	-2.349510243	0.0029462	3.17266678	3.8099383	3.17232976	4.16165755	3.45377331	3.80131951	2.58454581	2	2.5839675	2.3216648	2.5837918	2.8065305
ENSMUSG00000077431	Gm22591	-2.349610144	0.0018982	4.00370016	3.8099383	4.32538969	3.31555453	3.316593717	3.31686005	2.80681915	2.3209407	2.5839675	2.3216648	2.8058495	2.3215434
ENSMUSG00000031297	Slc7a3	-2.353648776	0.0010718	4.00370016	4.3952449	4.52713629	6.55966682	6.606172633	6.54649305	3.45863601	3.4562874	3.4575315	3.9990123	4.4565564	3.9985569
ENSMUSG00000096461	Igkv14-130	-2.354895026	0.0111291	4.70461358	4.70349952	4.17329055	7.80972963	7.939610206	7.87433013	4.69938173	4.3883165	3.4575315	5.1687544	5.0843618	5.4245194
ENSMUSG00000094686	Ccl21a	-2.373678825	7.02E-11	6.97055819	6.74494743	6.77235151	8.15943499	8.068046255	8.16158613	5.32080275	5.7503104	5.520835	5.2467492	4.8549513	5.3558154
ENSMUSG00000040907	Atp1a3	-2.385835463	0.0005949	6.13393312	5.61803048	6.37915695	8.9638612	8.921908906	9.02778156	5.69928551	6.0614409	5.8045815	5.8567548	5.8793666	5.7795753
ENSMUSG00000049100	Pcdh10	-2.392215398	0.0024843	3.8108791	3.5873738	4.09077189	3.79976415	4.452152566	2.99577786	2.32167809	2.3209407	2	2.9993416	2.5837918	2.9990381
ENSMUSG00000112797	Gm30034	-2.413884508	0.0260061	2.80947046	2.58616865	3.17232976	5.19996894	5.546446959	5.34992256	2.58454581	3.3189638	2.3213312	3.1691935	2.8058495	3.3207737
ENSMUSG00000012350	Ehf	-2.423718249	0.0057917	4.17376203	4.46239037	4.70410076	7.07713855	7.375016529	7.17168638	3.16923045	3.1671805	3.9977603	4.3912513	4.9511354	4.8563221
ENSMUSG00000095889	Ighv1-58	-2.435715517	0.0184221	4.58907321	4.32482117	3.58784774	7.82875198	7.939610206	8.00290208	3.584129	4.3883165	3.9047007	5.4906532	5.1261702	5.2077371
ENSMUSG00000076577	Igkv8-30	-2.4403939	0.0002292	8.43532692	8.54660853	8.50412385	11.4676407	11.44077569	11.4504746	8.05405081	8.4748918	8.3677366	8.1124442	8.1206568	8.0315279
ENSMUSG00000094787	Ighv1-54	-2.454515356	0.0162564	4.86223324	5.003164	4.09077189	8.50517823	8.594816539	8.60265489	4.6428059	3.9962936	4.804795	6.0862233	5.9739884	5.3905763
ENSMUSG00000043531	Sorcs1	-2.457804767	0.0042414	2.58660819	3.00180885	3.91006404	3.79976415	4.240904489	4.08100044	2.32167809	2.5833164	2.5839675	2.5845236	2.5837918	2.3215434
ENSMUSG00000094491	Igkv1-133	-2.496119535	0.0148386	4.70461358	4.52654927	4.17329055	7.94373022	8.041081703	8.07381756	3.80646187	3.4562874	3.9047007	5.0863008	5.7781007	5.3558154
ENSMUSG00000096670	Ighv2-6	-2.517592735	0.0307395	3.00246783	2.58616865	2.58640584	6.32973889	6.383840938	6.515474	3.45863601	3.5816684	3.5829719	3.1691935	3.4571958	3.6991077
ENSMUSG00000094051	Ighv1-36	-2.525454004	0.0049439	4.46346769	4.25078255	4.00324548	7.82875198	7.904135911	7.69214615	4.80628319	4.8031183	4.6413475	4.6993254	4.3894726	4.2464084
ENSMUSG00000030268	Bcat1	-2.545253757	3.80E-08	8.60479354	8.4589015	8.5892432	9.497215	9.520577265	9.52880739	5.58381631	5.9022768	5.1266377	7.1983912	7.0518733	7.3818259
ENSMUSG00000095981	Ighv10-1	-2.561629689	0.0048259	4.95849239	5.13248572	5.04819618	8.44481059	8.462874201	8.51911228	4.45840862	4.1660812	4.2455699	5.699224	5.520353	5.9289391
ENSMUSG00000076550	Igkv4-63	-2.562292137	0.010586	4.09123546	4.3952449	4.58856814	8.27951699	8.041081703	8.58408826	5.08635957	5.8533786	5.1672702	4.5224741	4.5820339	4.1684284
ENSMUSG00000095700	Ighv10-3	-2.565463433	0.0100645	4.75908943	5.46271875	5.5585469	9.30684125	9.3310035	9.36880488	5.28428008	5.0831014	4.804795	6.5685941	6.5044343	6.3380206
ENSMUSG00000094561	Ighv1-22	-2.566272178	0.0115536	4.75908943	4.81045442	5.25179848	9.6278512	9.444419964	9.51318993	5.80619384	6.0397503	6.206628	6.1072838	6.0627843	6.3019538
ENSMUSG00000097276	4930525G20Rik	-2.583426162	0.0481825	3.00246783	2.8089055	3.00216447	3.57787902	3.900368117	3.31686005	2	2.3209407	2	2	3.1679733	2
ENSMUSG00000069515	Lyz1	-2.586054955	7.62E-07	5.58948364	5.67575754	5.1737707	6.78416229	6.620815729	6.34950901	3.16923045	3.3189638	2.9985073	4.2468879	4.6409042	4.3203887
ENSMUSG00000044453	Ffar1	-2.612777249	0.0093738	3.70385559	4.52654927	3.17232976	3.57787902	3.316593717	3.57933023	2.32167809	2.3209407	2	2.3216648	3.3198201	2
ENSMUSG00000096672	Ighv1-63	-2.615708106	0.0258084	4.25182216	4.32482117	3.58784774	7.22804926	7.161271392	7.29553879	2.32167809	2.9975301	2.5839675	4.5838651	4.5820339	5.1275786
ENSMUSG00000022899	Slc15a2	-2.650478955	1.05E-09	7.81219846	7.86773959	7.86223222	9.52274907	9.478988158	9.5461773	6.68529867	6.5802249	6.7113724	5.699224	6.0190694	5.9050945
ENSMUSG00000043230	Fam124b	-2.668332141	0.0335007	3.00246783	2	3.00216447	4.23953538	3.801002232	4.45251622	2.32167809	2.3209407	2	2.8067906	2.3212258	2.5843213
ENSMUSG00000026616	Cr2	-2.69202042	0.0144066	5.55910126	5.42954425	5.91092831	2.99469065	2.995556056	2.58214912	2.99937492	3.4562874	2.5839675	2.3216648	3.1679733	2.9990381
ENSMUSG00000034486	Gbx2	-2.727323324	0.0044927	3.70385559	3.17193469	3.81044603	3.99202864	2.995556056	4.08100044	2	2	2	2.8067906	2.3212258	2.9990381
ENSMUSG00000094345	Igkv14-126	-2.733466338	0.001965	5.2138525	5.2511628	5.133115	9.09534772	9.15355204	9.20348884	5.64270583	5.5804312	5.752122	5.5837553	5.4562365	5.6420858
ENSMUSG00000035429	Ptprh	-2.772185218	0.0027258	3.17266678	3.32409844	3.46218583	3.79976415	3.316593717	3.45405584	2.32167809	2.3209407	2	2	2.3212258	2.8065305
ENSMUSG00000038086	Hspb2	-2.805994146	0.0105016	6.0707267	5.88601365	6.09153444	2.58142511	3.801002232	2.32024072	2.80681915	3.1671805	2.9985073	3.1691935	3.4571958	2.9990381
ENSMUSG00000096498	Ighv2-5	-2.81457046	0.01312	3.70385559	4.0902284	3.32452507	8.05021758	8.013603558	8.27705428	3.32117796	3.8038253	4.2455699	5.3911259	4.9969249	4.8057055
ENSMUSG00000074892	B3galt5	-2.822115619	0.0081977	3.32488899	3.17193469	3.17232976	7.23757017	7.024794002	7.03619444	3.69957415	4.2440258	3.3201366	3.9990123	3.3198201	3.9054796
ENSMUSG00000044550	Tceal3	-2.840159028	3.70E-05	8.2336845	8.4589015	8.10229472	6.38218749	6.349085887	6.36699145	4.90580695	3.4562874	3.1682663	5.7267029	5.520353	5.1682145
ENSMUSG00000094016	Trav15-1-dv6-1	-2.917505204	0.0026227	6.67716372	6.61817789	6.44707059	3.99202864	3.45377331	3.45405584	2.58454581	3.4562874	2.5839675	3.321138	4.0847757	3.8059806
ENSMUSG00000076552	Igkv4-61	-2.926722227	0.0002743	5.86257288	5.36081511	5.58892821	8.68990408	8.348759273	8.84023986	4.58392055	4.4553878	3.5829719	5.4906532	5.724671	5.3905763
ENSMUSG00000042359	Osbpl6	-3.003204091	0.0053577	3.17266678	2.58616865	4.09077189	6.70401392	6.811593384	6.69230923	3.69957415	3.3189638	3.9977603	2.8067906	3.6980072	2.5843213
ENSMUSG00000091345	Col6a5	-3.03071332	0.0099664	4.52763697	4.17273779	4.52713629	6.51338782	6.499285457	6.70611192	2.32167809	2	2	4.3208746	3.8048451	4.0859914
ENSMUSG00000038576	Susd4	-3.052445339	9.33E-07	10.8597892	10.929904	10.923925	8.62246447	8.530353201	8.61001516	6.26560109	6.0397503	6.1870014	7.8813484	7.7844513	7.5059125
ENSMUSG00000000794	Kcnn3	-3.127733986	0.0037076	8.07094716	7.99791223	8.10755067	4.94493511	5.036574414	5.03696515	2.80681915	2.5833164	2.5839675	5.2842203	4.5820339	5.3905763
ENSMUSG00000102301	Ighv8-2	-3.247346425	0.0280326	2.80947046	2	2	5.69062254	5.418193514	5.24036336	2.58454581	2.3209407	2.5839675	2.8067906	2.8058495	2.5843213
ENSMUSG00000076646	Ighv2-6-8	-3.251627789	0.0132579	2.80947046	3.17193469	2.58640584	4.69144319	4.747308112	5.12179534	2	2.5833164	2	3.1691935	2.5837918	2
ENSMUSG00000076547	Igkv4-70	-3.253045915	0.0101608	3.46257176	4.00271242	5.1737707	9.67941138	9.319828853	9.48944209	5.28428008	5.7767759	5.9041029	4.9988477	4.9511354	5.3201962
ENSMUSG00000076839	Trav13-1	-3.266104333	7.43E-08	4.52763697	5.13248572	4.09077189	6.01238644	5.922421116	5.99207333	2.99937492	3.1671805	2.3213312	2.9993416	2.8058495	3.5836798
ENSMUSG00000006154	Eps8l1	-3.278531001	1.93E-05	8.71224347	8.74504867	8.76583712	5.1198645	5.546446959	5.45174579	4.45840862	4.8031183	4.7523434	5.0863008	5.1261702	4.3907597
ENSMUSG00000030785	Cox6a2	-3.288989191	0.043464	2	2.58616865	2	5.19996894	5.515436574	5.12179534	2.58454581	2	2.5839675	2.5845236	2.8058495	2.5843213
ENSMUSG00000094164	Ighv2-3	-3.322598253	4.70E-34	6.71898941	6.67589916	6.58910821	7.30251325	7.151219462	7.40113382	4.16895254	3.4562874	3.9977603	4.0864558	4.3191168	4.0859914
ENSMUSG00000110386	Gm42031	-3.463473558	6.02E-21	7.81862512	7.7717335	7.75913321	7.52097401	7.663698793	7.37545076	4.08650672	3.4562874	3.1682663	5.2467492	4.6974661	4.9525203
ENSMUSG00000025330	Padi4	-3.534842273	1.12E-10	6.39701442	6.55805062	6.60406041	8.58566181	8.670665591	8.77298015	4.8569031	4.3883165	4.3898999	4.1689007	4.4565564	5.3558154
ENSMUSG00000076571	Igkv5-37	-3.542149346	0.0384967	2.32291573	2	2	5.41661938	5.576804784	5.20191333	2.32167809	2.5833164	2	2.5845236	2.8058495	2.5843213
ENSMUSG00000106387	Igkv4-73	-3.579990742	0.0452697	2.58660819	2.32265191	2	4.31342374	3.16498644	3.99366215	2	2.3209407	2.3213312	2.3216648	2	2
ENSMUSG00000076549	Igkv4-68	-3.6129163	0.0015478	6.6485907	6.64732718	6.7985859	11.9720094	11.89084227	12.0800081	7.4986231	7.3702148	7.1967667	7.4416568	7.6331804	7.4493306
ENSMUSG00000095711	Trav14-2	-3.710279243	0.0003322	3.46257176	3.00180885	3.32452507	6.46557494	6.313472863	6.66430124	3.16923045	2.3209407	2.3213312	2.9993416	3.3198201	2.9990381
ENSMUSG00000021313	Ryr2	-3.720813384	2.16E-07	8.26696215	8.46300602	8.47595224	6.49762561	6.705684016	6.6783732	3.16923045	2.5833164	3.1682663	4.9057492	4.7518938	5.3558154
ENSMUSG00000098161	Platr11	-3.749249395	0.0380006	2.58660819	2	2	4.38371152	4.080660667	4.69328731	2	2.3209407	2.3213312	2.3216648	2	2.3215434
ENSMUSG00000076484	Trbj1-2	-3.800643321	0.0172876	6.43096721	5.83625203	6.39643742	2.80280525	2.803546666	2.32024072	2	2	2	3.1691935	3.3198201	3.1688562
ENSMUSG00000085041	BB031773	-3.833191968	0.0059883	2.80947046	3.5873738	2.58640584	5.544859	5.546446959	5.57721245	2	2.5833164	3.4575315	2	2.3212258	2
ENSMUSG00000034009	Rxfp1	-3.867939335	5.75E-14	7.48055424	7.60345382	7.71160216	5.71808778	5.922421116	5.82502842	3.45863601	3.9032667	3.805222	3.1691935	3.4571958	3.8059806
ENSMUSG00000086503	Xist	-3.874310419	7.54E-06	16.5184892	16.4205777	16.4904377	12.6978054	12.72687116	12.6852532	11.1299657	11.156826	11.140402	12.067798	12.144329	12.118315
ENSMUSG00000095338	Igkv3-9	-3.89424805	1.98E-07	6.46413927	6.3957609	6.49598681	5.69062254	5.746647149	5.82502842	2.32167809	2	2	2.8067906	3.9043138	3.9985569
ENSMUSG00000030257	Srgap3	-3.910469444	0.0005291	5.28982865	4.81045442	5.3962317	10.2805665	10.26608768	10.3741928	6.0432195	5.3878451	5.5822247	5.5223595	5.5817408	5.042703
ENSMUSG00000096577	Ighv1-71	-3.936043964	0.0291132	2	2	2.58640584	5.44976368	5.692224792	5.20191333	2	2.3209407	2	2.8067906	2.5837918	2.5843213
ENSMUSG00000029651	Mtus2	-3.937942553	1.02E-05	6.17458292	6.1326921	5.95824332	8.30690819	8.29041978	8.45924472	4.75382239	4.9498913	4.5210949	2	2.8058495	2.9990381
ENSMUSG00000076480	Trbv29	-3.980654562	0.0002212	3.00246783	3.4617334	3.58784774	7.16956531	7.576246893	7.47554863	2.58454581	3.3189638	2.9985073	2.8067906	4.0847757	3.1688562
ENSMUSG00000013418	B4galnt2	-4.080490993	0.0277326	2	2.32265191	2	5.07808018	5.239965497	5.34992256	2.58454581	2	2.3213312	2.5845236	2	2.3215434
ENSMUSG00000027849	Syt6	-4.138467199	0.0280906	2.32291573	2.32265191	2	3.79976415	4.452152566	3.57933023	2	2.3209407	2	2	2	2.3215434
ENSMUSG00000095866	Ighv2-4	-4.154376117	4.62E-05	3.32488899	3.8099383	3.32452507	4.99069578	5.349521258	5.38466829	2.99937492	2.3209407	2	2	2.3212258	2.3215434
ENSMUSG00000044678	Ly6k	-4.18160157	1.76E-06	7.07087367	7.24192452	7.0265606	4.31342374	4.38511559	4.31516673	3.45863601	3.1671805	3.4575315	2.8067906	2	2.8065305
ENSMUSG00000026322	Htr4	-4.187846233	0.0044827	3.00246783	3.4617334	3.46218583	8.41993804	8.446527354	8.48349066	2.58454581	2.5833164	2.3213312	4.5224741	4.4565564	4.3203887
ENSMUSG00000106620	Trav7-5	-4.354587263	0.0001195	3.32488899	3.17193469	3.32452507	3.79976415	3.694282913	3.57933023	2	2	2	2.3216648	2	2.3215434
ENSMUSG00000076485	Trbj1-3	-4.448917925	1.79E-08	7.16466507	6.98078072	6.98146849	6.38218749	6.201034321	5.89899925	2	2	2	3.9059249	3.3198201	3.8059806
ENSMUSG00000100277	1810053B23Rik	-4.528205816	0.000223	5.13365172	4.75796789	4.81106345	2.80280525	3.16498644	3.31686005	2	2	2.3213312	2	2.5837918	2.3215434
ENSMUSG00000076846	Trav13-2	-4.550098383	0.001944	2.58660819	3.00180885	2.58640584	4.89767527	4.992214091	5.16241042	2	2.5833164	2	2	2.5837918	2
ENSMUSG00000018451	6330403K07Rik	-4.763356575	0.0321698	2	2.32265191	2.32279427	5.31235716	5.451341511	5.12179534	2	2.9975301	2	2	2	2
ENSMUSG00000072601	Ear1	-4.956717609	0.0017395	2.80947046	2.32265191	2.32279427	4.7458302	4.516212395	4.57791872	2.32167809	2	2.3213312	2	2	2
ENSMUSG00000076483	Trbj1-1	-5.231797932	0.0001963	7.19462112	7.24192452	7.2330292	2.80280525	3.579034195	2.8037367	2	2	2	2.8067906	2.9982436	3.1688562
ENSMUSG00000102524	Ighv1-2	-5.263155979	0.0002889	3.70385559	3.17193469	3.46218583	10.3469463	10.33431159	10.3101127	3.80646187	3.5816684	2.9985073	4.9988477	5.2063188	4.4578572
ENSMUSG00000076473	Trbv16	-5.382278919	2.02E-11	9.60853248	9.60536763	9.5608088	7.03407934	6.910256766	6.92255873	2.32167809	4.0836837	5.2067896	2.8067906	3.6980072	3.1688562
ENSMUSG00000114348	Gm41031	-5.471990443	3.84E-07	3.46257176	3.5873738	3.32452507	3.6930831	3.45377331	3.99366215	2	2	2	2	2	2
ENSMUSG00000030996	Art1	-5.644584746	4.07E-08	4.17376203	4.25078255	4.39582017	3.79976415	3.99332894	3.69459039	2	2	2	2.3216648	2	2
ENSMUSG00000093966	Trav4-3	-5.783417276	0.0012717	2	3.00180885	2.58640584	4.38371152	4.314811199	4.69328731	2	2	2	2	2	2
ENSMUSG00000096656	Trav12-2	-5.843904197	0.0014073	2.58660819	2	2.32279427	5.51385184	5.48374496	5.38466829	2.32167809	2	2	2	2	2.3215434
ENSMUSG00000095958	Trav12-3	-5.916142207	0.0054503	2	2.58616865	2	5.99002889	6.16151936	5.79950395	2	2	2	2.5845236	2.3212258	2
ENSMUSG00000057163	Prss2	-6.418945482	0.0002294	11.3064198	11.3721164	11.3177688	7.09819562	6.849387244	7.20122591	5.24680876	5.3174793	4.8554064	2	2	2
ENSMUSG00000120741	Gm33302	-7.019412621	4.18E-06	6.15440119	6.1326921	5.86200878	3.57787902	2.582001393	2.58214912	2.32167809	2	2	2	2	2
ENSMUSG00000076462	Trbv2	-7.051421853	8.22E-32	8.67730852	8.83647377	8.73560407	11.2828504	11.17536922	11.1463763	2.58454581	4.1660812	3.9047007	3.5840846	3.9043138	4.3907597
ENSMUSG00000076463	Trbv3	-7.247456903	6.74E-13	11.4977792	11.5941978	11.5425088	6.52897969	6.861768337	6.6783732	3.16923045	3.4562874	3.4575315	4.4583541	3.6980072	4.2464084
ENSMUSG00000094262	Igkv4-62	-8.560340112	4.58E-09	3.588252	3.32409844	3.91006404	8.08227528	8.041081703	8.03606595	2.32167809	2	2	2.3216648	2	2
ENSMUSG00000076475	Trbv19	-10.33295226	5.53E-77	10.8243013	10.8325373	10.7815712	12.7705225	12.74473817	12.6710286	2.58454581	3.1671805	3.1682663	2.5845236	2.8058495	2.8065305
ENSMUSG00000076474	Trbv17	-11.44185643	1.61E-23	12.5814126	12.562512	12.6502066	8.19895935	8.181045251	8.08969923	2.58454581	2.3209407	2	2.3216648	2.5837918	2.3215434

Table S3_Hallmark pathways enriched in Bcat1 WT and KO leukemias

Pathways enriched in Bcat1 WT leukemias	ES	NES	NOM p-val	FDR q-val
HALLMARK_G2M_CHECKPOINT	0.42567	1.71925	0	0.006739
HALLMARK_MITOTIC_SPINDLE	0.41392	1.68235	0	0.006137
HALLMARK_EPITHELIAL_MESENCHYMAL_TRANSITION	0.34885	1.423	0.004451	0.097323
HALLMARK_E2F_TARGETS	0.34738	1.40488	0.0118871	0.087318
HALLMARK_IL2_STAT5_SIGNALING	0.29979	1.21522	0.0751105	0.416291
HALLMARK_UV_RESPONSE_DN	0.31143	1.21287	0.1036496	0.353612
HALLMARK_COAGULATION	0.28995	1.13833	0.1869301	0.530567
HALLMARK_ESTROGEN_RESPONSE_EARLY	0.27199	1.10751	0.2315341	0.573327
HALLMARK_INFLAMMATORY_RESPONSE	0.2671	1.07843	0.2759104	0.6134
HALLMARK_HEDGEHOG_SIGNALING	0.34868	1.06397	0.3468697	0.604395
HALLMARK_TGF_BETA_SIGNALING	0.31186	1.04334	0.3811802	0.620579
HALLMARK_MYOGENESIS	0.25379	1.03423	0.3644444	0.600102
HALLMARK_TNFA_SIGNALING_VIA_NFKB	0.23717	0.97192	0.5369318	0.76375
HALLMARK_SPERMATOGENESIS	0.25016	0.96383	0.5342262	0.735256
HALLMARK_KRAS_SIGNALING_DN	0.23191	0.94643	0.6017442	0.739215
HALLMARK_ESTROGEN_RESPONSE_LATE	0.2323	0.94442	0.6143057	0.69889
HALLMARK_UNFOLDED_PROTEIN_RESPONSE	0.24033	0.91822	0.6308943	0.73008
HALLMARK_ANGIOGENESIS	0.26646	0.83742	0.744186	0.88554
HALLMARK_WNT_BETA_CATENIN_SIGNALING	0.21143	0.66439	0.9622642	0.992732

Pathways enriched in Bcat1 KO leukemias	ES	NES	NOM p-val	FDR q-val
HALLMARK_OXIDATIVE_PHOSPHORYLATION	-0.55955	-2.41774	0	0
HALLMARK_ADIPOGENESIS	-0.44633	-1.96541	0	0
HALLMARK_PEROXISOME	-0.42111	-1.68117	0.0026667	0.016598
HALLMARK_DNA_REPAIR	-0.39622	-1.6771	0	0.01317
HALLMARK_REACTIVE_OXYGEN_SPECIES_PATHWAY	-0.48062	-1.62967	0.0025063	0.014993
HALLMARK_XENOBIOTIC_METABOLISM	-0.36976	-1.60909	0	0.014463
HALLMARK_INTERFERON_ALPHA_RESPONSE	-0.40215	-1.58082	0.005102	0.016218
HALLMARK_APOPTOSIS	-0.35749	-1.53048	0	0.023055
HALLMARK_P53_PATHWAY	-0.34366	-1.52925	0.0030211	0.020832
HALLMARK_BILE_ACID_METABOLISM	-0.37796	-1.51214	0.0058651	0.021403
HALLMARK_IL6_JAK_STAT3_SIGNALING	-0.39037	-1.4898	0.0086207	0.023926
HALLMARK_FATTY_ACID_METABOLISM	-0.34599	-1.47731	0.0031847	0.02465
HALLMARK_HYPOXIA	-0.3309	-1.44721	0.006079	0.029479
HALLMARK_INTERFERON_GAMMA_RESPONSE	-0.3166	-1.39444	0.012945	0.045257
HALLMARK_PI3K_AKT_MTOR_SIGNALING	-0.3471	-1.38569	0.0258621	0.046325
HALLMARK_COMPLEMENT	-0.31305	-1.35672	0.0186916	0.056331
HALLMARK_ALLOGRAFT_REJECTION	-0.29664	-1.30317	0.020339	0.081336
HALLMARK_PANCREAS_BETA_CELLS	-0.37285	-1.26095	0.1234867	0.110291
HALLMARK_KRAS_SIGNALING_UP	-0.27289	-1.20407	0.070946	0.166313
HALLMARK_MTORC1_SIGNALING	-0.27663	-1.20235	0.0758621	0.160013
HALLMARK_APICAL_JUNCTION	-0.26799	-1.18999	0.0664452	0.170627
HALLMARK_GLYCOLYSIS	-0.26816	-1.18638	0.0827815	0.167523
HALLMARK_MYC_TARGETS_V1	-0.25788	-1.13489	0.1456954	0.234451
HALLMARK_HEME_METABOLISM	-0.25118	-1.09828	0.2024169	0.292568
HALLMARK_UV_RESPONSE_UP	-0.25492	-1.08273	0.2739274	0.316627
HALLMARK_PROTEIN_SECRETION	-0.26803	-1.05734	0.3164894	0.359791
HALLMARK_NOTCH_SIGNALING	-0.31323	-0.98176	0.4774347	0.565478
HALLMARK_CHOLESTEROL_HOMEOSTASIS	-0.249	-0.94304	0.5605263	0.671222
HALLMARK_ANDROGEN_RESPONSE	-0.22428	-0.88852	0.7147059	0.817348
HALLMARK_APICAL_SURFACE	-0.23808	-0.81848	0.8004751	0.938566
HALLMARK_MYC_TARGETS_V2	-0.16052	-0.5775	0.9976247	0.999054

Table S4: Primer sequences for amplification of BCAT1 promoter using Methylation Specific PCR (MSP)

TARGET LOCI	DIRECTION	SEQUENCE (5' to 3')
BCAT1-prom-T1-M	FORWARD	GAGAGATTTTATTATTTGGGGGC
BCAT1-prom-T1-M	REVERSE	CTAACCGTATAAACCGAATCTACGA
BCAT1-prom-T1-U	FORWARD	GAGAGATTTTATTATTTGGGGGTG
BCAT1-prom-T1-U	REVERSE	TAACCATATAAACCAAATCTACAAC
BCAT1-prom-T1-WT*	FORWARD	GTGTCTTCCTGCTGATGCAA
BCAT1-prom-T1-WT	REVERSE	AGATCCCAAGGGTCGTAGC
ACTB	FORWARD	GTGATGGAGGAGGTTTAGTAAGTT
ACTB	REVERSE	AATTACAAAAACCACAACCTAATAAA

*WT, represents unmodified or wild-type primers. M, methylation-specific primers; and U, unmethylated-specific primers.

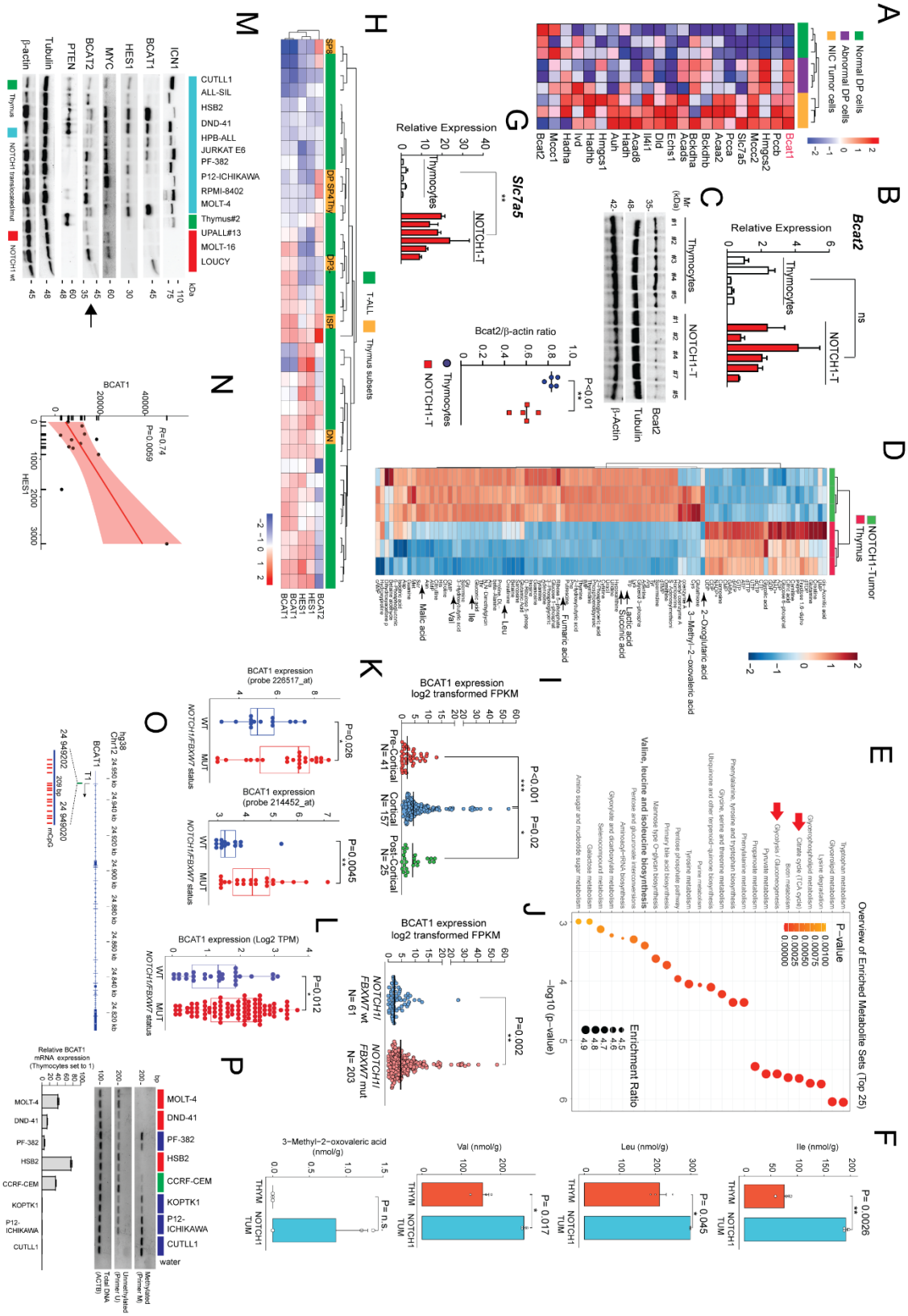

Figure S1. BCAT1 is highly expressed in NOTCH1 mutant T-cell acute lymphoblastic leukemia (T-ALL). (A) Heat map showing the expression levels of BCAA metabolic genes (N=22) between normal, abnormal (pre-

leukemic) DP cells and *ICN1*-induced DP leukemic cells (NIC Tumors). (B) Expression levels (qRT-PCR) of *Bcat2* in thymocytes obtained from 6-8 weeks old C57/Bl6 mice and leukemic cells from six *ΔE-NOTCH1* T-ALL tumors (NOTCH1-T). Significance was calculated using an unpaired two-tailed t-test. ns= not significant. (C) Western blot (top) showing protein expression levels of Bcat2. β-actin and tubulin are shown as loading controls. Graphical representation of Bcat2/β-actin ratios (bottom). Bars represent mean values. Significance was calculated using an unpaired two-tailed t-test. ***P*< 0.01. (D) Heatmap representation of metabolites identified by capillary electrophoresis time-of-flight mass spectrometry (CE-TOFMS) of thymic tissue (N=3) obtained from 6 weeks old C57/Bl6 mice and NOTCH1-induced *ΔE-NOTCH1* tumor tissue (spleen; N=3). (E) Metabolite Set Enrichment Analysis (MSEA) was used to determine differentially enriched metabolite sets between normal thymic tissue and *ΔE-NOTCH1* tumors. The top 25 enriched pathways are shown. (F) Quantification of tissue BCAA (isoleucine, leucine and valine) and BCKA (3-methyl-2-oxovaleric acid, KMV) in thymic tissue (N=3) obtained from 6 weeks old C57/Bl6 mice and NOTCH1-induced *ΔE-NOTCH1* tumor tissue (spleen; N=3). Significance was calculated using an unpaired two-tailed t-test. **P*< 0.05, ***P*< 0.01. (G) Expression levels (qRT-PCR) of *Lat1* (*slc7a5*) in thymocytes obtained from 6-8 weeks old C57/Bl6 mice and leukemic cells from six *ΔE-NOTCH1* T-ALL tumors (NOTCH1-T). Significance was calculated using an unpaired two-tailed t-test. **P< 0.01. (H) Heat map showing the expression levels of BCAT1 (two probes), BCAT2 and HES1 (surrogate of activated NOTCH1) between healthy human thymic subpopulations and total thymus and diagnostic pediatric T-ALL samples (N=32). SP8=CD8 single positive, DP= CD3 negative CD4 and CD8 double positive, SP4= CD4 single positive, Thy=total thymus, DP3= CD3 positive CD4 and CD8 double positive, ISP=intermediate single positive, DN= CD4 and CD8 double negative. (I) BCAT1 expression levels in immunophenotypically distinct T-ALL subtypes (pre-cortical, cortical and post-cortical). Significance was calculated using a nonparametric t-test (Mann-Whitney). **P*< 0.05, ****P*< 0.001. (J) BCAT1 expression levels in *NOTCH1/FBXW7* wild-type (wt) and *NOTCH1/FBXW7* mutated (mut) T-ALL in COG ALL TARGET cohort[14]. Significance was calculated using an unpaired two-tailed t-test. ***P*< 0.01. (K) BCAT1 expression levels in *NOTCH1/FBXW7* wt (wt) and *NOTCH1/FBXW7* mutated (mut) T-ALL in GSE14959 cohort (N=37)[10]. Two different probes are shown. Significance was calculated using a nonparametric t-test (Mann-Whitney). **P*< 0.05, ***P*< 0.01. (L) BCAT1 expression levels in NOTCH1 wild-type (wt) and NOTCH1 activated (*NOTCH1/FBXW7* mutated) T-ALL (adult and pediatric) (CGAS00000000002)[11]. Significance was calculated using an unpaired two-tailed t-test. **P*< 0.05. (M) Western blot analysis of ICN1, BCAT1, HES1, MYC, BCAT2, PTEN in T-ALL cell lines. Tubulin and β-actin are shown as loading controls. Cell lines with un-mutated NOTCH1 (wt) or activated NOTCH1 signaling (mutated/translocated) are shown. Arrow indicates specific band. (N) Correlation analysis between expression levels of BCAT1 and HES1 in T-ALL cell lines (ALL-SIL, CCRF-HSB2, DND41, HPB-ALL, Jurkat, PF-382, P12-Ichikawa, RPMI8402, MOLT4, CCRF-CEM, MOLT-3, MOLT-16; N=12) from GSE168386[28]. (O) Schematic drawing of BCAT1 gene structure (left) with amplicon coordinates indicated (UCSC Genome browser GRCh38/hg38 version). Methylated cytosines residing in CpG sites are depicted as red lines. (P) Methylation specific PCR (MSP) of BCAT1 promoter T1[29, 30]was set-up and used to evaluate methylation status of BCAT1 in T-ALL cell lines. Primer sets used for amplification are designated as unmethylated (U) and methylated (M). A bisulphite-conversion specific beta-actin gene (*ACTB*) PCR assay was performed as control assay to evaluate total amount of analyzed DNA. All DNA samples were bisulfite-treated. Relative BCAT1 transcript levels of the analyzed T-ALL cell lines are also shown (lower panel). BCAT1 expression is relative to a human thymocyte sample (#1).

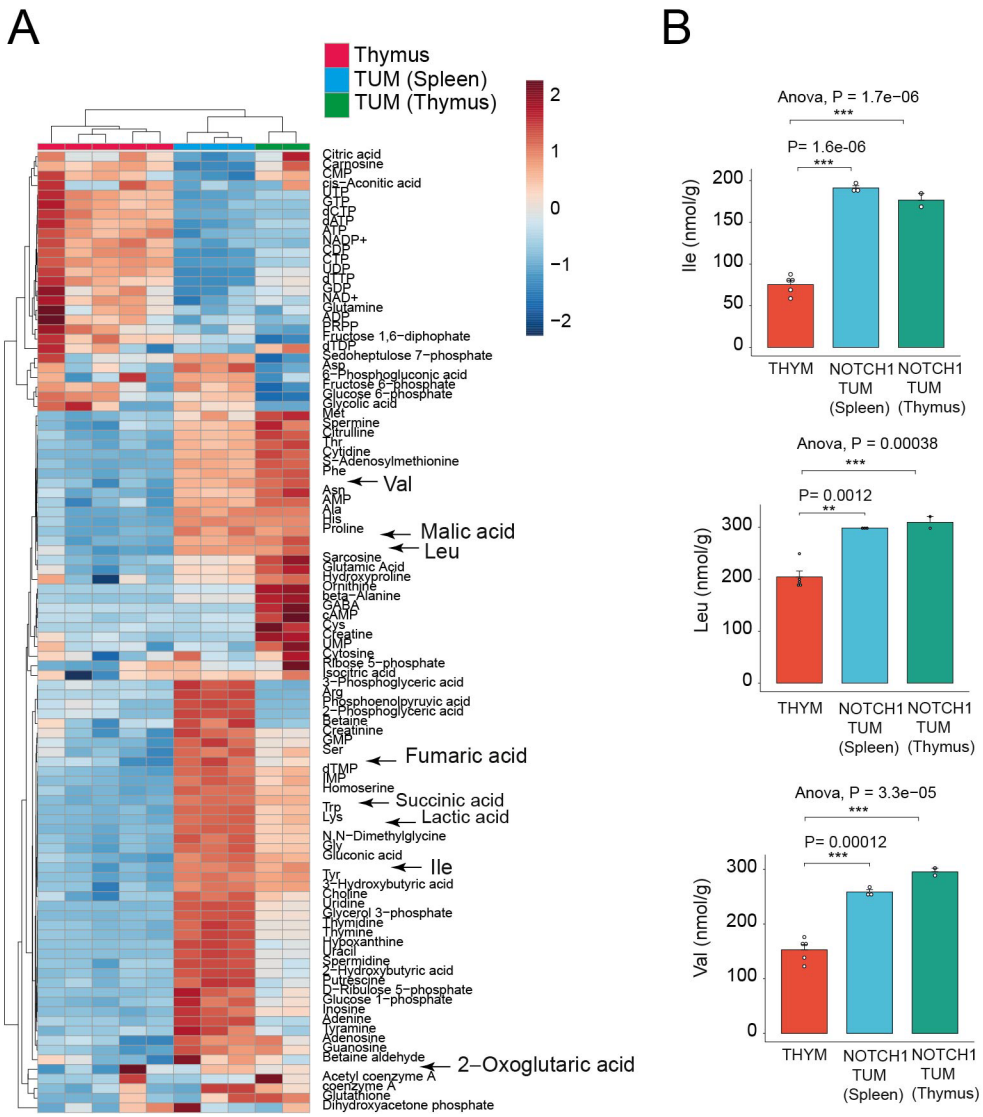

Figure S2. *ΔE-NOTCH1* tumors derived from infiltrated spleen and thymus have a similar metabolic profile. (A) Heatmap representation of metabolites identified by capillary electrophoresis time-of-flight mass spectrometry (CE-TOFMS) of thymic tissue (N=5) obtained from 6 weeks old C57/Bl6 mice and NOTCH1-induced *ΔE-NOTCH1* tumor tissue (spleen; N=3 or thymus; N=2). Selected metabolites differentially expressed between normal and leukemic tissue are remarked. (B) Quantification of tissue BCAA (isoleucine, leucine and valine) in thymic tissue (N=5) obtained from 6 weeks old C57/Bl6 mice and NOTCH1-induced *ΔE-NOTCH1* tumor tissue (spleen; N=3 or thymus; N=2). Significance was calculated using an unpaired two-tailed t-test or ANOVA test (normal versus leukemia). $^{**}P< 0.01$, $^{***}P< 0.001$.

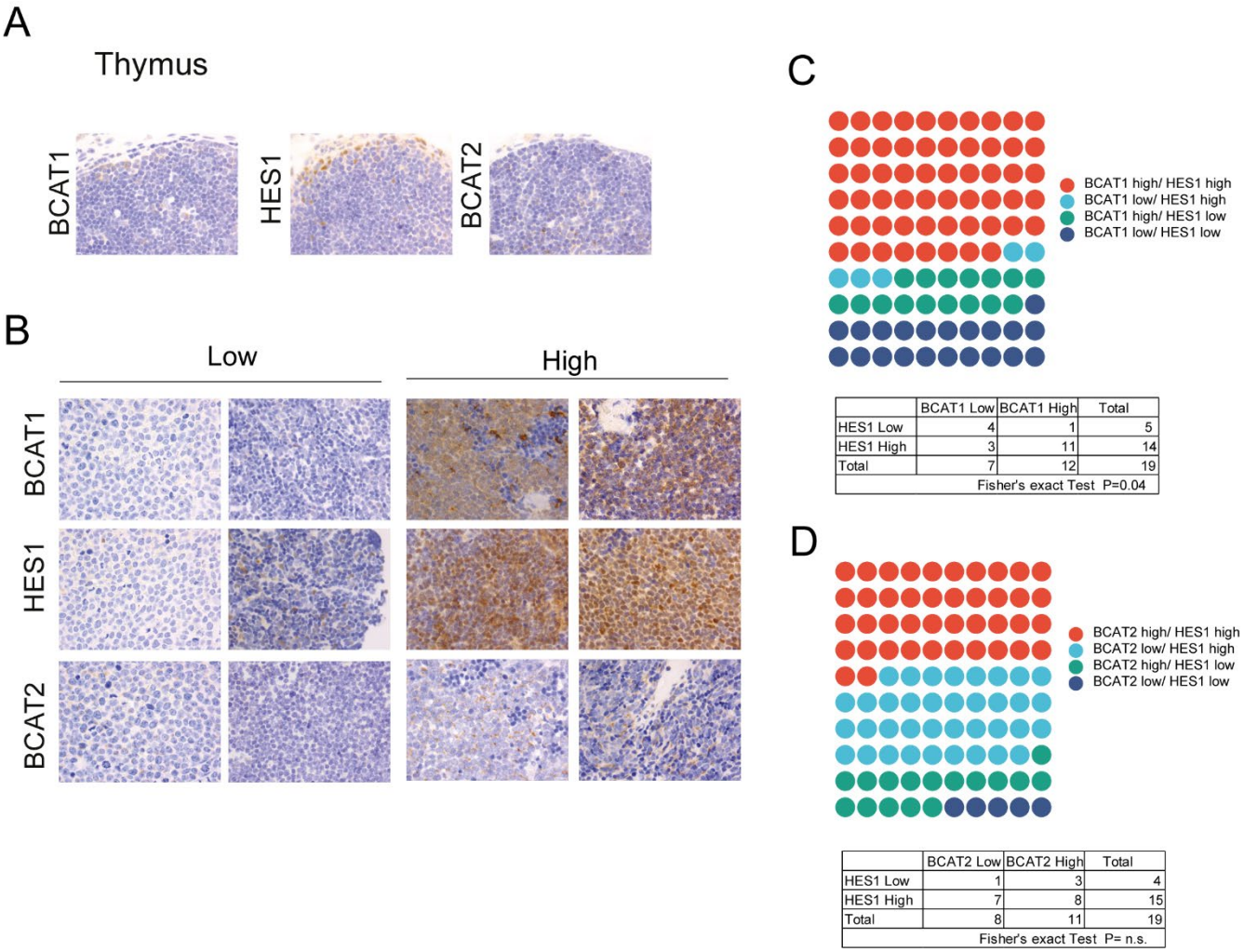

	BCAT1 Low	BCAT1 High	Total
HES1 Low	4	1	5
HES1 High	3	11	14
Total	7	12	19
Fisher's exact Test P=0.04			

	BCAT2 Low	BCAT2 High	Total
HES1 Low	1	3	4
HES1 High	7	8	15
Total	8	11	19
Fisher's exact Test P= n.s.			

Figure S3. BCAT1 expression associates with NOTCH1 activation in human T-ALL. (A) BCAT1 (left), HES1 (middle) and BCAT2 (right) immunohistochemical staining of human thymus (top): original magnification 400×. (B) Immunohistochemical staining for BCAT1 (top), HES1 (middle), and BCAT2 (bottom) in representative cases of T-ALL showing low (0, +1) and high (+2, +3) expression levels. Original magnification ×400. (c) Circle waffle representation of BCAT1 immunohistochemical staining results obtained in T-ALL/T-LBL/PDX samples analysed (top) and correlation table for Fisher's exact test (bottom). (D) Circle waffle representation of BCAT2 immunohistochemical staining results obtained in T-ALL/T-LBL/PDX samples analysed (top) and correlation table for Fisher's exact test (bottom).

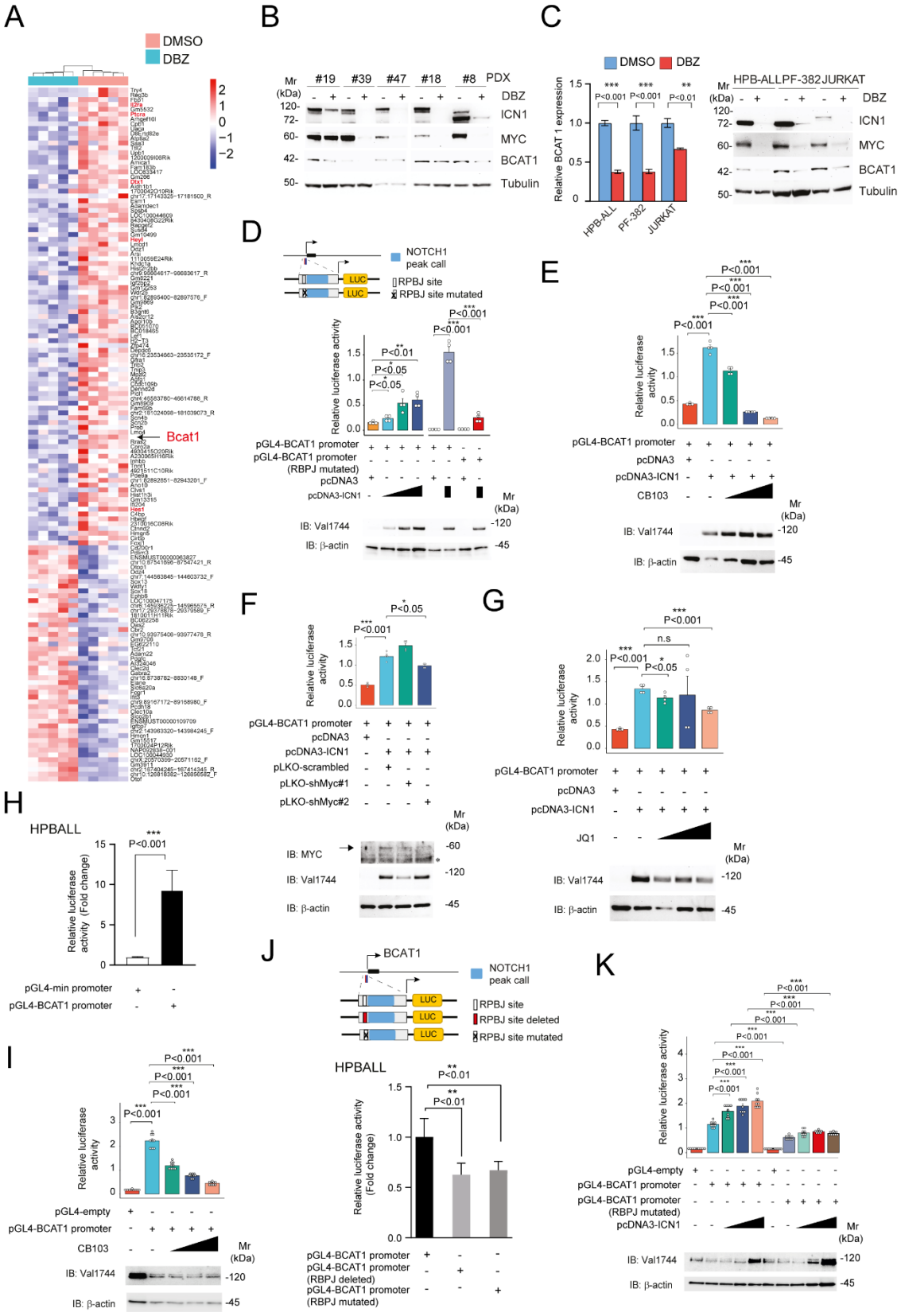

Figure S4. BCAT1 is modulated upon NOTCH1 inhibition. (A) Heat map representation of the top down-regulated genes following in vivo DBZ treatment of five *ΔE-NOTCH1* tumors. BCAT1 and selected known

NOTCH1 target genes are shown[1]. (B) PDX samples were treated in vivo with DBZ (10 μg/kg every 8 hours for a total of 3 injections) or vehicle (DMSO) for 24h before analysis of BCAT1 protein levels. ICN1 and MYC proteins are also shown. Tubulin is shown as loading control. (C) T-ALL cell lines were treated with DBZ (250 nM) or vehicle for 72h before analysis of BCAT1 transcript (left) or BCAT1 protein levels (right). ICN1 and MYC proteins are also shown. Tubulin is shown as loading control. Mean value and SD are shown. For statistical analysis, an unpaired t-test was used. $^{**}P< 0.01$. $^{***}P< 0.001$. (D) Schematic representation (top) of *BCAT1* promoter construct (BCAT1-Luc) containing the region –1407 to +195 from the transcription start site (TSS) including the proximal RBPJ binding site. The location of the NOTCH1 ChIP peak is also depicted on the reporter construct. HEK 293T cells were co-transfected with pGL4 luciferase reporter construct (BCAT1-Luc) and different amounts of pcDNA3-ICN1 or control plasmid. In some experiments, HEK 293T cells were also co-transfected with BCAT1-Luc having the RBPJ site mutated and ICN1 plasmid. Immunoblot shows expression levels of ICN1 in transfected cells. β-actin is shown as loading control. Error bars indicate ± SD. Results from one of two independent experiments performed in quadruplicate are shown. Significance was calculated using an unpaired two-tailed t-test. $^{*}P< 0.05$, $^{**}P< 0.01$, $^{***}P< 0.001$. (E) HEK 293T cells were co-transfected with pGL4 luciferase reporter construct (BCAT1-Luc) and ICN1 or control plasmid. After 24h, ICN1 transfected cells were treated with increasing concentration of CB103 (10 nM-1 μM) or vehicle for 48h. Immunoblot shows expression levels of ICN1 in transfected cells. β-actin is shown as loading control. Error bars indicate ± SD. Results from one of two independent experiments performed in quadruplicate are shown. Significance was calculated using an unpaired two-tailed t-test. $^{***}P< 0.001$. (F) HEK 293T cells were co-transfected with pGL4 luciferase reporter construct (BCAT1-Luc) and ICN1 or control plasmid. After 24h, ICN1 transfected cells were transfected with plasmids silencing MYC (pLKO-shMYC#1, pLKO-shMYC#2) or non-silencing control (pLKO-shscrambled). Cells were harvested 48h later. Immunoblot shows expression levels of MYC and ICN1 in transfected cells. β-actin is shown as loading control. Arrow indicates specific band. Asterisc (*) indicates non-specific band. Error bars indicate ± SD. Results from one of two independent experiments performed in quadruplicate are shown. Significance was calculated using an unpaired two-tailed t-test. $^{*}P< 0.05$, $^{***}P< 0.001$. (G) HEK 293T cells were co-transfected with pGL4 luciferase reporter construct (BCAT1-Luc) and ICN1 or control plasmid. After 24h, ICN1 transfected cells were treated with increasing concentrations of JQ1 (10 nM-1 μM) or vehicle for 48h. Immunoblot shows expression levels of ICN1 in transfected cells. β-actin is shown as loading control. Error bars indicate ± SD. Results from one of two independent experiments performed in quadruplicate are shown. Significance was calculated using an unpaired two-tailed t-test. $^{*}P< 0.05$, $^{***}P< 0.001$. n.s=not significant. (H) Relative luciferase reporter activity in HPB T-ALL cells transfected with a BCAT1 promoter construct (BCAT1-Luc) or empty pGL4minP plasmid. Mean value and SD are shown (N =6). For statistical analysis, an unpaired t-test was used. $^{***}P< 0.001$. The experiment was repeated three times with similar results. (I) Relative luciferase reporter activity in HPB T-ALL cells transfected with pGL4 luciferase reporter construct (BCAT1-Luc) or control plasmid. After 24h, transfected cells were treated with increasing concentration of CB103 (0.5 μM-5 μM) or vehicle for 48h. Immunoblot shows expression levels of ICN1 in transfected cells. β-actin is shown as loading control. Error bars indicate ± SD. Results from one of two independent experiments performed is shown. Significance was calculated using an unpaired two-tailed t-test. $^{***}P< 0.001$. (J) Relative luciferase reporter activity in HPB T-ALL cells transfected with BCAT1-Luc wt construct, BCAT1-Luc having the RBPJ site deleted or mutated. Mean value and SD are shown (N=6). For statistical analysis, an unpaired t-test was used. $^{**}P< 0.01$. The experiment was repeated three times with similar results. (K) Relative luciferase reporter activity in HPB T-ALL cells transfected with BCAT1-Luc wt construct, BCAT1-Luc having the RBPJ site mutated or control vector. These cells were co-transfected with increasing concentrations of pcDNA3-ICN1 or control plasmid (100-500 ng). Error bars indicate ± SD. For statistical analysis, an unpaired t-test was used. $^{***}P< 0.001$. Immunoblot shows expression levels of ICN1 in transfected cells. β-actin is shown as loading control.

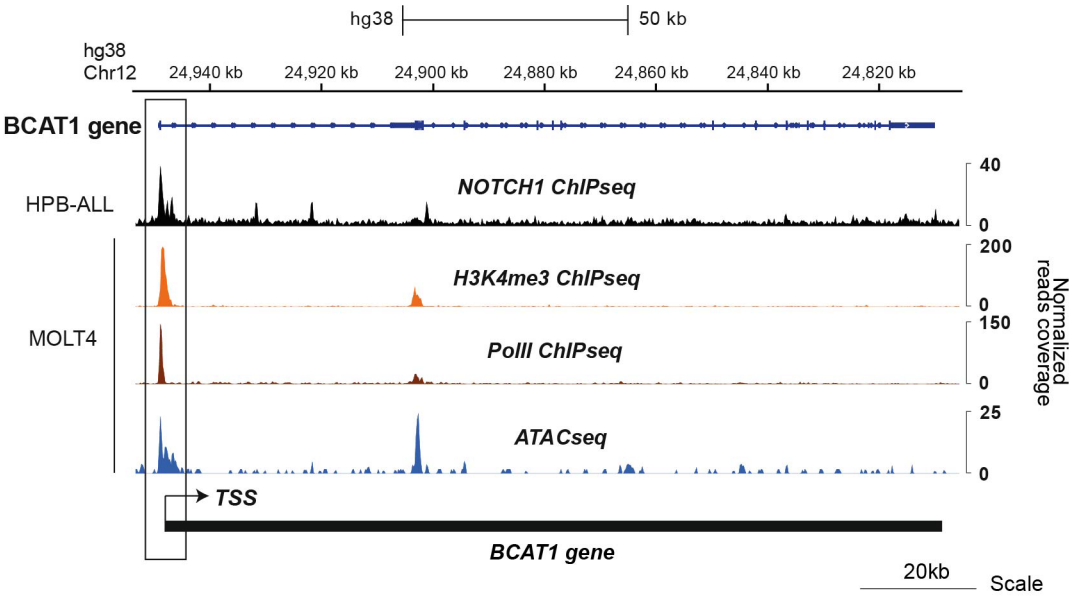

Figure S5. The NOTCH1 binding region in the BCAT1 locus is associated with promoter features in T-ALL cells. Profiles of H3K4me3, Pol II and NOTCH1 ChIP-seq binding in the BCAT1 locus in T-ALL cells. ATAC-seq data for the same region is also shown.

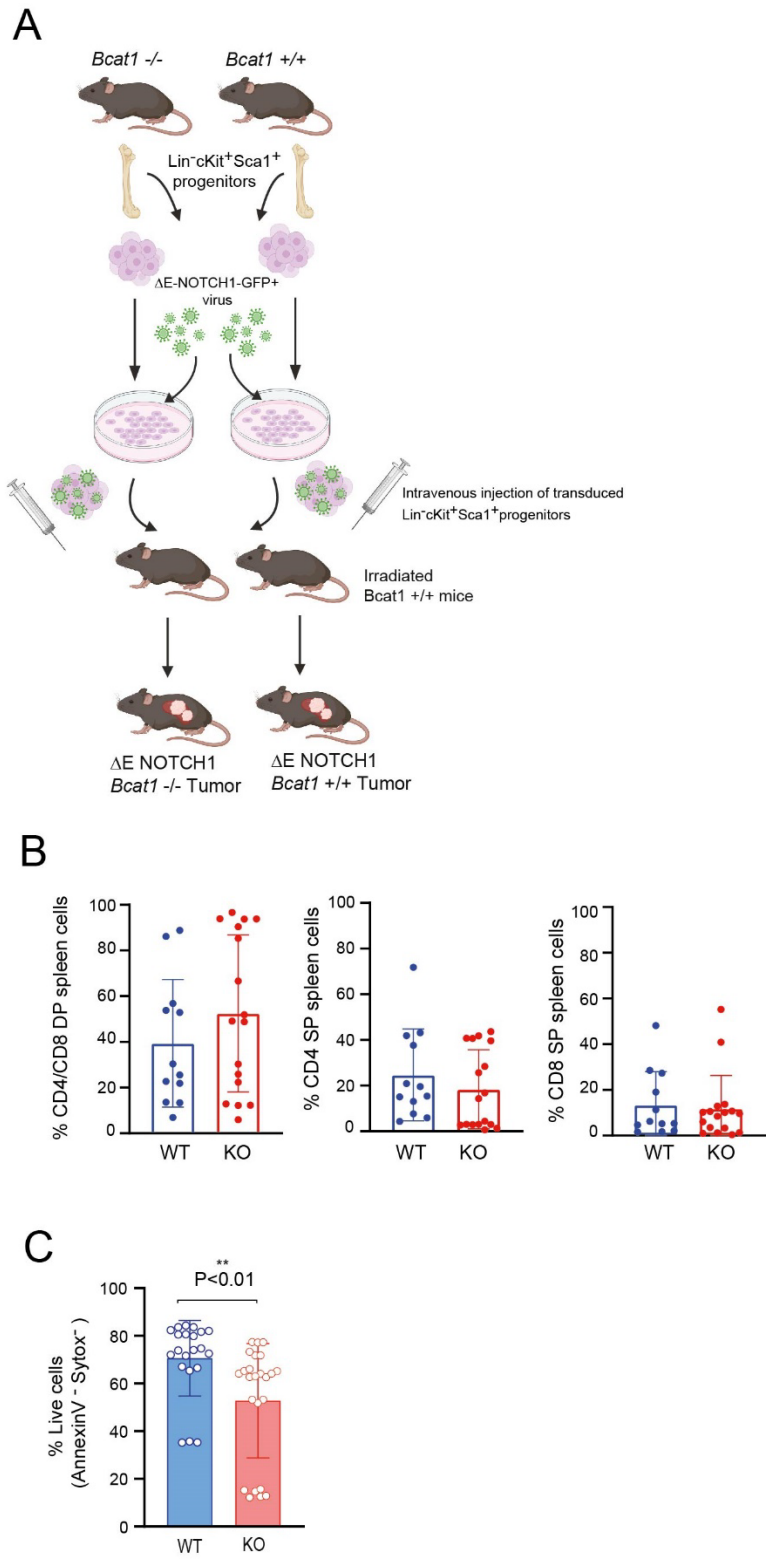

Figure S6. Bcat1 promotes NOTCH1-dependent leukemia onset. (A) Schematic representation of the experimental procedure for the generation of *ΔE-NOTCH1* leukemias wild-type (WT; +/+) and null (KO; -/-) for *Bcat1*. Image was generated with BioRender software. (B) Immunophenotype distribution showing the expression levels of CD4 and CD8 in *ΔE-NOTCH1*-induced leukemias at the moment of sacrifice. DN, double negative; DP,

double positive; SP, single positive. WT, *Bcat1* wild-type; KO, *Bcat1* null. (C) Quantification of viable cells (Annexin V^- Sytox Red^-) in *ΔE-NOTCH1* leukemias WT and null for *Bcat1* obtained ex vivo (bar graph). Data for bar graph is shown as mean ± SD. Significance was calculated using an unpaired two-tailed t-test. $^{**}P < 0.01$.

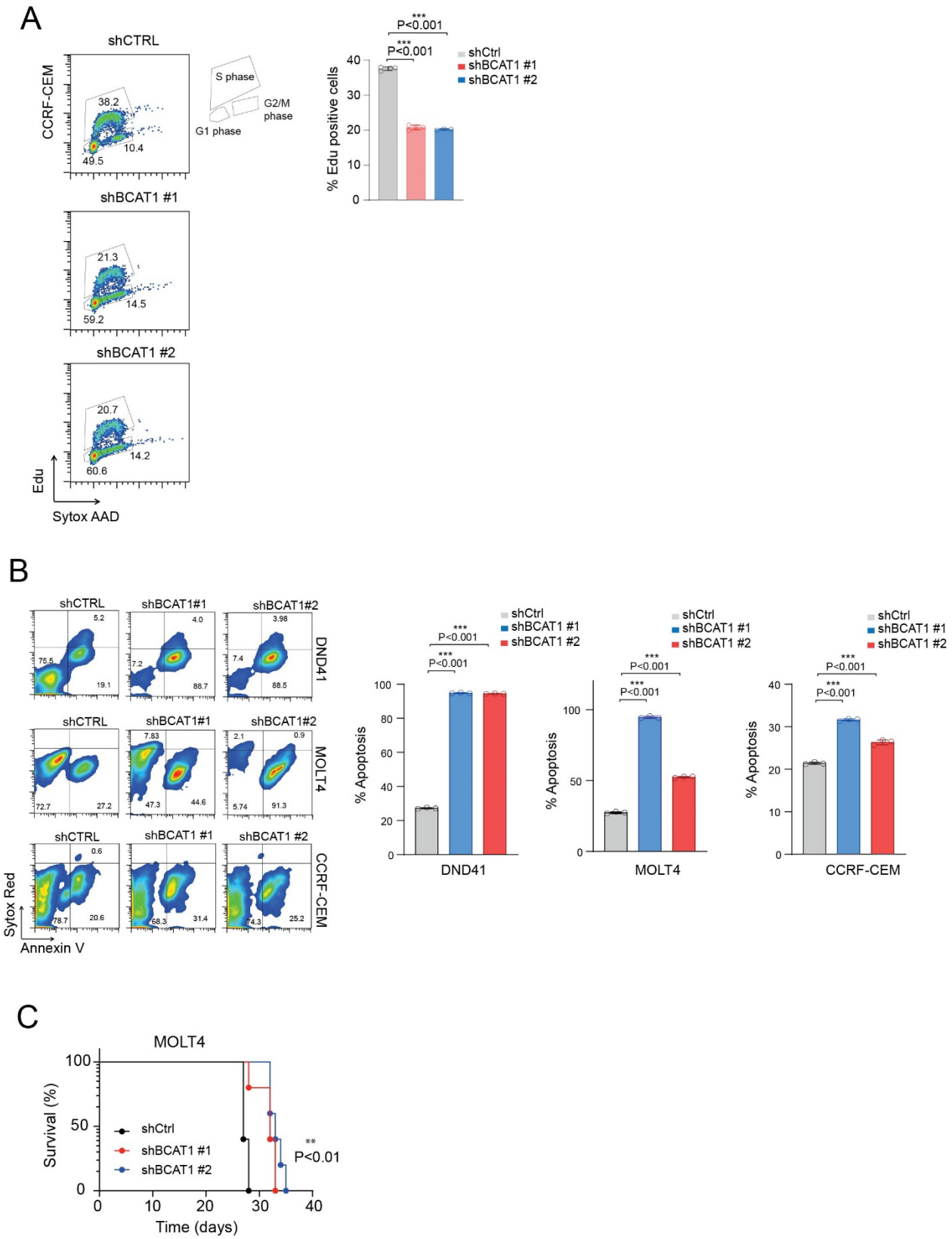

Figure S7. Functional effects of BCAT1 depletion. (A) Representative plots (left) and bar graph representation (right) of CCRF-CEM cells transduced with shCTRL, shBCAT1#1 or shBCAT1#2 twelve days post-puromycin

selection and assessed for EdU incorporation by fluorescence-activated cell sorting (FACS) analysis. Data for bar graph is shown as mean ± SD. Significance was calculated using an unpaired two-tailed t-test. ***$P< 0.001$. (B) Representative plots of apoptosis (left) and quantification of apoptosis (right) in in DND41, MOLT4 and CCRF-CEM T-ALL cells transduced with shCTRL, shBCAT1 #1 and shBCAT1 #2 constructs 3-5 days post-puromycin selection. Data for bar graph is shown as mean ± SD. Significance was calculated using an unpaired two-tailed t-test. ***$P< 0.001$. (C) Kaplan-Meier survival curves of overall survival in NSG mice xenografted with MOLT4 cells expressing luciferase and transduced with shCTRL or shBCAT1 (#1 and #2). Log-rank test was performed to calculate *P* value. **$P< 0.01$.

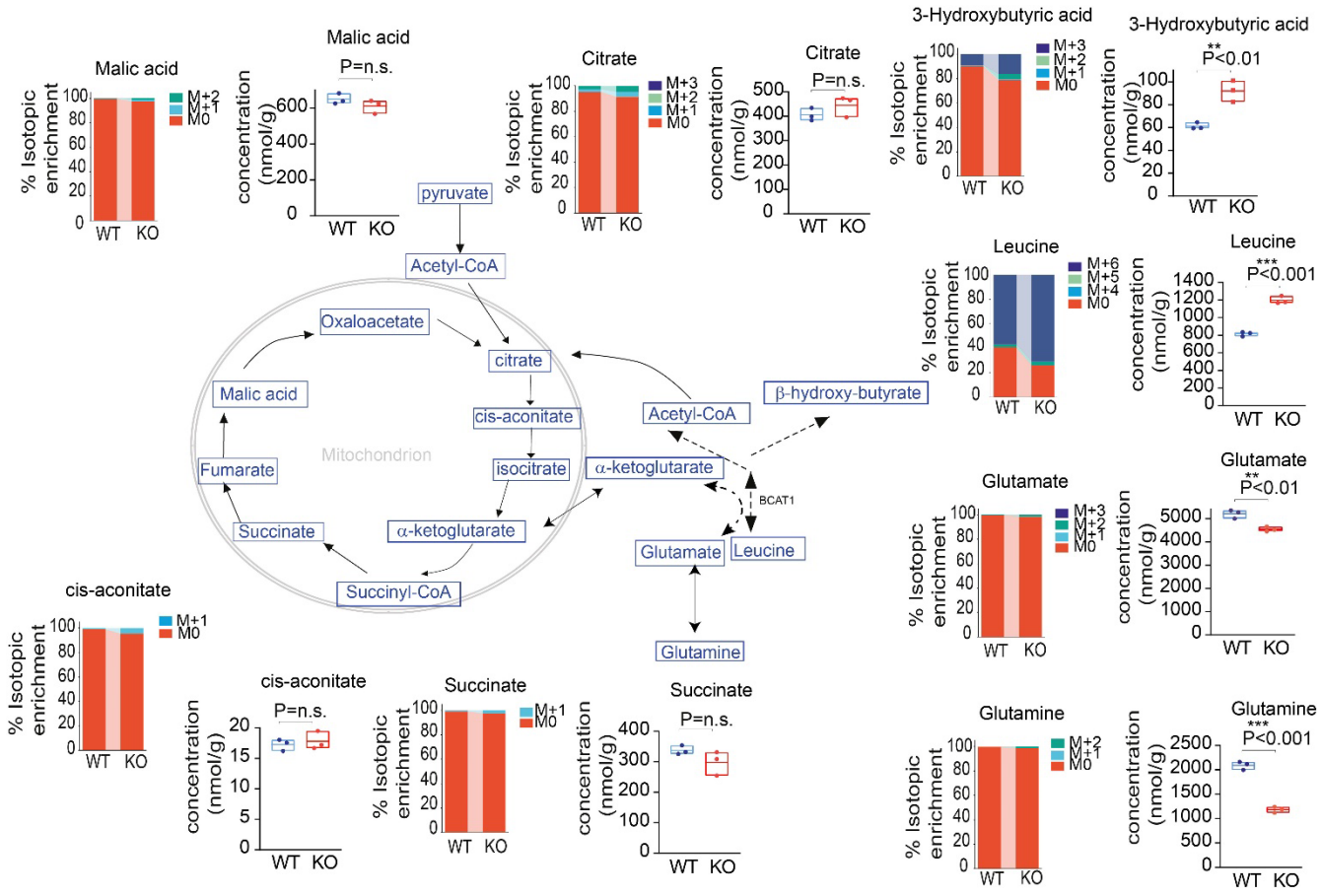

Figure S8. **Metabolic impact of Bcat1 depletion on *ΔE-NOTCH1* leukemias.** Results for *in vivo* isotope-tracing experiments following i.v. administration of $^{13}C_6$ Leu in *ΔE-NOTCH1* leukemias WT and KO for *Bcat1*. Mean percentages (from N=3 determinations) of $^{13}C_6$ Leu derived: (i) TCA intermediates: citrate (M0, M+1, M+2, M3), cis-aconitate, (M0, M+1), malic acid (M0, M+1, M+2), succinate (M0, M+1); (ii) BCAA and derivatives: leucine (M0, M+4, M+5, M+6), glutamate (M0, M+1, M+2, M3), glutamine (M0, M+1, M+2) and beta-hydroxybutyrate (M0, M+1, M+2, M+3) are shown. F-scope metabolic quantification for selected metabolites in the same tumors is also shown. Changes in glutaminolysis, TCA cycle intermediates, and BCAA and intermediates are shown as floating bars representing mean ± SD. Significance was calculated using a nonparametric t-test (Mann-Whitney). **P*< 0.05, ***P*< 0.01, ***P< 0.001. n.s.= not significant.

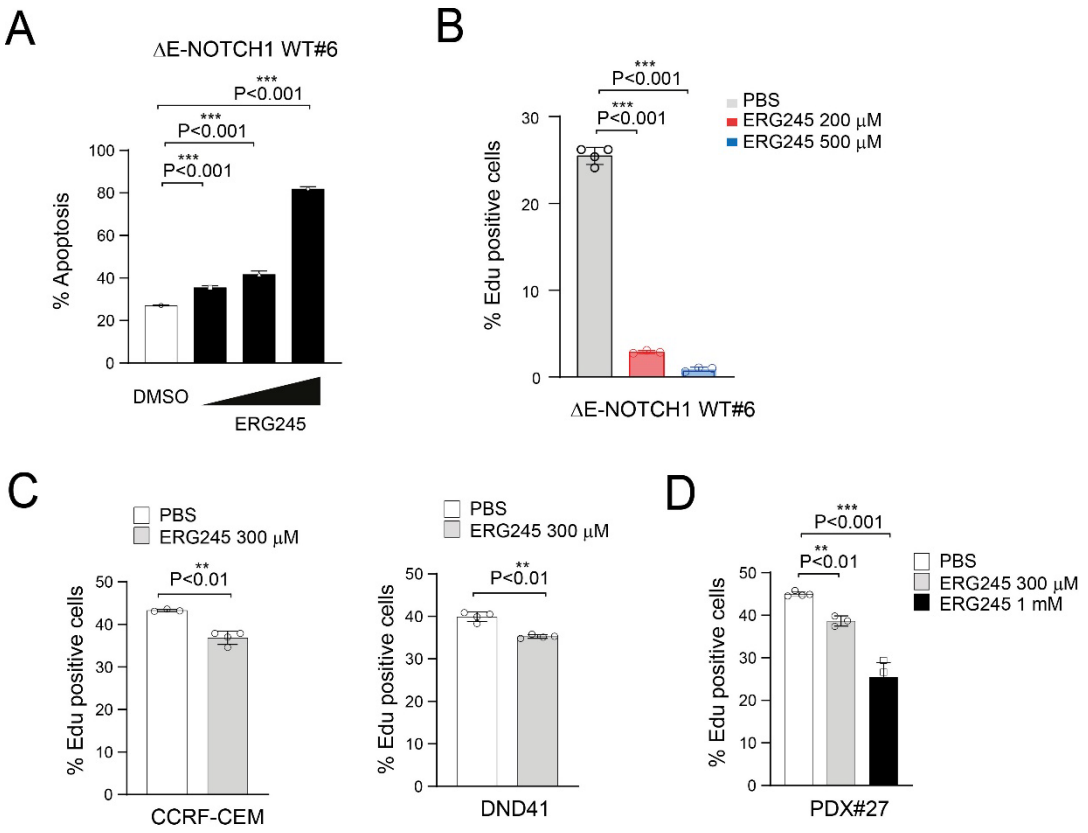

Figure S9. Functional effects of a BCAT1 specific inhibitor, ERG245. (A) Quantification of apoptosis in *ΔE-NOTCH1* leukemia wild-type for *Bcat1* (WT#6) treated in vitro for 48h with PBS (vehicle) or increasing doses of ERG245 (200 μM-1 mM). Data for bar graph is shown as mean ± SD. Significance was calculated using an unpaired two-tailed t-test. ****P*< 0.001. (B) Quantification of EdU incorporation (S-phase cells) in *ΔE NOTCH1* leukemia wild-type for Bcat1 (WT#6) treated in vitro for 48h with PBS (vehicle) or increasing doses of ERG245 (200 μM- 500 μM). Data for bar graph is shown as mean ± SD. Significance was calculated using an unpaired two-tailed t-test. ****P*< 0.001. (C) Quantification of EdU incorporation (S-phase cells) in T-ALL cell lines (CCRF-CEM, DND41) treated in vitro for 72h with PBS (vehicle) or ERG245 (300 μM). Data for bar graph is shown as mean ± SD. Significance was calculated using an unpaired two-tailed t-test. ***P*< 0.01. (D) Quantification of EdU incorporation (S-phase cells) in PDX#27 treated in vitro for 72h with PBS (vehicle) or increasing doses of ERG245 (300 μM-1 mM). Data for bar graph is shown as mean ± SD. Significance was calculated using an unpaired two-tailed t-test. ***P*< 0.01, ****P*< 0.001.

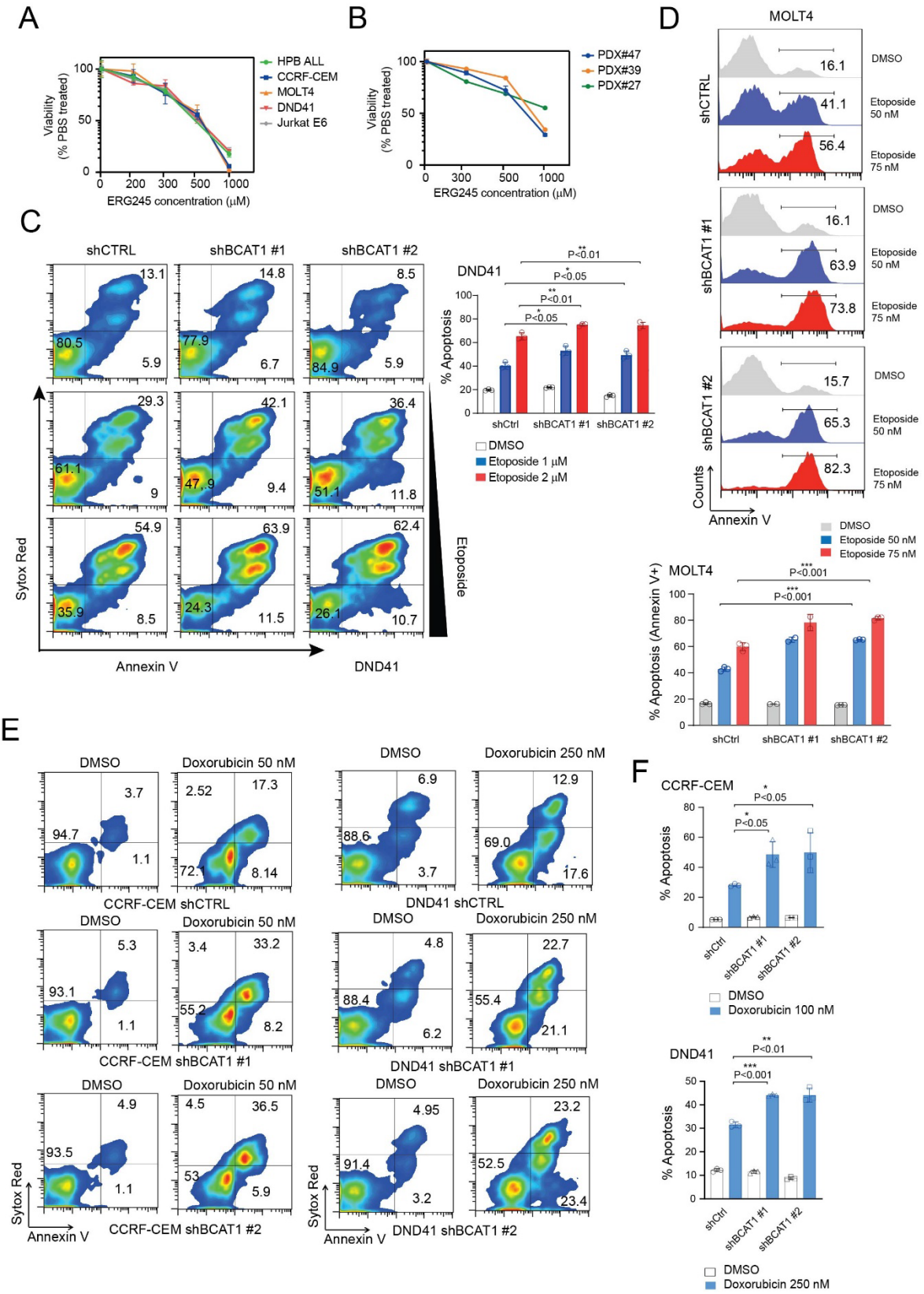

Figure S10. BCAT1 specific inhibition has modest cytotoxic effects on human T-ALL, while BCAT1 depletion increases sensitivity to DNA damaging agents. (A) Cell viability analysis in T-ALL cell lines (HPB-

ALL, CCRF-CEM, MOLT4, DND41, Jurkat E6). T-ALL cells were treated in vitro for 72h with PBS (vehicle) or increasing doses of ERG245 (200 μM-1 mM). Data is shown as mean ± SD. (B) Cell viability analysis in PDX samples (PDX#47, PDX#39, PDX#27). T-ALL cells were treated in vitro for 72h with PBS (vehicle) or increasing doses of ERG245 (300 μM-1 mM). Data is shown as mean ± SD. (C) Representative plots of apoptosis (left) in DND41 T-ALL cells transduced with shCTRL or shBCAT1 (#1 and #2) and treated in vitro for 48h with DMSO (vehicle) or etoposide (1 μM or 2 μM). Quantification of apoptosis (right) in DND41 T-ALL cells transduced with shCTRL or shBCAT1 (#1 and #2) and treated in vitro for 48h with DMSO (vehicle) or etoposide (1 μM or 2 μM). Significance was calculated using an unpaired two-tailed t-test. * $P< 0.05$, ** $P< 0.01$. (D) Representative plots (top) and bar graph representation (bottom) of annexin V staining in MOLT4 T-ALL cells transduced with shCTRL or shBCAT1 (#1 and #2) and treated with vehicle (DMSO) or etoposide (Etop; 50-75 nM) for 48h. (E) Representative plots of apoptosis in CCRF-CEM (left) or DND41 (right) T-ALL cells transduced with shCTRL, shBCAT1#1 or shBCAT1#2 and treated with vehicle (DMSO) or doxorubicin (Doxo; 50 or 250 nM, respectively) for 48h. (F) Bar graph representation of apoptosis in CCRF-CEM (top) or DND41 (bottom) T-ALL cells transduced with shCTRL, shBCAT1#1 or shBCAT1#2 and treated with vehicle (DMSO) or doxorubicin (Doxo; 50 or 250 nM, respectively) for 48h. Significance was calculated using an unpaired two-tailed t-test. * $P< 0.05$, ** $P< 0.01$, *** $P< 0.001$.

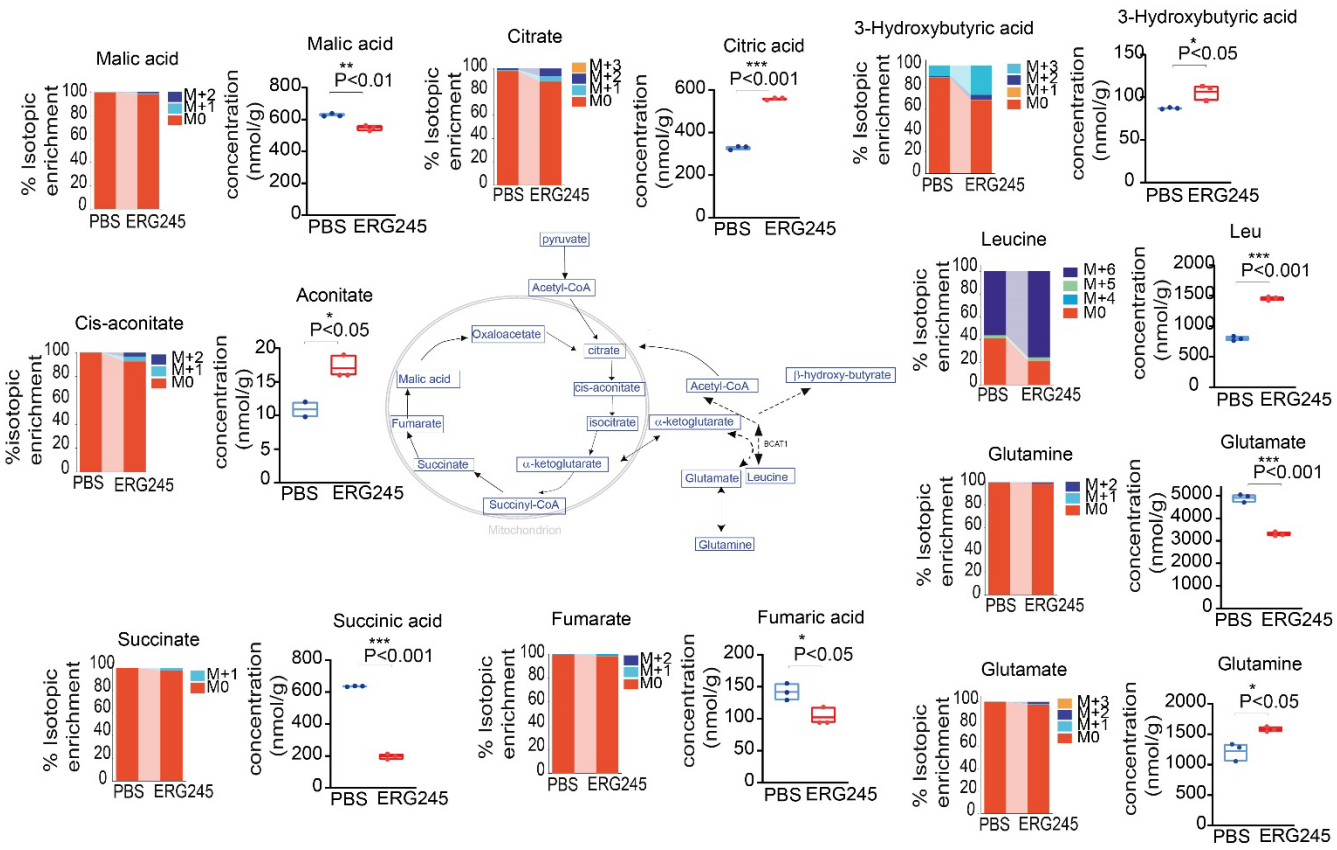

Figure S11. Metabolic impact of BCAT1 inhibition on *ΔE-NOTCH1* leukemias. Results for *in vivo* isotope-tracing experiments following i.v. administration of $^{13}C_6$ Leu in primary *ΔE-NOTCH1* leukemic tissue (N=3) treated with vehicle (PBS) or BCAT1-specific inhibitor, ERG245 (30 mg/kg every 8 hours for 24h). Percentages of $^{13}C_6$ Leu derived: (i) TCA intermediates: citrate (M0, M+1, M+2, M3), cis-aconitate, (M0, M+1, M+2), fumarate (M0, M+1, M+2), malic acid (M0, M+1, M+2), succinate (M0, M+1); (ii) BCAA and derivatives: leucine (M0, M+4, M+5, M+6), glutamate (M0, M+1, M+2, M3), glutamine (M0, M+1, M+2) and beta-hydroxybutyrate (M0, M+1, M+2, M3) are shown. F-scope metabolic quantification for selected metabolites in the same tumors is also shown. Changes in glutaminolysis, TCA cycle intermediates, and BCAA and intermediates are shown as floating bars representing mean ± SD. Significance was calculated using a nonparametric t-test (Mann-Whitney). **P*< 0.05, ***P*< 0.01, ***P< 0.001. n.s.= not significant

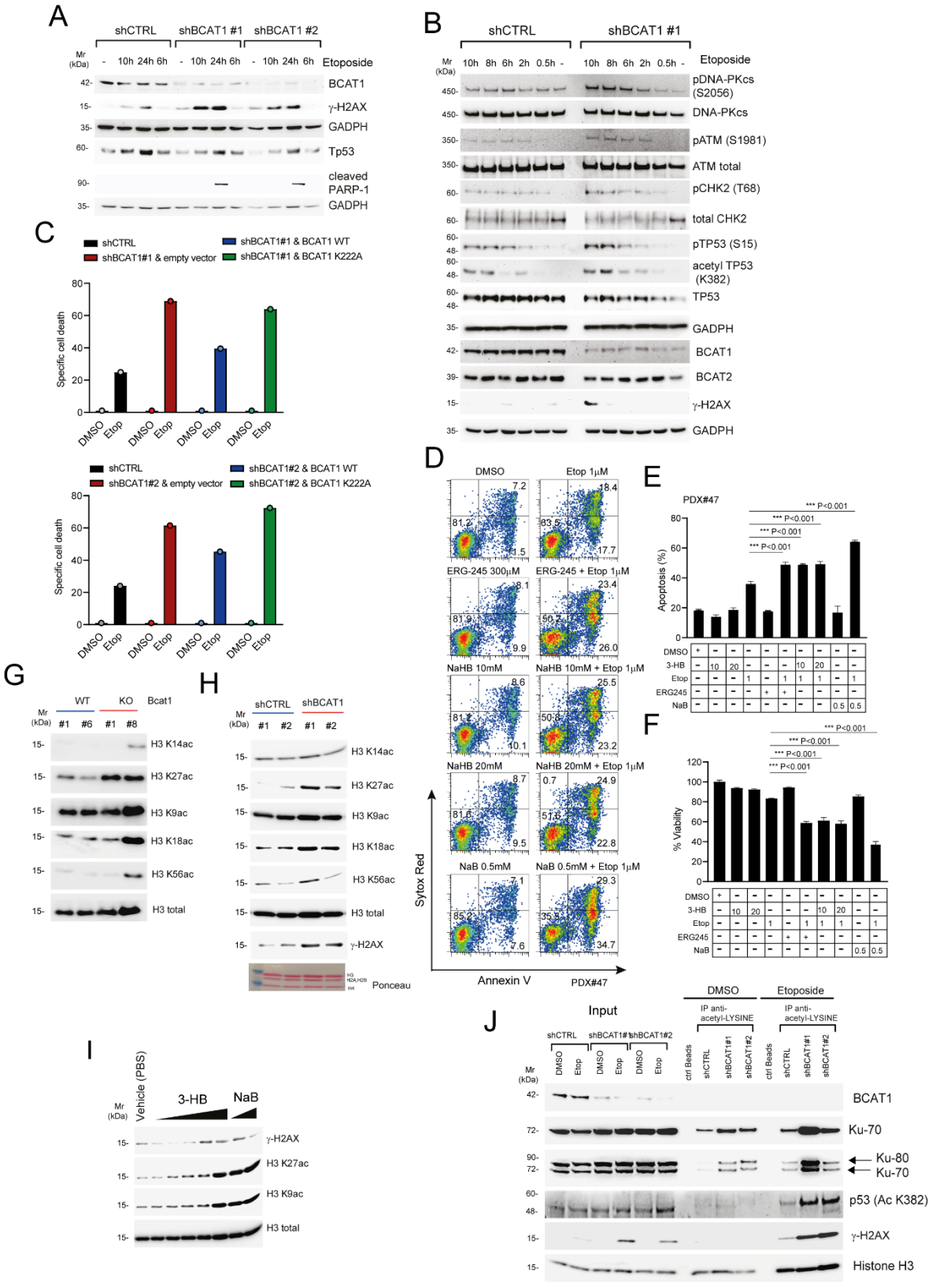

Figure S12. Increased responsiveness to DNA damaging agents in BCAT1 depleted cells is associated with an altered DNA damage response and dependent on its catalytic activity. (A) CCRF-CEM T-ALL cells

transduced with shCTRL or shBCAT1 (#1 and #2) were treated with 1 μM etoposide for the indicated time. Subsequently, whole cell lysates were collected and analyzed by immunoblotting for proteins implicated in the DNA damage response and apoptosis (γH2AX, TP53, cleaved PARP-1). GADPH is shown as loading control. (B) CCRF-CEM T-ALL cells transduced with shCTRL or shBCAT1 #1 were treated with 1 μM etoposide for the indicated time (0-10 hours). Subsequently, whole cell lysates were collected and analyzed by immunoblotting for proteins implicated in the DNA damage response. Total DNA-PKcs, ATM, CHK2 and GADPH are shown as loading controls. (C) Specific apoptosis[31] analysis in BCAT1 depleted CCRF-CEM T-ALL cells (shBCAT1#1 or shBCAT1#2) engineered to express empty vector, wild-type (WT) or catalytic inactive (K222A) BCAT1 and treated in vitro for 48h with DMSO (vehicle) or etoposide (1 μM). Specific apoptosis analysis of CCRF-CEM cells infected with a control shRNA (shCTRL) and treated in vitro for 48h with DMSO (vehicle) or etoposide (1 μM) is also shown. Significance was calculated using an unpaired two-tailed t-test. ** $P< 0.01$, *** $P< 0.001$. (D) Representative plots of apoptosis in PDX#47 cells treated with vehicle (DMSO), 3-HB (10-20 mM), NaB (0.5 mM), ERG245 (300 μM) etoposide (Etop; 1 μM)) or the combination (ERG245 + Etop or 3-HB + Etop or NaB + Etop) for 48h. (E) Quantification of apoptosis in PDX#47 cells treated in vitro with vehicle (DMSO), 3-HB (10-20 mM), NaB (0.5 mM), ERG245 (300 μM), etoposide (Etop; 1 μM)) or the combination (3-HB + Etop or ERG245 + Etop or NaB + Etop) for 48h. Significance was calculated using an unpaired two-tailed t-test. *** $P< 0.001$. (F) Cell viability analysis in PDX#47 cells treated in vitro with vehicle (DMSO), 3-HB (10-20 mM), NaB (0.5 mM), ERG245 (300 μM), etoposide (Etop; 1 μM)) or the combination (3-HB + Etop or ERG245 + Etop or NaB + Etop) for 48h. Significance was calculated using an unpaired two-tailed t-test. *** $P< 0.001$. (G) Total histones were extracted from tumors WT or KO for *Bcat1* and immunoblots were performed for acetylated histone H3 variants. Total H3 is shown as loading control. (H) Total histones extracted from CCRF-CEM cells transduced with shCTRL (#1, #2) or shBCAT1 (#1 and #2) were analyzed by immunoblotting for acetylated histone H3 variants and γH2AX. Total H3 and Ponceau staining are shown as loading controls. (I) CCRF-CEM TALL cells were treated for 24h with vehicle or increasing concentrations of 3-HB (1-40 mM) or NaB (0.5-1 mM). Total histones were extracted and analyzed by immunoblotting for selected acetylated histone H3 variants (K27ac, K9ac) and γH2AX. Total H3 is shown as loading control. (J) CCRF-CEM T-ALL cells transduced with shCTRL or shBCAT1 (#1 and #2) were treated with vehicle (DMSO) or 1 μM etoposide for 24h, subsequently whole cell lysates were collected and immunoprecipitated using anti-acetyl-lysine affinity beads or control beads and probed for KU70, KU80, γH2AX. Total H3 was used as loading control (for input).

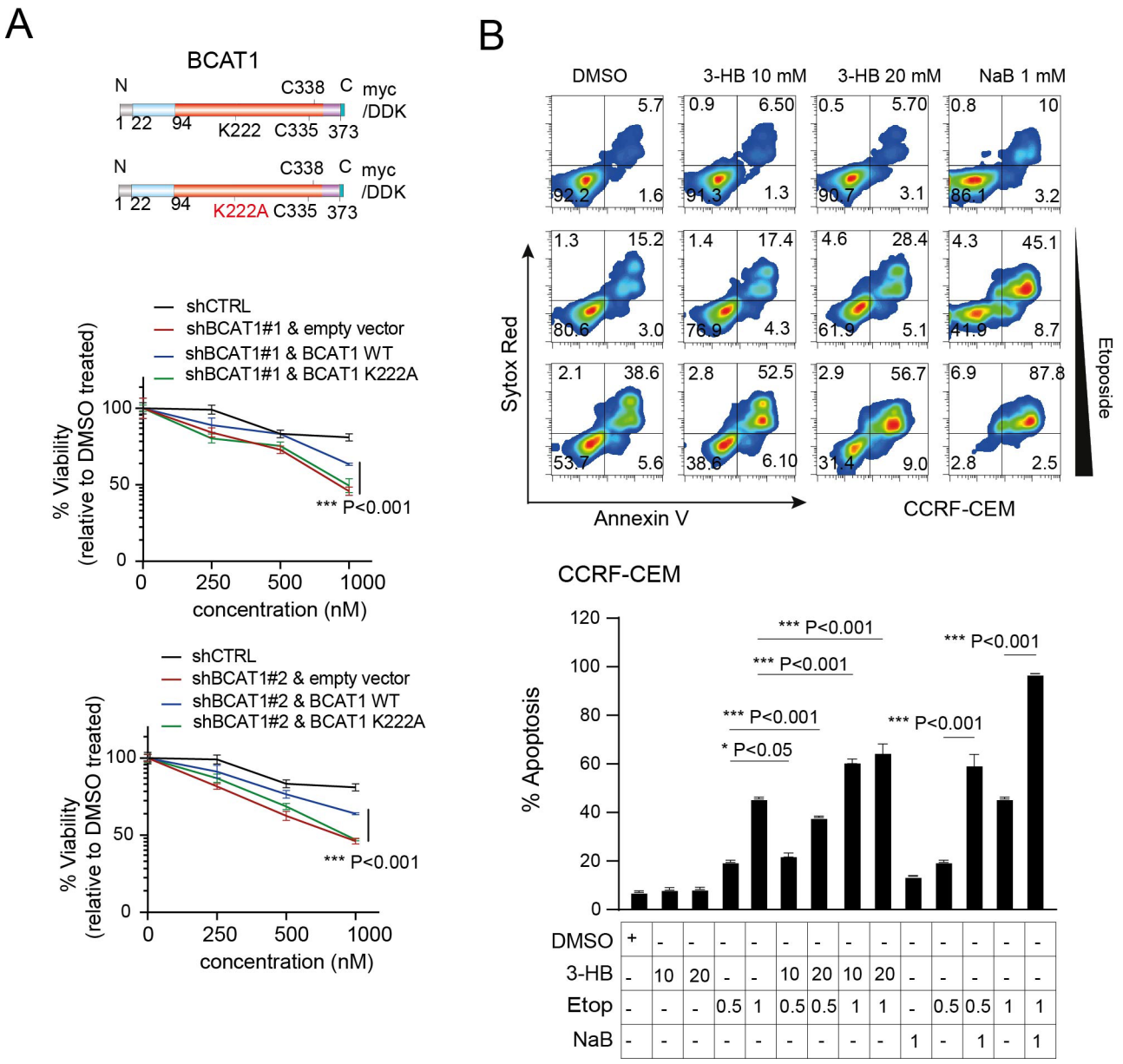

Figure S13. Metabolic function of BCAT1 contributes in modulating the sensitivity to DNA damaging agents. (A) Schematic representations (top) of the constructs encoding full-length (WT) and catalytic inactive mutant of BCAT1 (K222A). Cell viability analysis (lower panels) in BCAT1 depleted CCRF-CEM T-ALL cells (shBCAT1#1 or shBCAT1#2) engineered to express empty vector, wild-type (WT) or catalytic inactive (K222A) BCAT1 and treated in vitro for 48h with DMSO (vehicle) or etoposide (250 nM– 1 µM). Cell viability analysis of CCRF-CEM cells infected with a control shRNA (shCTRL) and treated in vitro for 48h with DMSO (vehicle) or etoposide (250 nM– 1 µM) is also shown. Significance was calculated using an unpaired two-tailed t-test. *** $P<$ 0.001. (B) Representative plots of apoptosis (top) or quantification of apoptosis (bottom) in CCRF-CEM T-ALL cells treated with vehicle (DMSO), 3-HB (10-20mM), NaB (1mM), etoposide (Etop; 0.5-1 µM) or the combination (3-HB + Etop or NaB + Etop) for 48h. Significance was calculated using an unpaired two-tailed t-test. * $P<$ 0.05, *** $P<$ 0.001.

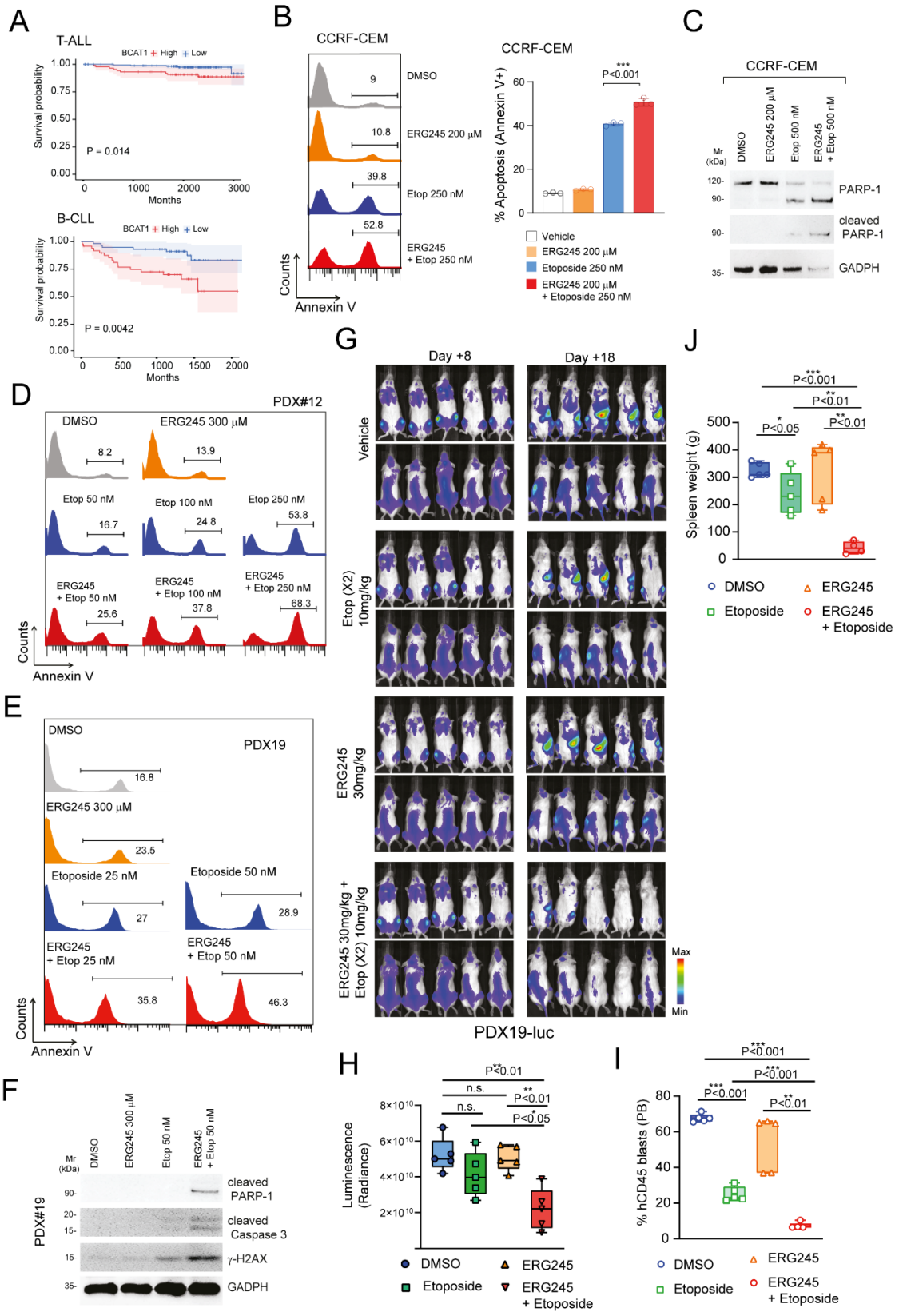

Figure S14. BCAT1 expression correlates with prognosis in NOTCH1-dependent leukemias and represents a therapeutic target in T-ALL. (A) Kaplan–Meier survival curves (top) of the entire series of 261 T-ALL patients

(with reported OS). BCAT1 high cases (> mean expression) or BCAT1 low cases (< mean expression). Log-rank Mantel-Cox test was performed to calculate *P* value. **P*< 0.05. Shaded area represents 95% CI. Kaplan–Meier survival curves of a cohort of 107 B-CLL patients (bottom). BCAT1 (probe 22585_at) high cases (> mean expression) or BCAT1 low cases (< mean expression). Log-rank Mantel-Cox test was performed to calculate *P* value. ***P*< 0.01. Shaded area represents 95% CI. (B) Representative plots (left) and bar graph representation (right) of annexin V staining in CCRF-CEM T-ALL cells treated with vehicle (DMSO), BCAT inhibitor (ERG245), etoposide (Etop) or the combination (ERG245 + Etop) for 48h. Significance was calculated using an unpaired two-tailed t-test. *** *P*< 0.001. (C) Western blot analysis of PARP-1 (total or cleaved PARP-1) in CCRF-CEM cells treated for 48h with DMSO (vehicle), ERG245 (200 μM), etoposide (Etop; 500 nM) or ERG245 + Etop. GADPH was used as protein loading control. (D) Representative plots of annexin V staining in PDX#12 T-ALL cells treated with vehicle (DMSO), BCAT inhibitor (ERG245; 300 μM), etoposide (Etop: 50, 100, 250 nM) or the combination (ERG245 + Etop) for 48h. (E) Representative plots of annexin V staining in PDX#19 T-ALL cells treated with vehicle (DMSO), BCAT inhibitor (ERG245; 300 μM), etoposide (Etop: 25, 50 nM) or the combination (ERG245 + Etop) for 48h. (F) Western blot analysis of cleaved PARP-1, cleaved caspase 3 and phosphorylated γH2AX in PDX#19 cells treated for 48h with DMSO (vehicle), ERG245 (300 μM), etoposide (Etop; 50 nM) or ERG245 + Etop. GADPH was used as protein loading control. (G) Representative images of bioluminescence in NSG mice xenografted with PDX#19 cells expressing luciferase (PDX#19-luc) and treated with vehicle (DMSO), BCAT inhibitor (ERG245; 30 mg/kg three times a week), etoposide (Etop; 10 mg/kg twice a week) or the combination (ERG245 + Etop). Analysis before (day 8 post-transplantation) and 10 days after start of treatment (day 18 post-transplantation) is shown. (H) Quantitative analysis of tumor load via in vivo bioluminescence imaging of NSG mice xenografted with PDX#19-luc 10 days after treatment with vehicle (DMSO), BCAT inhibitor (ERG245), etoposide (Etop) or the combination (ERG245 + Etop). Significance was calculated using an unpaired two-tailed t-test. n.s: not significant. **P*<0.05, ** *P*<0.01. (I) Quantitative analysis of tumor burden in NSG mice xenografted with PDX#19-luc and treated with vehicle (DMSO), BCAT inhibitor (ERG245), etoposide (Etop) or the combination (ERG245+Etop), estimated by analyzing human CD45 expression in the blood (PB) at sacrifice (t=18 days). Significance was calculated using an unpaired two-tailed t-test. ***P*< 0.01, *** *P*< 0.001. (J) Analysis of spleen weight in NSG mice xenografted with PDX#19-luc and treated with vehicle (DMSO), BCAT inhibitor (ERG245), etoposide (Etop) or the combination (ERG245+Etop). Significance was calculated using an unpaired two-tailed t-test. **P*< 0.05, ***P*< 0.01, *** *P*< 0.001.

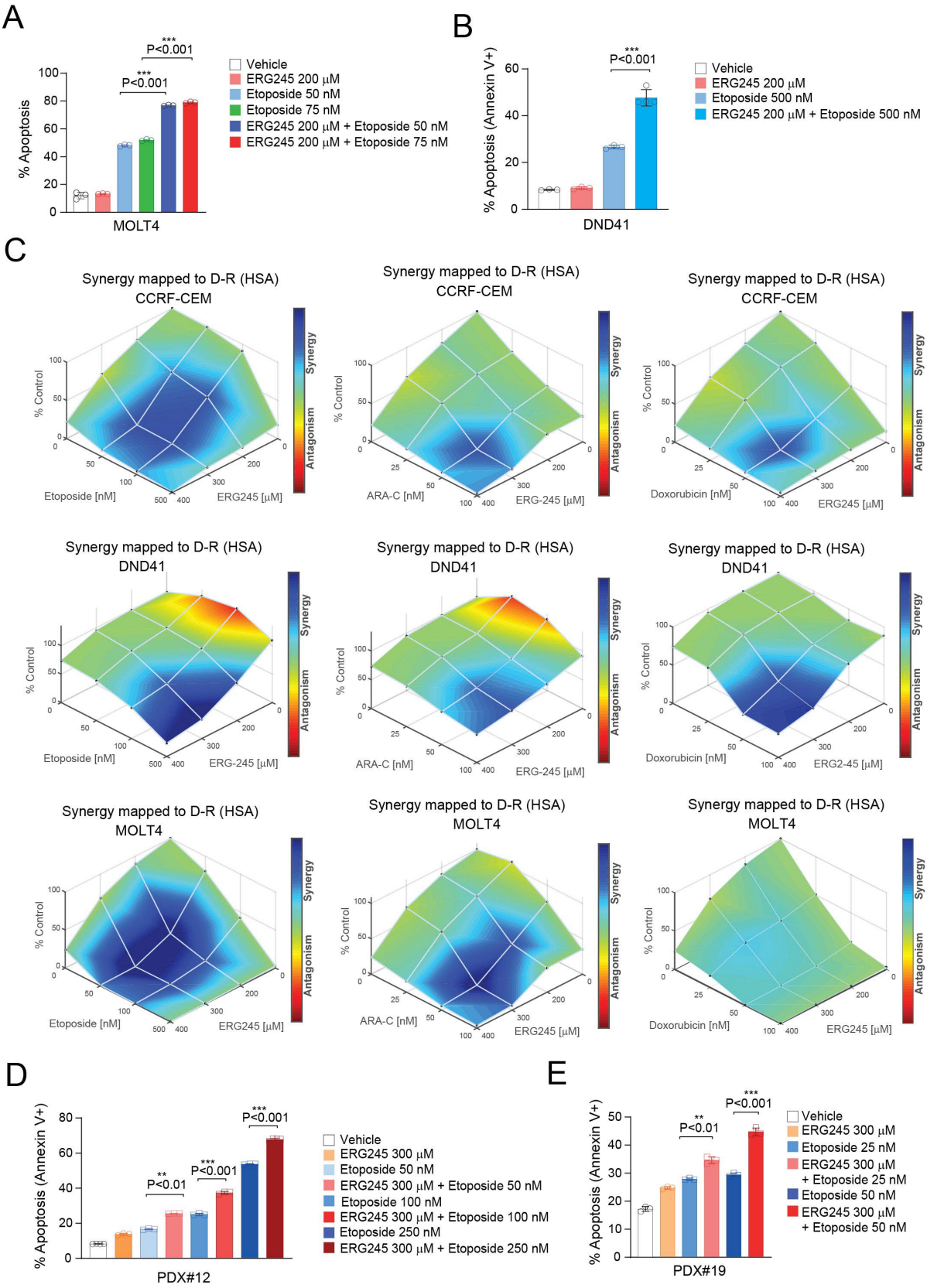

Figure S15. BCAT1 inhibition synergizes with numerous chemotherapeutic drugs to reduce cell viability. (A) Quantification of apoptosis in MOLT4 T-ALL cells treated with vehicle (DMSO), BCAT inhibitor (ERG245),

etoposide (Etop; 50-75 nM) or the combination (ERG245 + Etop) for 48h. Significance was calculated using an unpaired two-tailed t-test. *** $P< 0.001$. (B) Quantification of apoptosis (Annexin V positive) in DND41 T-ALL cells treated with vehicle (DMSO), BCAT inhibitor (ERG245), etoposide (Etop) or the combination (ERG245 + Etop) for 48h. Significance was calculated using an unpaired two-tailed t-test. *** $P< 0.001$. (C) CCRF-CEM, DND41 and MOLT4 T-ALL cells were incubated with different concentrations of etoposide (0- 500 nM, left panels), cytarabine/ara-C (0- 100 nM, middle panels) or doxorubicin (0- 100 nM, right panels) and ERG245 (0-400 μM) for 72h. After treatment, cell viability was assessed using a bioluminescent assay (Vialight plus). Analysis of combination efficacy and synergy for chemotherapeutic drugs (etoposide, ara-C and doxorubicin) and the BCAT inhibitor ERG245 was done using the HSA model with Combenefit software. (D) Quantification of apoptosis (Annexin V positive) in PDX#12 T-ALL cells treated with vehicle (DMSO), BCAT inhibitor (ERG245; 300 μM), etoposide (Etop: 50, 100, 250 nM) or the combination (ERG245 + Etop) for 48h. Significance was calculated using an unpaired two-tailed t-test. ** $P< 0.01$, *** $P< 0.001$. (E) Quantification of apoptosis (Annexin V positive) in PDX#19 T-ALL cells treated with vehicle (DMSO), BCAT inhibitor (ERG245; 300 μM), etoposide (Etop: 25, 50 nM) or the combination (ERG245 + Etop) for 48h. Significance was calculated using an unpaired two-tailed t-test. ** $P< 0.01$, *** $P< 0.001$.

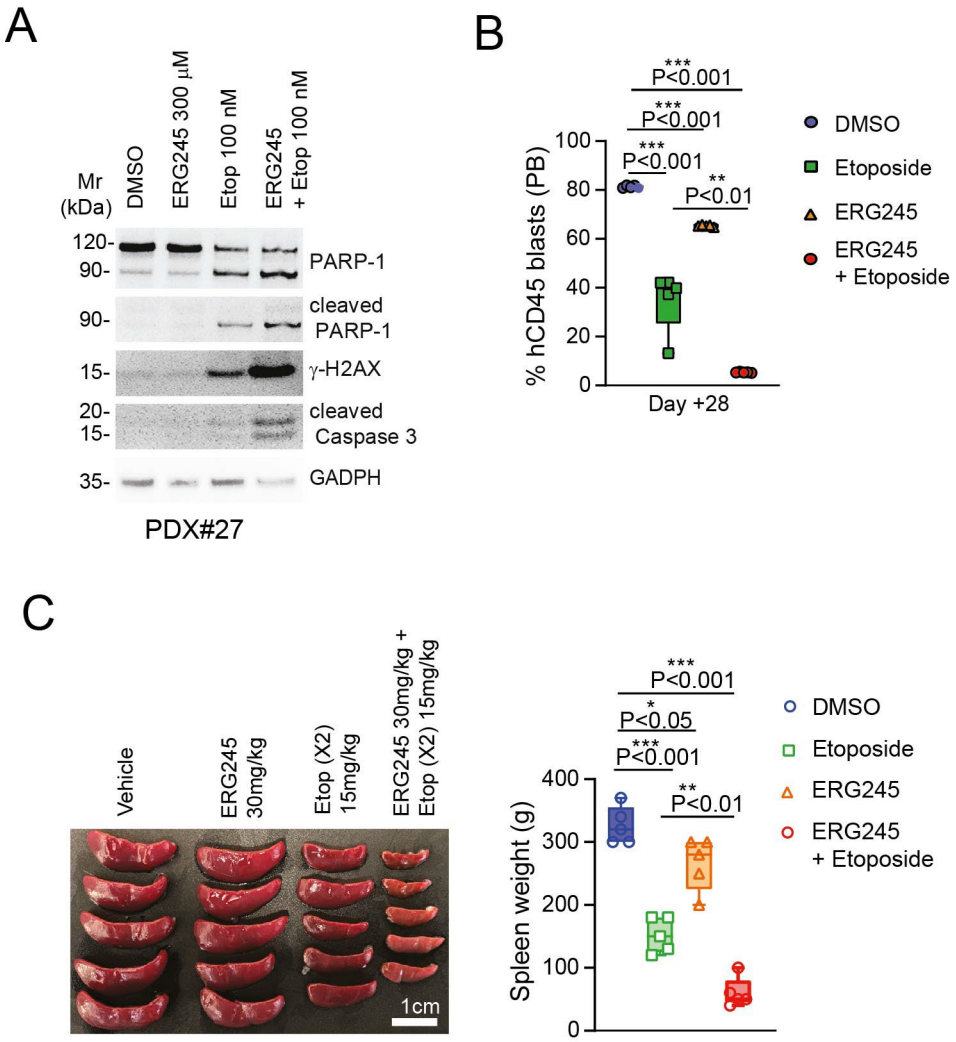

Figure S16. BCAT1 inhibition synergizes with etoposide to reduce viability. (A) Western blot analysis of PARP-1 (total or cleaved PARP-1), phosphorylated γH2AX and cleaved caspase 3 in PDX#27 cells treated for 48h with DMSO (vehicle), ERG245 (300 µM), etoposide (Etop; 100 nM) or ERG245 + Etop. GADPH was used as protein loading control. (B) Quantitative analysis of tumor burden in NSG mice xenografted with PDX#27-luc and treated with vehicle (DMSO), BCAT1 inhibitor (ERG245), etoposide (Etop) or the combination (ERG245+Etop), estimated by analyzing human CD45 expression in the blood (PB) at sacrifice. Significance was calculated using an unpaired two-tailed t-test. ***P*< 0.01, *** *P*< 0.001. (C) Representative images of spleens (left) and analysis of spleen weights (right) in PDX#27-luc xenografted mice at the end of treatment in NSG mice xenografted with PDX#27-luc and treated with vehicle (DMSO), BCAT1 inhibitor (ERG245), etoposide (Etop) or the combination (ERG245+Etop). Significance was calculated using an unpaired two-tailed t-test. **P*< 0.05, ***P*< 0.01, *** *P*< 0.001.

Bibliography

1. Saccomani V, Grassi A, Piovan E, et al. miR-22-3p Negatively Affects Tumor Progression in T-Cell Acute Lymphoblastic Leukemia. Cells. 2020;9(7):
2. Chiang MY, Xu L, Shestova O, et al. Leukemia-associated NOTCH1 alleles are weak tumor initiators but accelerate K-ras-initiated leukemia. The Journal of clinical investigation. 2008;118(9):3181-3194.
3. Ghisi M, Corradin A, Basso K, et al. Modulation of microRNA expression in human T-cell development: targeting of NOTCH3 by miR-150. Blood. 2011;117(26):7053-7062.
4. Agnusdei V, Minuzzo S, Frasson C, et al. Therapeutic antibody targeting of Notch1 in T-acute lymphoblastic leukemia xenografts. Leukemia. 2014;28(2):278-288.
5. Bordin F, Piovan E, Masiero E, et al. WT1 loss attenuates the TP53-induced DNA damage response in T-cell acute lymphoblastic leukemia. Haematologica. 2018;103(2):266-277.
6. Pizzi M, Friziero A, Vianello F, et al. Histology of the spleen in immune thrombocytopenia: clinical-pathological characterization and prognostic implications. European journal of haematology. 2021;106(2):281-289.
7. Gyori BM, Venkatachalam G, Thiagarajan PS, Hsu D, Clement MV. OpenComet: an automated tool for comet assay image analysis. Redox biology. 2014;2(457-465.
8. Ng OH, Erbilgin Y, Firtina S, et al. Deregulated WNT signaling in childhood T-cell acute lymphoblastic leukemia. Blood cancer journal. 2014;4(e192.
9. Sanda T, Li X, Gutierrez A, et al. Interconnecting molecular pathways in the pathogenesis and drug sensitivity of T-cell acute lymphoblastic leukemia. Blood. 2010;115(9):1735-1745.
10. Gutierrez A, Sanda T, Grebliunaite R, et al. High frequency of PTEN, PI3K, and AKT abnormalities in T-cell acute lymphoblastic leukemia. Blood. 2009;114(3):647-650.
11. Chen B, Jiang L, Zhong ML, et al. Identification of fusion genes and characterization of transcriptome features in T-cell acute lymphoblastic leukemia. Proceedings of the National Academy of Sciences of the United States of America. 2018;115(2):373-378.
12. Van Vlierberghe P, Ambesi-Impiombato A, Perez-Garcia A, et al. ETV6 mutations in early immature human T cell leukemias. The Journal of experimental medicine. 2011;208(13):2571-2579.
13. Thandapani P, Kloetgen A, Witkowski MT, et al. Valine tRNA levels and availability regulate complex I assembly in leukaemia. Nature. 2022;601(7893):428-433.
14. Liu Y, Easton J, Shao Y, et al. The genomic landscape of pediatric and young adult T-lineage acute lymphoblastic leukemia. Nat Genet. 2017;49(8):1211-1218.
15. Herold T, Jurinovic V, Metzeler KH, et al. An eight-gene expression signature for the prediction of survival and time to treatment in chronic lymphocytic leukemia. Leukemia. 2011;25(10):1639-1645.
16. Reich M, Liefeld T, Gould J, Lerner J, Tamayo P, Mesirov JP. GenePattern 2.0. Nat Genet. 2006;38(5):500-501.
17. Ge X. iDEP Web Application for RNA-Seq Data Analysis. Methods Mol Biol. 2021;2284(417-443.
18. Subramanian A, Tamayo P, Mootha VK, et al. Gene set enrichment analysis: a knowledge-based approach for interpreting genome-wide expression profiles. Proceedings of the National Academy of Sciences of the United States of America. 2005;102(43):15545-15550.
19. Pang Z, Chong J, Zhou G, et al. MetaboAnalyst 5.0: narrowing the gap between raw spectra and functional insights. Nucleic Acids Res. 2021;49(W1):W388-W396.
20. Ngondo-Mbongo RP, Myslinski E, Aster JC, Carbon P. Modulation of gene expression via overlapping binding sites exerted by ZNF143, Notch1 and THAP11. Nucleic Acids Res. 2013;41(7):4000-4014.
21. Winter GE, Mayer A, Buckley DL, et al. BET Bromodomain Proteins Function as Master Transcription Elongation Factors Independent of CDK9 Recruitment. Molecular cell. 2017;67(1):5-18 e19.
22. Gopi LK, Kidder BL. Integrative pan cancer analysis reveals epigenomic variation in cancer type and cell specific chromatin domains. Nature communications. 2021;12(1):1419.
23. Massarat AR, Sen A, Jaureguy J, et al. Discovering single nucleotide variants and indels from bulk and single-cell ATAC-seq. Nucleic Acids Res. 2021;49(14):7986-7994.
24. Langmead B, Salzberg SL. Fast gapped-read alignment with Bowtie 2. Nature methods. 2012;9(4):357-359.

25. Zhang Y, Liu T, Meyer CA, et al. Model-based analysis of ChIP-Seq (MACS). Genome biology. 2008;9(9):R137.
26. Lopez-Delisle L, Rabbani L, Wolff J, et al. pyGenomeTracks: reproducible plots for multivariate genomic datasets. Bioinformatics. 2021;37(3):422-423.
27. McBrayer SK, Mayers JR, DiNatale GJ, et al. Transaminase Inhibition by 2-Hydroxyglutarate Impairs Glutamate Biosynthesis and Redox Homeostasis in Glioma. Cell. 2018;175(1):101-116 e125.
28. Leo IR, Aswad L, Stahl M, et al. Integrative multi-omics and drug response profiling of childhood acute lymphoblastic leukemia cell lines. Nature communications. 2022;13(1):1691.
29. Tonjes M, Barbus S, Park YJ, et al. BCAT1 promotes cell proliferation through amino acid catabolism in gliomas carrying wild-type IDH1. Nature medicine. 2013;19(7):901-908.
30. Pedersen SK, Baker RT, McEvoy A, et al. A two-gene blood test for methylated DNA sensitive for colorectal cancer. PloS one. 2015;10(4):e0125041.
31. Epling-Burnette PK, Liu JH, Catlett-Falcone R, et al. Inhibition of STAT3 signaling leads to apoptosis of leukemic large granular lymphocytes and decreased Mcl-1 expression. The Journal of clinical investigation. 2001;107(3):351-362.